TECHNISCHE UNIVERSITÄT DRESDEN

Faculty of Science Institute of Microbiology
Chair of Molecular Biotechnology

Dissertation

The Agarolytic System of *Microbulbifer elongatus* PORT2, Isolated from Batu Karas, Pangandaran West Java Indonesia

by

Santi Rukminita Anggraeni

born July 20, 1979 in Lampung

for the award of the academic degree
***Doctor rerum naturalium* (Dr. rer.nat.)**

Submission: 30.06.2020

Public defence: 03.11.2020

Dresden, 2020

The work of this dissertation was performed between November, 14th 2015 until June, 30th 2020 at the Molecular Biotechnology Research Group of Prof. Dr. Marion B. Ansorge Schumacher, the Institute of Microbiology, Technische Universität Dresden. This work has not been previously done or identical to any previous related topics.

Dresden, November 3, 2020

Santi Rukminita Anggraeni

PhD Committee and Examination Board:

1st reviewer and supervisor	Prof. Dr. Marion B. Ansorge Schumacher	Technische Universität Dresden
2nd reviewer	Dr. Mirjam Czjzek	Station Biology Roscoff-CNRS
The Chair	Prof. Dr. Michael Rother	Technische Universität Dresden
Member	Prof. Dr. Thorsten Mascher	Technische Universität Dresden
Member	Prof. Dr. Stefan Wanke	Technische Universität Dresden

Indeed, in the creation of the heavens and the earth and the alternation of the night and the day are signs for those of understanding (Al Imran: 190),

Who remember Allah while standing or sitting or [lying] on their sides and give thought to the creation of the heavens and the earth, [saying], "Our Lord, You did not create this aimlessly; exalted are You [above such a thing]; then protect us from the punishment of the Fire (Al Imran: 191).

Summary

Agar is a marine heteropolysaccharide with repeating units consisting of 3,6-α-anhydro-L-galactopyranose and D-galactopyranose linked by α-(1,3) and β-(1,4) linkages. It has been promoted as a prospective replacement for petroleum-based feedstocks and other applications. Enzymatic biotransformation of agar generates high specific products: It is also more environmentally friendly than chemical hydrolysis. In particular, agarolytic bacteria and their agarases are preferred for the processing of agar into sugar derivatives.

Agar-producing macroalgae are one of Indonesia's national commodities. However, agar-based products and technology are rarely developed in Indonesia. This research is aimed to explore the potential of an Indonesian marine bacterium and its agarases as bioagents for agar bioprocessing. The research objectives are to identify the novelty of the isolate among known agarolytic bacteria using microbiology and molecular biology approaches, to elucidate the agarolytic system of the bacterium using *in silico* genome analysis, to express and characterize the recombinant agarases, and to elucidate their potential for producing agar-derived saccharides from Indonesian natural agar.

Microbulbifer elongatus PORT2 is a gram-negative marine bacterium that had been isolated from Batu Karas seawater, Pangandaran, West Java Indonesia. PORT2 shows potential as biocatalysts for agar saccharides conversion by showing remarkable agar liquefaction. The annotation of the draft genome identifies six putative β-agarases consist of three GH50, two GH86, and one GH16 in *M. elongatus* PORT2. Those agarases are clustered at two different contigs. Besides agarases, other genes for D-galactose and 3,6 anhydro-L galactose metabolism, sugar transports and regulatory system are found in the vicinity of the agarases clusters. Despite the ability to utilize agar as a sole carbon sole, PORT2 lacks any putative α-agarase GH117 or GH96. Both are responsible for the cleavage of α-glycosidic bonds in agar. Indeed, several hypothetical proteins are in the neighborhood of the agarase gene clusters in *M. elongatus* PORT2. They probably could have a function as the alternative machinery or pathway for agar monomerization that needs clarification in future research work.

Four recombinant β-agarases from PORT2; AgaA50, AgaB50, AgaC50, and AgaF16A have been successfully overexpressed in *E.coli* and characterized. The AgaA50 and AgaC50 exhibit metal-dependent activity. They perform exo-agarolytic modes and generates neoagarobiose (NA2). The AgaB50 can act as endo-and exo-β-agarase without any additional activator and produces neoagarohexaose (NA6), neoagarotetraose (NA4), and NA2. AgaF16 produces NA6 and NA4. The enzyme shows pure endo-catalytic action which thiol agents positively affect its activity. The synergetic reaction of AgaF16A and AgaA50 converts Indonesian *Gelidium* agar into NA2 and *Gracilaria* agar into modified NA2. The modified NA2 from *Gracilaria* agar could promise new potential bioactivity that is different from agarose-derived NA2 due to the presence of additional side chains on the saccharide backbone. The NA6, NA4, and NA2 products from agarose have shown potential pharmaceutical applications such as immunomodulator, anti-tumor, antioxidant, anti-diabetic, and moisturizer.

Despite being isolated from a mesophilic marine bacterium, the recombinant agarases from *M. elongatus* PORT2 are active at 50 °C and pH between 6.5 to 8. They maintain more than 75% of their activities even after 1 h preincubation at 50 °C, except for AgaC50. Their thermostability gives advantages for the effective biocatalytic conversion of agar because the substrate is more accessible at mild pH and the temperature above the sol-gel condition (> 40 °C).

Abbreviations

AA	Auxiliary activity
AI	Aliphatic index
ANI	Average nucleotide identity
AOS	Agarooligosaccharides
BN-PAGE	Blue native polyacrylamide gel electrophoresis
CAPS	N-cyclohexyl-3-aminopropanesulfonic acid
CAT	Catalase
Cazymes	Carbohydrate-active enzymes
CBM	Carbohydrate-binding module
CDS	Coding sequence
CE	Carbohydrate esterase
COG	Cluster of orthologous group
ED	Entner-Doudoroff
gDNA	genomic deoxyribose nucleic acid
GGDC	Genome to genome distance comparison
GH	Glycoside hydrolase
GoR	Glutathione reductase
GRAS	Generally recognized as safe
GT	Glycoside transferase
HEPES	Hydroxyethyl piperazineethanesulfonic acid
HSP	High scoring segment pairs
isDDH	*In silico* DNA-DNA hybridization
II	Instability index
IMAC	Immobilized metal affinity chromatography
NAOS	Neoagarooligosaccharides
NA8	Neoagarooctaose
NA6	Neoagarohexaose
NA4	Neoagarotetraose
NA2	Neoagarobiose
AHG	3,6- α-anhydro-L-galactose
NABH	Neogarobiose hydrolase
Ni-NTA	*Nickel*–nitrilotriacetic acid
ORF	Open reading frame
PAGE	Polyacrylamide gel electrophoresis

PCR	Polymerase chain reaction
PDB	Protein database
PL	Polysaccharide lyase
RBS	Ribosomal binding site
RDP	Ribosomal database project
SDS	Sodium dodecyl sulfate
SIM	Sulfide, Indole, and Motility
SP	Signal peptide
SOD	Superoxide dismutase
TCA	Tricarboxylic acid cycle
YEAas	Yeast extract agar in the artificial seawater

Contents

1. Introduction

1.1. Motivation and Scientific Goals

Global climate change and sustainable living concepts have triggered the effort to identify renewable resources as a replacement for petroleum-based feedstock. Biomass provides carbon materials similar to fossilized resources. Therefore, it has been considered a prominent candidate for renewable fuel and chemical staples. Transition into alternative feedstock requires not only adequate raw materials supply but also chemical pathways and processing technologies into novel final products. The derived processes and products should be profitable, sustainable, and environmentally harmless. Among potential biomass resources, macro algae offer the aforementioned features.

Out of 221 commercial macro algae species, a few have been intensively cultivated such as brown algae *Sargassum* sp., kelp red alga *Porphyra* red algae *Eucheuma* sp., *Kapphaphycus* sp., and *Gracilaria* sp. Their cultivation is simple without any additional fertilizer, growth factors, or hormones. Macro algae farming does not compete with food or land-usage issues. It also enhances CO_2 absorption beneficial for reducing greenhouse effects. Notably, red algae farming in developing countries has assisted the improvement of coastal community livelihood by generating employment activity. Other fisheries cultivation such as shrimp, abalone, and sea cucumber often combine with red alga *Gracilaria* sp. due to its ability to ameliorate water quality and for additional economic value as agar producer (Ferdouse et al. 2018). Agar-derived saccharides have been considered not only as a potential prospective replacement for petroleum-based feedstock but also as bioactive compounds such as antioxidants, anti-inflammatory, anti-tumor, immuno-modulator, and whitening agent (Park et al. 2020).

Agar-derived saccharides production can use a chemical and/or enzymatic process. The latter is preferable due to homogenous highly-specific products and more environmentally friendly. Biotechnology has been used as an effective tool for generating high added-value products. It offers a sustainable approach for enzymatic agar conversion while optimizing viable domestic bio resources.

One crucial part of biotechnology research and development is the establishment of bio agents for alga polysaccharides transformation, the organisms and/or the enzymes (Renn 1997; Pulz and Gross 2004; van Hal et al. 2013). Exploration of local microorganisms where the red algae originate could be a feasible way to obtain the appropriate bio agents needed.

Indonesia is the second-largest cultivated *Gracilaria* producer in the world after China and shares around 38% of the market. Around 60-70% of Indonesian agar production was exported as dried red alga to Chile, China, the Philippines, and some other countries. However, at the same time, Indonesia imports macro algae colloids for food and pharmaceutical industry applications due to inadequate macro algae-based research technology and development (Mazarrasa et al. 2014; Ferdouse et al. 2018). As a result, potential production and utilization of agar-derived saccharides also reduce. Substantial research development is needed to support the scale-down process technologies that efficiently extract agar-derived saccharides and economically improve agar-value chain competitiveness.

An agarolytic bacterium had been isolated from Batu Karas seawater, Pangandaran, West Java Indonesia. It forms a pit and liquefies the agar plate indicating agar utilization. The bacterium should have an agarase system and therefore is a potential candidate for converting agar to smaller saccharides. This research aims to elucidate the bacterium capability for agar-derived saccharides conversion by:

1. Identifying the bacterium isolate to determine its uniqueness compared to the known agarolytic bacteria (**Chapter 3**).
2. Examining the isolate genome to explain its agarolytic system *in silico* in comparison to the known agarolytic bacteria (**Chapter 4**).
3. Mining the agarase genes and engineering recombinant agarases to elucidate the functionality of the enzymes (**Chapter 5**).
4. Determining the agarolytic performance and potential added value-product that can be derived from Indonesian agar using recombinant agarases (**Chapter 5**).

The studies in this dissertation have revealed several findings for supporting macro algae biotechnology development in Indonesia. The first is the discovery and characterization of a mesophilic marine bacterium from the Indonesian coastal

seawater. The bacterium produces thermostable agarases and designates as *Microbulbifer elongatus* PORT2. Second, the first part of the agar degradation pathway in PORT2 that represents *M.elongatus* has been elucidated through genome profiling and characterization of recombinant β-agarases. The finding implies the possibility of discovering neoagarobiose hydrolase-like enzyme for the completion of the agar degradation pathway in *Microbulbifer* spp. The third is the potential application of the thermostable recombinant agarases for the conversion of Indonesian agar into agar-derived saccharides

1.2. Literature Review

1.2.1. Agar and Agar Derived Saccharides

Agar is a heteropolysaccharide with a repeating backbone consisting of 3,6- α-anhydro-L-galactopyranose and D-galactopyranose linked by alternating α-(1,3) and β-(1,4) linkages (**Figure 1.1**). This structure is typical neutral agar or agarose. The 3,6- α-anhydro-L-galactopyranose gives unique gelling property to the agar. Physico-chemical properties of agar depend on producing-species, harvesting period, method of extraction, and environmental factors such as nutrient availability and hydrodynamic condition (Usov 2011; Lahaye and Rochas 1991; Rebello et al. 1997; Sousa et al. 2013).

Agar backbone can be masked by various side-chain groups such as methyl, sulfate, or pyruvate. The side-chain modifies not only the structure but also the agar's physical properties. Natural methyl at C6 of the galactose increases the gelling temperature and agar solubility in hot ethanol (Guiseley 1970). Pyruvate and sulfate augment agar polarity and reduce the gelling property (Morrice et al. 1983; Lahaye and Rochas 1991). An example is porphyran, sulfate masking of 6-sulfate-L-galactopyranoses significantly diminish the gelling property and increased cold water solubility. Indeed, 6-sulfate-L-galactopyranose is purposed as the precursor of anhydro-L-galactose during the biosynthesis of agar (Usov 2011).

Agar has covalent alpha (α) and/or beta (β) glycosidic linkages reflecting the stereochemistry of the hydroxyl group at the anomeric carbon (Sinnot 2007). By convention, the reducing-end residue within the structure is drawn furthest to the right and the non-reducing end positioned at the furthest left (Baker et al. 1997). The glycosidic cleavage can generate two distinct agar oligomers. The cleavage of

β-linkage generates neoagarooligosaccharide with D-galactose at the reducing end (e.g neoagarobiose) while the α-cleavage produces agarooligosaccharide (e.g. agarobiose) with 3,6- α-anhydro-L-galactose as the reducing end (**Figure 1.1**) (Ekborg 2005).

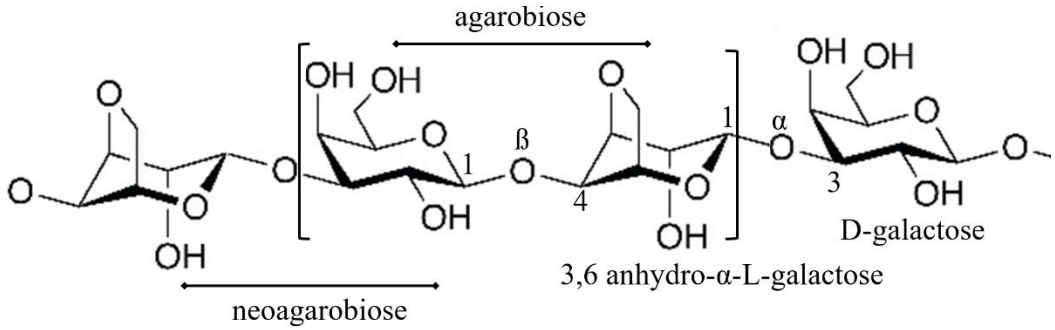

Figure 1.1. Neutral agar (agarose) repeating units. The smallest repeating disaccharide is designated as a neoagarobiose if D-galactose is at a reducing end position or agarobiose if 3,6- α-anhydro-L-galactose as the reducing end.

Agar has been widely used as a food additive, solidifying reagent, and supporting materials for electrophoresis and chromatography techniques. Recently, it has been applied in various industries as carrier materials for drug delivery (Kazimierczak et al. 2019), encapsulation (Guerrero et al.2017), immobilization (Elkahlout et al. 2017), and prospective biodegradable polymers for replacing petroleum-based feedstock (Liu et al. 2018).

Agar-derived saccharides show numerous biological activities. A mixture of neoagarohexaose (NA6) and neoagarotetraose (NA4) show anti-obesity and antidiabetic effects (Hong et al. 2017). NA4 demonstrates various activities such as immunomodulatory activity (Kang et al. 2017), anti-inflammatory effect (Wang et al. 2017), anti-fatigue agent (Zhang et al. 2017), and antitumor activity (Lee et al. 2017) while neoagarobiose (NA2) exhibits antioxidant activity, skin-whitening, and moisturizing activity (Kobayashi et al. 1997; Lee et al. 2008; Yun et al. 2013).

1.2.2. Glycoside Hydrolases (GHs)

Glycoside hydrolases or glycosidases are enzymes that catalyze the hydrolysis of glycosidic linkages. Their classifications imply the structural complexity of the substrate (Vocadlo and Davies 2008). The EC number classifies glycoside hydrolase based on the chemical reaction catalyzed by the enzyme thus inferring substrate specificity. An example is the O-Glycoside hydrolases which are classified into EC 3.2.1.X. The first three digits 3.2.1. instantiates the type of

glycosidic bond cleavage and the last digit indicates the substrate structure. The EC number classification was proposed by the International Union of Biochemistry and Molecular Biology (IUMB) to avoid trivial name ambiguity but unable to describe the enzyme structure and mechanism (Zhang et al. 2010).

A sequence-based classification of glycoside hydrolase is well documented in the carbohydrate-active enzymes database (Lombard et al. 2014). The classification was proposed in 1995 by Davies and Henrissat based on the hypothesis that most functional domain/region responsible for the mechanism is conserved and sequence defines protein fold. Thus, preliminary structure and mechanism can be predicted from sequence similarity. The availability of experimental 3D protein structure with minimum sequence length around 150 residues and 50% of homology could facilitate *in silico* mechanism prediction of an unknown protein (Krieger et al. 2003). The database classifies enzymes into family, subfamily, and clan. Sequence and folding similarity, conserved catalytic apparatus, and mechanism delineate a GH family and clan (Cantarel et al. 2009; Davies and Williams 2016).

Mechanism

In 1953, Koshland postulated that glycoside hydrolase performs bio catalysis either via a retaining or inverting mechanism. Both mechanisms need a nucleophile and a proton donor residues to perform the cleavage. Catalysis by a retaining GH involves two transition steps due to the proximity of two catalytic residues. In-between, a glycosyl-enzyme intermediate complex is formed to facilitate hydrolysis reaction before product release (**Figure 1.2.a**). In contrast, an inverting GH has a wider distance between catalytic residues that can accommodate a one-step hydrolysis reaction and is illustrated in **Figure 1.2**.**b.** Recently, a new glycoside hydrolase mechanism involving a NAD-cofactor dependent has been discovered. The reaction proceeds via an anionic transition state with elimination and redox steps (Yip et al. 2004; Rajan et al. 2004).

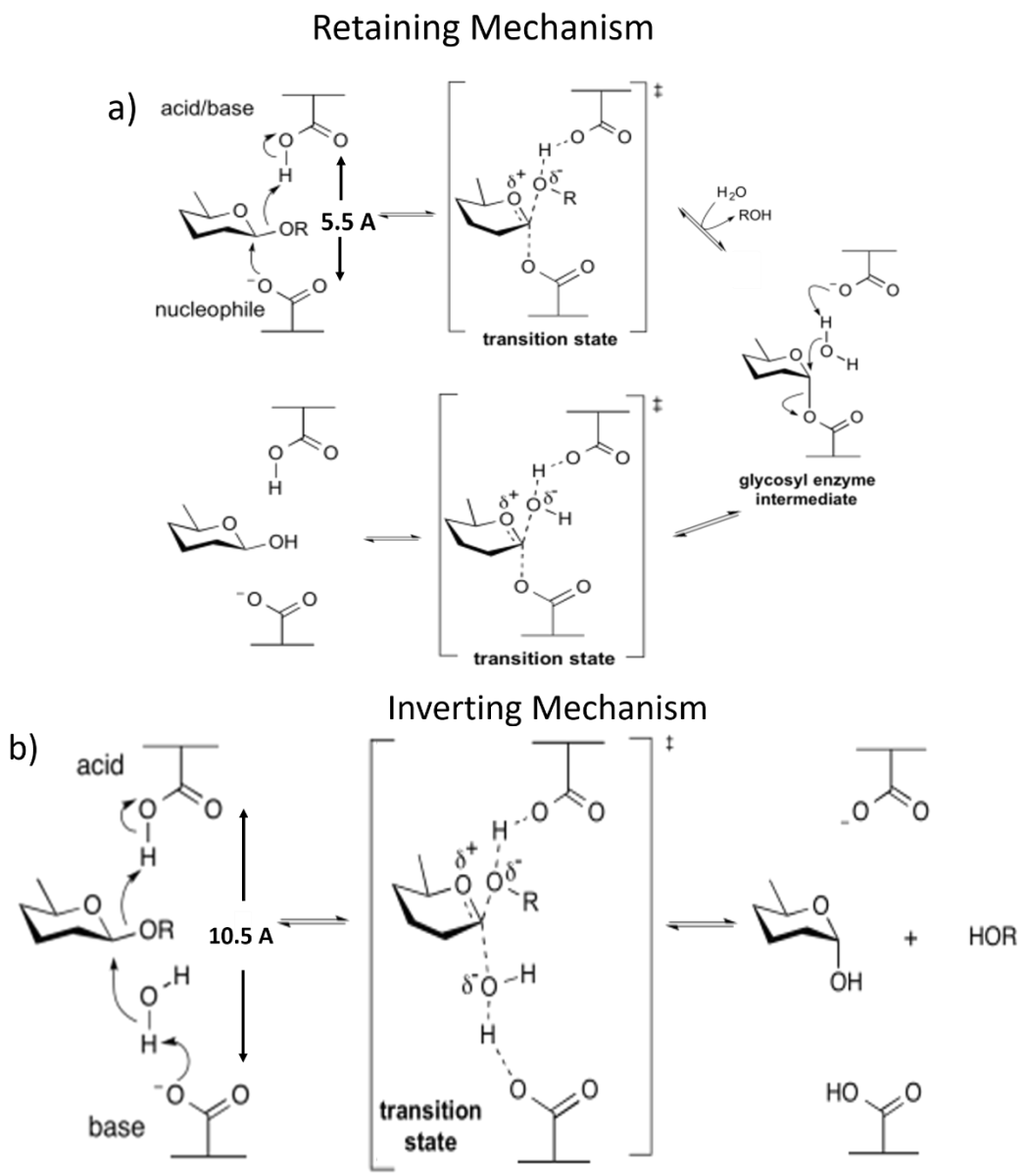

Figure 1.2. Catalytic mechanisms of glycoside hydrolase (modified from https://www.cazypedia.org/index.php/Glycoside_hydrolases). a) A retaining glycosidase performs the glycosidic bond cleavage using two steps displacement. In the first step, a residue acts as a nucleophile attacking the anomeric center. At the same time, other residue acts as an acid/base and protonates the cleaving glycosidic oxygen. A covalent glycosyl-enzyme is formed. In the second step, the base residue deprotonates water for hydrolyzing the glycosyl-enzyme intermediate. b) an inverting glycosidase cleaves the glycosidic bonds using a single displacement mechanism. One residue plays a role as a general base deprotonates water that attacks the anomeric carbon. At the same time, the other residue plays a role as a general acid protonates the glycosidic oxygen as the bond cleaves. An oxocarbenium ion-like transition state is formed and hydrolyzed by the water.

The action of glycoside hydrolase on catalyzing the hydrolysis of glycosidic bonds can be differentiated into endo- and exo-mode. The exo-glycosidase acts on the

glycosidic bonds from the end part of sugar while endo-glycosidase cuts inner glycosidic bonds randomly (**Figure 1.3.**). Glycoside hydrolase also has different modes of enzyme-substrate interaction, either processive or dissociative (Vocadlo and Davies 2008). A processive glycosidase interacts continuously with the substrate during hydrolysis until it reaches the final reaction capacity. Meanwhile, the dissociative glycosidase cleaves the glycosidic linkages once or a few times randomly releasing different sizes of products with accessible termini (Taylor et al.2013).

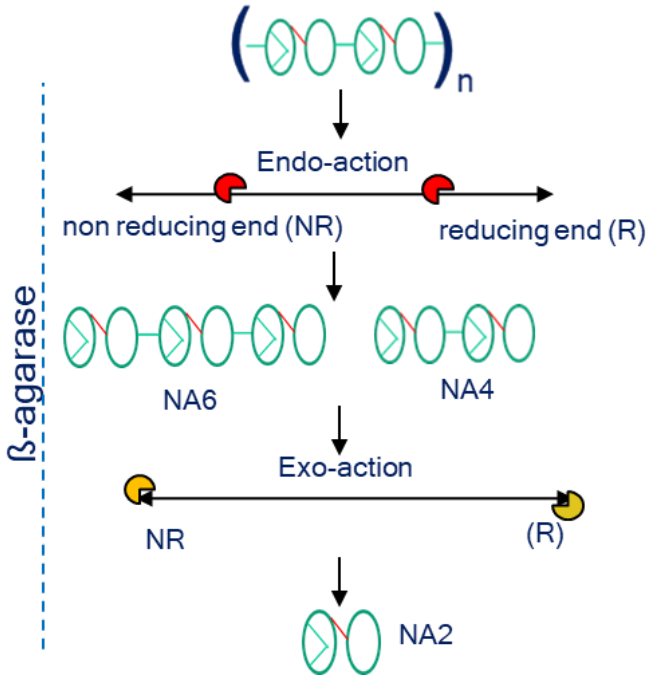

Figure 1.3. Mode of glycosidase actions: endo and exo-activity (e.g. β-agarase). Endo-glycosidase (*red packman*) cleaves inner glycosidic bonds randomly releasing products of different sizes. An exo-glycosidase (*yellow packman*) performs the cleavage from the end of saccharides resulting in a single product size.

Substrate Binding Site

A substrate-binding site is a region within an enzyme where the catalysis reaction proceeds. Specific amino acid residues interact with the substrate through non-polar and non-covalent hydrogen-bonding networks to form a transition state with lower activation energy before releasing the product (Wilson 2010). In glycoside hydrolase, arginine, aspartate, glutamate, and aromatic amino acids have a strong propensity to be the substrate-binding residues. Specifically, two glutamates or aspartic acid play a role as the catalytic residues, either proton donor or nucleophile (Davies and Henrissat 1995; Tsai 2012).

The substrate-binding site in glycoside hydrolase has a specific nomenclature which indicates the position of catalytic subsite relative to the point of cleavage and indirectly illustrates the mode of action. The number of binding subsites can be increased or reduced when different sugar-units of the substrate are introduced into the enzyme but the pre-existing nomenclature sequence may not change (Davies et al 1997). The nomenclature applies several rules as below:

1). The - n to + n is the label of the subsites at the non-reducing end to the reducing end, respectively.

2). The cleavage occurs between -1 and +1 sites.

3). The –n to + 2 is used for exo-glycosidase that cleaves from the reducing end (**Figure 1.4.a**).

4). The -2 to + n is used for exo-glycosidase that cleaves from the non-reducing end (**Figure 1.4.b.**).

5). The -1 to n is used for a glycosidase that cleaves a monosaccharide from the non-reducing end (**Figure 1.4.c**).

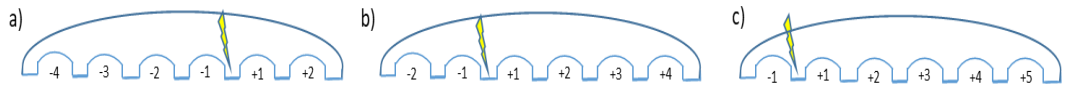

Figure 1.4. Sugar-binding sub sites nomenclature for different actions of glycoside hydrolases: **a**) exo-glycosidase that cleaves from reducing end **b**) exo-glycosidase that cleaves from non-reducing end **c**) a glycosidase that cleaves a monosaccharide from the non-reducing end.

Active Site Topology

Up to date, only three types of active site topologies are known. Exo-glycoside hydrolase such as β-galactosidase or cellohydrobiolase generally adopts a pocket-like active site suitable for a small substrate (Vonossowski et al. 2003) (**Figure 1.5.a**). Endo-acting GHs such as agarases from the GH16 family, chitinases, and endocellulases adopt an open structure-active site such as a cleft or groove (Viborg et al. 2019) (**Figure 1.5.b**). A processive GH mostly adopts tunnel topology such as cellobiohydrolase II from *Trichoderma reesei* (Vonossowski et al. 2003) (**Figure 1.5.c**).

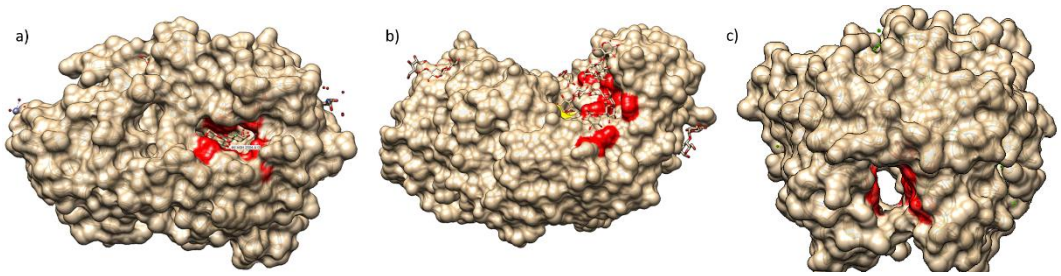

Figure 1.5. Active site topology in glycoside hydrolase: **a**). Pocket/crater of Cel7A *Aspergillus fumigatus* (PDB id 4V20) **b**). Cleft/Groove from GH6-amylase alkalophilic *Bacillus* sp.707 (PDB id 2D3N) **c**). Tunnel of cellobiohydrolase II *Trichoderma reesei* (PDB id 1CB2); amino acid residues at substrate binding site (*red*).

1.2.3. Agarases

Agarases are glycoside hydrolases that catalyze glycosidic bonds cleavage of agar by adding water. They are differentiated into two groups. The α- agarase has activity on (1→3)-α-L-galactoside linkages while β-agarase on (1→4)-β-D-galactoside linkages. The CAZY system classifies β-agarase into GH16, GH50, GH86, and GH118 with E.C number 3.2.1.81 and α-agarase into GH96 and GH117 with E.C number 3.2.1.158 (Hehemann et al. 2012c; Michel and Czjzek 2013). Currently, more β-agarases have been characterized and structurally elucidated than α- agarase.

Glycoside hydrolase 16 (GH16) is a polyspecific β-glycanase family clan B in which β-agarase is a member of subfamily 16 (GH16-16). This family is composed of endo-retaining enzymes. Some of them also show transglycosylation activity. GH16 has a β-jelly roll sandwich structure forming a cleft-shaped active site with motif either β-bulge or β-strand and two catalytic glutamates or aspartic acid in the middle of the cleft. The β-bulge motif has a consensus active-site sequence of EXDXXE and presents more frequently than the β-strand (EXDXE) (Viborg et al. 2019; www.cazypedia.org). Members of GH16 can be equipped with additional non-catalytic carbohydrate-binding modules (CBMs) which specifically recognize the non-reducing end of the substrate and enhance the catalytic efficiency (Henshaw et al. 2006).

GH50 is a retaining-β-agarases family within the $(\alpha/\beta)_8$ barrel-clan A. Most of them are exo-retaining agarases. The exo-action was resolved from the protein structure of Aga50D (*Saccharophagus degradans* 2-40). Aga50D has a CBM-like domain at the N terminus fuses to an $(\alpha/\beta)_8$ barrel at the C terminus via α-helix coils. The

enzyme has two catalytic glutamates locate in a pocket tunnel-shaped active site (Pluvinage et al. 2013).

GH86 is also a member of clan A with an $(\alpha/\beta)_8$ barrel and two β-sandwich domains at the C terminus. Members of GH86 are β-agarase and β porphyranase with endo- or exo-hydrolytic retaining mechanism. An agarase from *Bacteroidetes plebeius,* BpGH86A, showed two catalytic glutamates in the middle of a long deep cleft-shaped active site (Hehemann, et al. 2012c).

GH96 is an α-agarase and GH118 is a β-agarase. Both enzymes have an inverting mechanism and are rarely found. Only their biochemical characteristics are available within the CAZY database without any structural information. Nine GH118s have been reported but only three have been characterized, AgaXa from *Catenovulum* sp. X3, AgaB from *Pseudoalteromonas* sp. CY24 and AgaC from *Vibrio* sp. PO-303 (Xie et al. 2012; Ma et al. 2006; Dong et al. 2006).

GH117 or α-neoagarobiose hydrolase (NABH) is the substantial enzyme for the conversion of agar disaccharides into the monomers through an inverting exo-α-hydrolytic action. Generally, an agarolytic bacterium has at least one GH117 (Hehemann et al. 2012a). This enzyme can be secreted extracellularly by Zobellia *galactanivorans* and *Bacillus* sp. MK03 (Rebuffet et al. 2011; Suzuki et al. 2002). It can also be produced in the periplasm by *Pseudomonas atlantica* (Day and Yaphe 1975). Marine bacteria *Cytophaga flevensis, Vibrio* sp. strain JT0107, and *S degradans* 2-40 produce a cytosolic NABH (Meulen and Harder 1976, Sugano et al. 1994; Ha et al. 2011). GH117 forms a homodimer structure, each consists of a fivefold-β-propeller catalytic domain with catalytic residues aspartate (base) and histidine (acid) (Ha et al. 2011; Hehemann et al. 2012a).

1.2.4. Agarolytic Pathway

The first agarolytic bacterium designated as *Bacillus gelaticus* was observed by Gran in 1902. New agar-degrading bacteria and fungi are continuously reported afterward dominated by marine *Bacteroidetes* and *Gammaproteobacteria* such as *Zobellia, Microbulbifer, Cellvibrio, Saccharophagus, Pseudoalteromonas,* etc (Michel et al 2006). Some others have been isolated from soil, freshwater, and human gut indicating a horizontal gene transfer from marine microorganisms (Hehemann et al. 2010; Song et al. 2016).

The agar degradation in bacteria had been proposed as an inducible pathway (Van der Meulen and Harder 1976; Furusawa et al. 2017). An agarolytic bacterium produces a basal amount of extracellular agarase consecutively as substrate-sensing machinery. When an appropriate substrate such as agar is available, the extracellular β-agarase hydrolyzes it and releases agar oligosaccharides such as neoagarooctaose (NA8), neoagarosehexaose (NA6), and neoagaraotetraose (NA4). Those molecules trigger the expression of cognate agarases to start the agarolytic pathway.

In general, the pathway involves the action of endo-agarases either β-or α-agarases to hydrolyze the agar polymer into neoagarooligosaccharides (NAOS) or agaroligosaccharides (AOS). The NAOS or AOS are converted further into the smallest repeating unit neoagarobiose or agarobiose (NA2) by exoagarases or β-galactosidases. The last step is the cleavage of α-1,3 linkages in NA2 by an α-agarase GH96 or neoagarobiose hydrolase (NABH) GH117 to release the monomers, D-galactose and 3,6 anhydro-L-galactose (Chi et al. 2012; Park et al. 2020).

Three agarolytic bacteria models have been studied extensively. They are a Flavobacteriia *Zobellia galactanivorans,* a Gammaproteobacteria *Saccharophagus degradans* 2-40, and an Actinobacteria *Streptomyces coelicolor* A3(2). Those models feature a combination of β- and α-agarases pathways. *Z.galactanivorans* performs agar degradation through serial actions of extracellular GH16, porphyranase, and NABH, while *S. degdradans* 2-40 and *S.coelicolor* A3(2) release extracellular GH16, GH50, and GH86 for agar degradation into NA2 and cytosolic GH117 for NA2 monomerization (Chi et al. 2012).

2. Materials and Methods

2.1. Materials

Chemicals and Reagents

Common chemicals, buffers, reagents, and microbiological media were obtained from Roth, Sigma Aldrich, or VWR except specifically mentioned. Neogarobiose, neoagarotetraose, neoagarohexaose, and neoagarooctaose were purchased from Qingdao BZ Oligo Biotech (China). Porphyran was purchased from Carbosynth (UK). Laminarin, κ-carrageenan, high molecular weight chitosan, and low molecular weight chitosan were products from Sigma Aldrich. *Gelidium* sp., *Gracilaria* sp., and *Ulva* sp. were harvested from Sayang Heulang Beach, Pamengpeuk, Garut, West Java, Indonesia in January 2018. The primers were listed in **Table 2.1**. (16S rRNA) and **Table 2.2**. (gene isolation).

Table. 2.1. 16S rRNA primers

Name	Sequence (5' – 3')	Position (*E. coli*)
TPU1 (27f)	AGAGTTTGATCMTGGCTCAG	8 – 27
TPU2 (forward)	CCARACTCCTACGGGAGGCA	334 - 353
RTU5 (reverse)	CCGTCAATTCMTTTRAGTTT	907–926
1492r	TACGGYTACCTTGTTACGACTT	1492 – 1513

Table 2.2. Primers for agarase genes isolation

Gene	Size (bp)	Restriction Enzyme	Primer Pairs	Plasmid & Size (bp)
agaA50	2313	BamHI/ EcoRI	F: 5'-ttttttggatccgagcagaaaggtggcgagactg-3' R: 5'-aaaaaagaattctcactcggcaggcttcacatcg-3'	pME1-8002
agaB50	2229	XhoI/ NsiI	F: 5'-ttttttctcgagctgctgtctgcctgtggtcagt-3' R: 5' aaaaaaatgcattcaatcatttttttgcccatagcgg-3'	pME2-7930
agaC50	2280	XhoI/ NsiI	F: 5'-ttttttctcgagaatgatgtccggtccacgattaca-3' R: 5'-aaaaaaatgcatttactctggcgccactgccaatt-3'	pME3-7981
agaD86T	1423	XhoI/ NsiI	F: 5'-ttttttctcgagccaaccgaagcccgtatttctgg-3' R: 5'-aaaaaaatgcatttattcacgggcgccgcgcac-3'	pME46-7123
agaE86	2103	XhoI/ NsiI	F: 5'-ttttttctcgagtccgcttcgcaagtaggcaacag-3' R: 5'- aaaaaaatgcatttagttgcgtacaggtacggtact-3'	pME6-7804
agaF16A	837	BamHI/ EcoRI	F: 5'-ttttttggatccgcggactgggatggcatcccg-3' R: 5'-aaaaaagaattcttaggagccgccaccggtcgcc-3'	pME9-6529

Bacterial Strain and Growth Condition

M. elongatus strain PORT2 was isolated from the surface seawater of coastal area Batu Karas Pangandaran, West Java Indonesia (7°45'0"S, 108°30'0"E). Seawater sample was taken using a sterile bottle, transported in a cold box, and processed for isolation using serial dilution on sterile KNO_3 agar media (yeast extract 1 g, KNO_3 0.2 g, agar 15 g, seawater 1 L, pH 8 ± 0.2). The colonies that formed a pit on the surface of the media were further purified using the streak plate method on sterile KNO_3 agar media. Incubation was performed for 24 to 48 h at 28 to 30 °C. Other media for maintenance of isolate or experiments were marine broth (Roth, Germany, Germany), Vattuone media (1975) (peptone 0.25 g; agar 0.2 g; K_2HPO_4 0.2 g; NaCl 3 g, H_2O 100 mL) or yeast extract agar (Hadm) (Roth, Germany) (tryptone 6 g, yeast extract 3 g, agar 15 g in 1 L modified artificial seawater; $NaSO_4$ 3.24 g; Na_2HPO_4 0.008 g; $FeSO_4.7H_2O$ 0.2 g; $CaCl_2.2H_2O$ 2.38 g; $MgCl_2.2H_2O$ 12.58 g; NH_4NO_3 0.016 g; $NaHCO_3$ 0.16 g; KCl 0.55 g; NaCl 25 g; 1 L H_2O) (modified from Difco, USA).

Escherichia coli DH5α and BL21 (DE3) were from New England Biolabs (NEB, Germany). *E. coli* Artic Express was from (Agilent Technology, Germany). They were maintained using Luria-Bertani (LB) media (tryptone 10 g; yeast extract 5 g; NaCl 10 g; H_2O 1 L; pH 7 ± 0.2) (Roth, Germany). All bacteria were also prepared as glycerol stock for -80 °C storage.

2.2. Methods

Isolate Characterization. The isolate was grown on a marine agar plate at 28 °C; 24 to 48 h. The growth was examined at temperatures of 4, 28, 30, 37, and 45 °C. Gram staining was performed according to the ASM protocol (Smith and Hussey 2005). Briefly, a small drop of sterile distilled water was put onto a glass slide. A single colony was spread onto a water drop, air-dried, and heat-fixed. The sample was then flooded with crystal violet reagent for one min, washed gently with distilled water, and air-dried for one min. A mordant reagent (gram's iodine) was spread onto the sample for one min and then washed gently with distilled water and air-dried. A decolorizing agent was spread on the sample until the running flow was clear, then air-dried. A counterstaining was spread onto the sample for one min, washed gently with distilled water, and air-dried for microscopic observation using

phase-contrast microscopy Axio Imager M1 (Zeiss, Germany) equipped with an HBO 100 light source. The observation parameters were Gram type and cell morphology. Cell motility and morphology were also observed using living cells. Sodium tolerance was measured at 30 °C using Vattuone medium (1975) without NaCl and marine broth (Roth, Germany) with the addition of NaCl into the final concentration of 8 and 10% w/v.

Assimilation tests were examined using the API NE20 test system (Biomerieux, USA) with modification. The API AUX media from the kit was diluted into the final concentration of 70% w/v sterile artificial seawater. The other procedure was performed according to manual instruction. The SIM media (sulfide, indole, and motility) was prepared using artificial seawater. A colony was stabbed into two-third of the medium and then incubated at 30 °C until the growth was visible. The H_2S production was indicated by a blackening along the stab line. The indole production was indicated by color change after Kovac's and negative motility by growth along the stab line. A catalase test was performed by putting a colony on a drop of 3% v/v hydrogen peroxide. Production of catalase was indicated by bubble formation. Oxidase test was performed by spreading the colony onto the oxidase strip (Microbiology Bactident oxidase, Merck). Production of cytochrome oxidase was indicated by purple color formation.

Single carbon utilization was examined using Vattuone media (1975) by replacing the organic protein with NH_4SO_4 and agar with other polysaccharides such as sodium alginate, κ-carrageenan, high molecular weight chitosan, low molecular weight chitosan, D-galactose, and D-glucose monohydrate. The agarolytic activity was assayed qualitatively by dispersing Lugol onto agar plate colonies. A clear zone formation indicated agarase activity.

Agar Extraction. Naturally grown macro algae were harvested from Sayang Heulang Beach. The algae were cleaned from sands and marine biota, air-dried for 2 days, washed trice with fresh water, and then sun-dried. For each sample, 5 g of dried-alga was washed with distilled water and then cut into smaller sizes using scissors. A 700 mL distilled water was added to the sample and incubated in a water bath at 95 °C for 6-8 h, then autoclaved at 121 °C for 15 min. The agar solution was filtered using Whatman paper grade 1. Two volumes of technical ethanol 99, 5% v/v were added into 350 mL of filtrates for agar precipitation in the cold room for

2 h. The filter was centrifuged at 8000 rpm for 30 min at 4 °C and concentrated using a rotary evaporator (Heidolph, Germany) at 40 °C for collecting the precipitate. The extract was freeze-dried, stored at -20 °C, and designated as an alcohol insoluble residue (AIR).

Analysis of 16s Ribosomal DNA. The isolate was grown on the marine agar plate for 24 h. A toothpick-single colony was dispersed in 10 µL sterile ultrapure water, heated at 95 °C for 10 min, and short-spined. Directly,1 µL of supernatant (10-50 ng genomic DNA) was mixed with 1x DreamTag green buffer (Thermo Fischer Scientific, USA), 10 mM of dNTPs, 25 µM of each universal primers for 16S rRNA (TPU1f and 1492r), 5U Dream Taq polymerase in a total volume of 50 µL. The 30 cycles-PCR condition for 16S rRNA was 95 °C, 5 min for initial denaturation; 95 °C, 2 min for denaturation; 50 °C, 1 min for annealing; 72 °C, 1 min for elongation; and 72 °C, 10 min for terminal elongation. The PCR amplicon was observed on 1% w/v agarose gel and sent for sequencing (GATC Biotech Eurofins Genomics, Germany).

The 16S rRNA sequence consensus was assembled and examined manually to resolve nucleotide conflicts on CLC Workbench 8.0. The sequence was compared with 16S rRNA databases such as EZbiocloud (https://www.ezbiocloud.net/), Ribosomal Database Project (RDP) (https://rdp.cme.msu.edu/), and NCBI databases (https://blast.ncbi.nlm.nih.gov/Blast.cgi). Mega X package was used for phylogeny analysis. Multiple sequence alignments were created using the Muscle algorithm. Phylogeny tree was constructed by using the maximum likelihood heuristic method with best-fit nucleotide substitution model Kimura 2 plus gamma distribution (G) and invariant sites (I) (K2+G+I); initial tree: neighbor-joining; 1000 bootstraps.

Genome extraction. PORT2 was cultured aerobically overnight in 10 mL of marine broth (Roth, Germany) at 30 °C, 180 rpm. The gDNA was extracted using the Wizard Genomic DNA Purification Kit (Promega USA) according to the manufacturer's protocol. The integrity of gDNA extract was assessed by using 0.8% w/v agarose gel electrophoresis and quantified using NanoDrop 1000 Spectrophotometer (Thermo Scientific, USA).

Genome Sequencing. PORT2 genomic sequencing library was constructed from 1 ng of gDNA with the Nextera XT DNA Sample Preparation Kit (Illumina, UK) according to the manufacturer's protocol. The library quality was controlled by analysis on an Agilent 2000 Bioanalyzer with Agilent High Sensitivity DNA Kit (Agilent Technologies, Germany) for fragment sizes of around 300-700 bp. Sequencing on a MiSeq sequencer (Illumina; 2x250 bp paired-end sequencing, v3 chemistry) was performed in the Genomics Service Unit (LMU Biocenter, Martinsried, Germany), resulting in 2.9 Mio raw reads. Raw reads were trimmed for quality (>Q20) and adapter sequences. De-novo assembly was performed using CLC Genomics Server 8.0 (Qiagen) with the following parameters: bubble size = 194, minimum contig length = 1000, word size = 21, perform scaffolding = Yes, auto-detect paired distances = Yes, mismatch cost = 2, insertion cost = 3, deletion cost = 3, length fraction = 0.5, similarity fraction = 0.8.

***In silico* agarase genes analysis**. The genome sequencing resulted in a draft genome with a size of 4,156,734 bp in 59 contigs or scaffolds and GC content of 57.6% without any extrachromosomal element. The N50 value of the contigs was 197,941 bp. The draft genome was submitted to the Microscope platform together with other *Microbulbifer* genomes from EZBiocloud and NCBI databases for comparative genome analysis and functional annotation. Genome quality was assessed using an integrated tool CHECKM analysis within the Microscope platform (Vallenet et al. 2017). The translated coding sequences output for agarases genes and proteins were further analyzed using several online platforms such as BLASTp against PDB and non-redundant protein database (nr) for pairwise comparison (https://blast.ncbi.nlm.nih.gov/Blast.cgi), Protparam analysis for calculation of protein physical and chemical properties (https://web.expasy.org/protparam/), and SignalP 5.0 for signal peptide prediction (http://www.cbs.dtu.dk/services/SignalP/). The abundance of carbohydrate-active enzymes within the genome was assessed using dbCAN meta server analysis (http://bcb.unl.edu/dbCAN2).

Agarases Genes Amplification and Transformation. Specific primers were designed to amplify the catalytic domain of agarase genes from the PORT2 gDNA together with the restriction site (**Table 2.2**.). The signal peptides were excluded to enhance intracellular heterologous-protein expression. The PCRs were performed

in 50 µL of PCR mixture mix composed of Q5 Taq polymerase (NEB, Germany) (3 U/µL), primer pair (10 µM of each), dNTPs (25 mM), and genomic DNA as a template (50-100 ng) (**Appendix 1., Table 1.1**). The PCR products were purified using the Qiaquick PCR Purification Kit (Qiagen) and cloned into pFO4 (a courtesy from Glycobiology Groups of Station Biology of Roscoff) using a standard ligation strategy with different combinations of *Xho*I-*Nsi*I-*Bam*HI-*Eco*RI (NEB, Germany).

Each plasmid encoding an N-terminal His_6 tag fused to agarase was transformed into *Escherichia coli* NEB5α cells (NEB, Germany). The cells were grown in LB media at 37 °C, 220 rpm. The positive clones were validated using *Hinc*II (NEB, Germany) mapping to verify the fidelity of the plasmid constructs. (**Appendix 1., Table 1.2.**). The plasmids were designated as pMEn (n: 1-9) (**Appendix 3**). After validation, they were transformed into *E. coli* BL21 (DE3) cells or Artic Express (Agilent Technology) for overexpression according to the manufacture's manual.

Protein Overexpression and Purification. Briefly, *E. coli* BL21(DE3) cells harboring the plasmid were cultured in 250 mL auto-induction media ZYP 5052 (Studier 2005) supplemented with ampicillin (100 µg/mL) for 48 h at 20 °C, 220 rpm.

For Artic Express expression, the *E.coli* was grown using LB media supplemented with ampicillin (final concentration 100 µg/mL) and gentamycin (final concentration 20 µg/mL) at 30 °C, 220 rpm until OD_{600nm} reached 0.7-0.8 and equilibrated at 10 °C for 10 min before the addition of 1 mM IPTG (final concentration). The cells then were incubated at 10 °C, 220 rpm for 24 h.

Unless specified, protein purification was always performed at 4 °C. The cells were harvested by centrifugation at 8000 g for 15 min and resuspended in cold lysis buffer (20 mM Tris HCl pH 8.0; 500 mM NaCl; 1 mM EDTA, 0.1% v/v Triton X-100, 5 mM $MgCl_2$) with fresh addition of DNAseI 10 mg/µL. The cell suspension was disrupted by sonication (LabSonic M Sartorius) (100% amplitude, 1 to 1 min/cycle) and then centrifuged at 12.000 g for 1 h. The soluble fraction was collected and loaded onto the HisTrap FF crude 5 mL column (GE, Germany) according to the manufacture's manual. The column was washed using buffer A (HEPES 50 mM pH 8, imidazole 10 mM, and 500 mM NaCl). The binding protein

was eluted using buffer B (HEPES 50 mM pH 8, imidazole 250 mM, 500 mM NaCl).

The quality of protein expression was checked on the SDS-PAGE 10% (w/v) using Coomassie brilliant blue R-250 gel staining (Laemmli 1970). Protein concentration was determined using the Rotinanoquant-Bradford method (Roth, Germany) with bovine serum albumin as a standard according to the manufacturer' manual and verified using nanodrop ((Thermo Scientific, USA) (equilibration buffer: HEPES 50 mM pH 7.5-8, imidazole < 0.05 mM, NaCl < 3 mM).

Enzyme Characterization. The enzymatic reaction of AgaB50 (final concentration was 2,5 µg/mL) and 375 µL of 0.2% (w/v) of agarose in KPi 50 mM pH 7 or AgaF16A (final concentration 1 µg/mL) and 390 µL of 0,2% w/v agarose in HEPES 50 mM pH 8 were performed at 50 °C for 20 min in a 400 µL system. The initial rate of each reaction was defined.

The reaction was stopped by adding dinitro salicylic acid (DNS) reagent (1% 3,5 dinitro salicylic acid; 0.2% phenol; 1% NaOH; 20% potassium sodium tartrate tetrahydrate, 100 mL dH_2O) (w/v) (Miller, 1959). The ratio of the DNS reagent to the sample was 1:1. The mixtures were incubated in 96 wells thermal cycler (Advanced Primus 96, Germany) at 98 °C for 10 min and 4 °C for at least 15 min and measured at 540 nm absorbance using 96 multiwells microplate reader (Tecan Infinite 200, Switzerland). The amount of reducing sugar in the sample was calculated using the D-galactose standard curve. The enzyme activity was measured from the increase of D-galactose concentration and reported from the slope value of the initial rate of reaction (µM/min) at a defined condition. One unit of enzyme activity was defined as the amount of enzyme that produced 1 µmol of D-galactose per minute at a defined condition. Appropriate enzyme and substrate controls were used during the experiment. All measurements were performed in triplicate.

The pH range was determined at buffer concentration 50 mM using sodium acetate (pH 4); KPi (pH 6-7.5); HEPES (pH 6-8): Tris (pH 9) and CAPS (pH 10). Temperature range and stability were measured at 20 to 80 °C. Preincubation 1 h at a certain temperature followed with incubation on ice for 5 min was used for measuring temperature stability. The enzymatic reaction was performed with the presence of a certain chemical to determine its influence on the enzyme activity.

The tested chemicals were β-mercaptoethanol (BME), dithiothreitol (DTT) (each final concentration 1 mM); $MgCl_2$ (1; 5; 10) mM, ethylenediaminetetraacetic acid (EDTA) (1 and 2.5) mM, NaCl (1; 5; 10; 150) mM; $CaCl_2$ (0.5 and 10) mM, KCl (1 and 10) mM; sodium dodecyl sulfate (SDS) (1 mM and 2.5% v/v) and glycerol (2.5% v/v.).

Characterization of AgaA50, AgaC50, and AgaD86T was performed using an artificial substrate *para* nitrophenyl β-D-galactopyranoside (β-*p*npg). The concentration of *p*-nitrophenol in the sample was monitored at 405 nm and calculated using the *p*-nitrophenol standard curve. The absorption coefficient (ε) of *p*-nitrophenol was defined specifically in each assay condition (Lieshout 2007).

The enzyme activity was measured from the increase of *p*-nitrophenol concentration and corrected from the non-enzymatic hydrolysis of β-*p*npg. It was reported from the slope value of the initial rate of reaction (μM/min) at a defined condition. Appropriate enzyme and substrate controls were used during the experiments. All measurements were performed continuously in triplicate using Cary 60 UV-Vis system (Agilent Technology).

Briefly, a 50 μL of a diluted enzyme (final concentration: 6 μg/mL for AgaA50; 18.4 μg/mL for AgaC50 and 74 μg/mL for AgD86T) was used for conversion β-*p*npg into p-nitrophenol and D-galactose in 1 mL system. Substrate concentration was adjusted accordingly, 1mM β-*p*npg for AgaA50, AgaD86T, and 0.1 mM for AgaC50. The sample minus enzyme was preincubated for 2 min at each reaction condition.

For each enzyme, the pH range was determined at buffer concentration 50 mM using sodium acetate (pH 5.1); HEPES (pH 6-8.6): Tris (pH 9.1) and CAPS (pH 10). Temperature range and stability were measured at 30 to 80 °C. Temperature stability was determined by measuring the activity after 1-h enzyme preincubation at a certain temperature followed by incubation on ice for 5 min. The effect of a certain chemical presence on the enzyme activity was tested using NaCl, $CaCl_2$ and $MgCl_2$, (each final concentration: 1 mM and 10mM); $NiSO_4.6H_2O$; $FeCl_3.6H_2O$, DTT (each final concentration 5 mm); EDTA 2.5 mM; SDS 0.5% v/v); and glycerol 0.25% (v/v). Kinetics parameters were defined for AgaA50 and AgaC50 using β-

*p*npg concentrations of (0; 1; 2.5; 5; 7.5; 10; 12.5; 15; 20) mM at pH 7; 60 °C and (0; 0.1; 0.25; 0.5; 1; 2; 5; 10) mM at pH 7.5, 50 °C, respectively.

Products and Substrate Specificity Analysis. Substrate specificity was examined in ultrapure water (milli-Q, Merck) at a concentration of 0.2% w/v for polysaccharides and 0.5 mg/mL for neoagaroligosaccharides. Agarose, agar kobeI, amylose, kappa-carrageenan, alcohol insoluble residue (AIR) of *Gracilaria* sp. (AIRG), *Gelidium* sp. (AIRS), and *Ulva* sp. (AIRU) were heated at 95 °C and kept at 50 °C for maintaining their water solubility before enzymatic reaction. Other substrates such as laminarin, porphyran, β-lactose monohydrate, sucrose, maltose, neoagarooctaose (NA8), neoagarohexaose (NA6), neoagarotetraose (NA4), neoagarobiose (NA2) were soluble in cold water. The NA8, NA6, NA4, NA2, D-glucose, and D-galactose were used as standards.

The products were analyzed using double ascending thin layer chromatography on precoated TLC sheet alugram 0.2 mm silica gel 60 (Macherey Nagel, Germany) with a solvent system: water:acetic acid:n-butanol (1:1:2) (v/v). Visualization of the spot was performed by short dipping in H_2SO_4 10% v/v in ethanol absolute and then dried with hot air at 150 °C for 5-10 min. The product was also analyzed using a high-performance liquid chromatography-refractive index detector (HPLC-RID) (Knauer, Germany) with the REZEX-RSO column (Phenomenex, Germany). This column can resolve oligosaccharides with a degree of polymerization of 1-20 (DP1-DP20). The mobile phase was isocratic ultrapure water (milli-Q, Merck) with a flow rate of 0.3 mL/min at 75°C, and the sample volume injection 20 µL. The EZChrom Elite software (Knauer, Germany) was used for data acquisition and processing.

Fourier Transform Infrared Spectroscopy (FTIR). FTIR spectra were recorded on an FTIR spectrometer Tensor II (Bruker, Germany) with an ATR unit. Background and sample spectra were recorded at resolution 4 cm^{-1}, scan time 32 times, and wavenumber range from 400 to 4000 cm^{-1}. Baseline correction and normalization of the spectra was performed using OPUS 7.5 software.

Protein Homology Modelling. The modeling was performed using an online platform SWISS model server (https://swissmodel.expasy.org/). The tool used BLAST and HHblits for template-target sequence identification and alignment analysis. It integrated ProMod-II and Modeller for a model built up. Model quality

parameters GMQE and QMEAN and their values were observed and recorded. The GMQE scored from 0 to 1 indicating the increase of the tertiary structure accuracy. Meanwhile, the QMEAN Z-score value represented global and local quality estimation based on statistical potentials of mean force. The score value between 0 to -4 indicated a good agreement between the model and template (Benkert et al. 2011; Bertoni et al. 2017). A PDB file of the best-recommended template and model of each enzyme was downloaded. Protein structure visualization, analysis, and comparison were performed using UCSF Chimera (Pettersen et al 2004).

Nucleotide Sequence Accession Number. All the gene sequences and draft genome were deposited in NCBI. The Draft genome of PORT had bioproject, biosample, and accession numbers PRJNA642745, SAMN15398149, and JACASI000000000, respectively. Meanwhile, the accession numbers for 16S rRNA, agaB50, agaF16, agaA50 and AgaC50 sequences were MH622756, MH996638, MH996639, MT682142 and MT682143 respectively.

3. Agarolytic Bacterium *Microbulbifer elongatus* PORT2

3.1. Results

Phenotypic Characterization of Isolate PORT2

PORT2 was identified as a non-sporulating gram-negative bacterium. Its ability to liquefy yeast extract agar (YEAas) was observed after 4 days of incubation at 30 °C (**Figure 3-1.a**). The bacterium was immotile (**Figure 3.1.b)**. The cell morphology was rods with 2-13 µm length, 0.8-1 µm width, and afterward became thin long-rods and coccoid (**Figure 3.1.c**). The cells formed aggregates in liquid minimal media culture (**Figure 3.1.d)**. Colonies on a marine agar plate were circular with 1-2 mm in diameter, crater form, entire edge, and smooth. After 48 h, the colony color was opaque on marine agar and mucoid-brownish on yeast extract agar-artificial seawater (YEAas) (**Figure 3.1.e**)

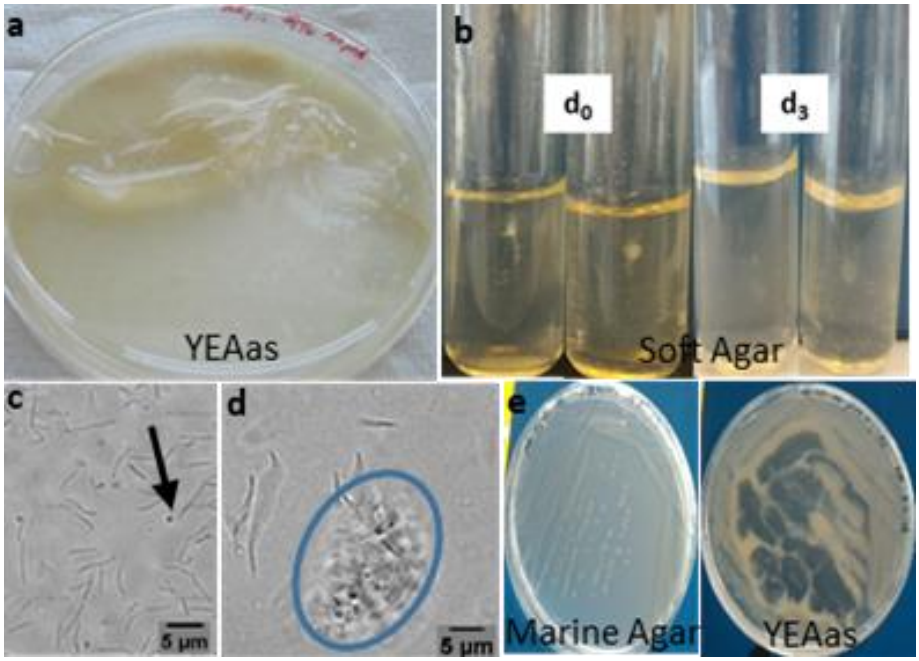

Figure 3.1. Growth characteristics of isolate PORT2: **a**) Yeast extract agar-artificial seawater (YEAas) plate liquefaction after 4 days incubation at 30 °C **b**) motility test in soft agar media; 30 °C (d_0: day 0 & d_3: day 3) **c**) cell morphology variation in marine broth at 30 °C, 48 h (coccoid cell *black arrow*) **d**) cell aggregates in glucose minimal media at 30 °C, 96 h (**e**) Morphologies of 48 h cultures (marine agar and YEAas). Microscopic magnification: oil immersion 10x100).

Growth occurred at a temperature between 28 to 37 °C and optimum at 30 °C. The growth existed at pH 6 to 8 and optimal at pH 8. PORT2 showed no growth on yeast extract agar media without NaCl or artificial seawater. It tolerated NaCl range from 2% to 10% (w/v). Besides Na^+, the bacterium also required, K^+, $Ca^{2+,}$ and Mg^{2+} for growth.

Nutrient assimilation and other biochemical properties of PORT2 were examined. The bacterium reduced nitrate to nitrite (denitrification) and gave positive catalase and oxidase reactions. PORT2 did not utilize L-arginine, urea, and gelatin. It produced neither indole nor H_2S when it was grown on SIM media (Sulfide, Indole, and Motility). The bacterium utilized esculin, ferric citrate, agar, alginate, chitosan, and κ-carrageenan. Rapid growth on agar and carrageenan was observed (**Figure 3.2**).

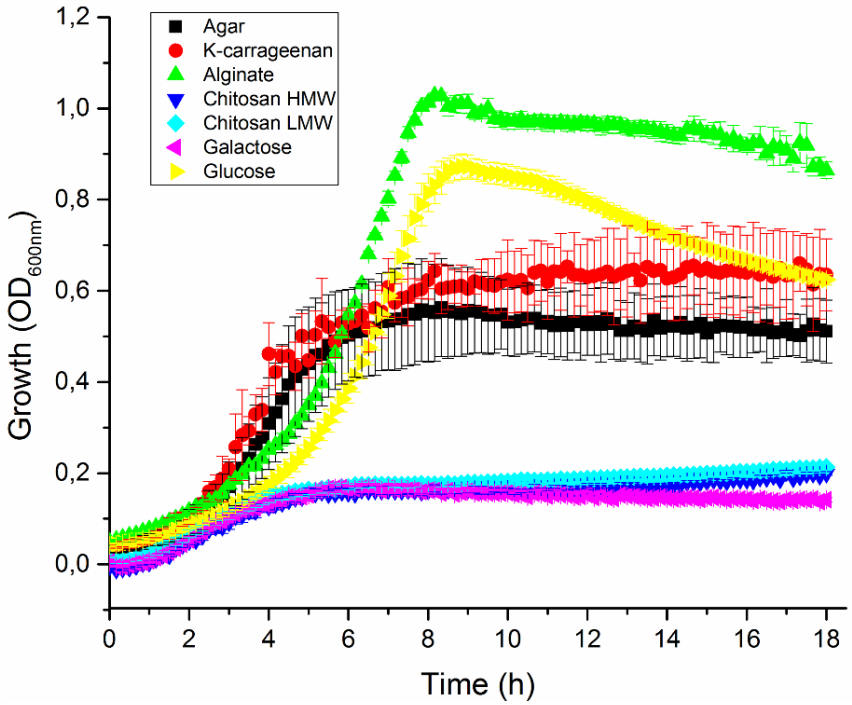

Figure 3.2. **Growth of PORT2 on different sole carbon source media indicates on the legend**. Growth condition: 30 °C; 220 rpm; Each medium was composed of: 0.2 g carbon source; 0.25 g NH_4SO_4, 0.2 g K_2HPO_4, 3 g NaCl, 100 mL dH_2O.

PORT2 demonstrated agar liquefaction during screening and maintenance indicated agarolytic activity. The colonies created craters on minimum agar media without any additional growth factor. PORT2 exhibited diauxic growth patterns and agarase production either in HAdm 0.3% w/v (yeast extract, agar 0.3% w/v in artificial seawater) or in soft agar media Vattuone (1975). Both media contained proteinous

substrates. Vattuone media facilitated more cell growth but not agarase production. The agarase production was detected after 10 h of incubation. It started with a low activity which continuously increased especially after the first stationary phase (**Figure 3.3.**).

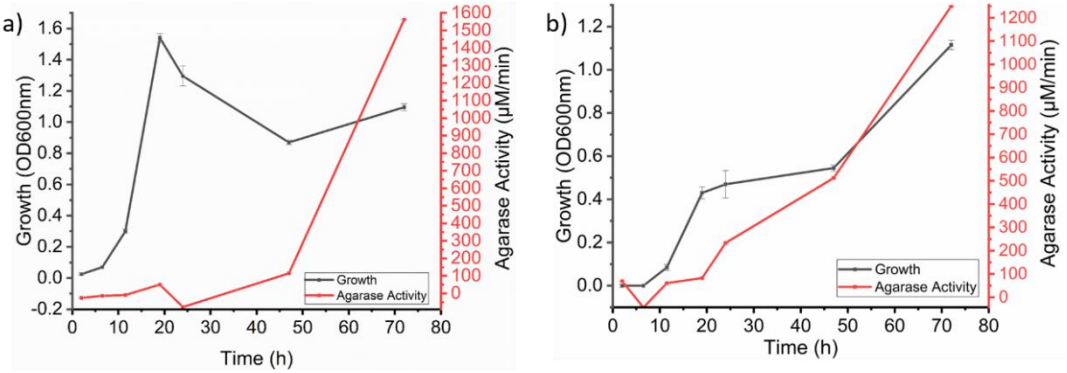

Figure 3.3. **Cell growth and agarase activity in different media.** a) Soft agar Vattuone b) YEAas 0.3%. Culture condition: 30 ºC, 72 h incubation, 150 rpm.

Molecular Identification and Determination

The 16S rRNA sequence assembly resulted in 1444 bp nucleotides length. The assembly also included corrections of two ambiguous nucleotides M366A and R943G according to the peak of electropherogram (M represented A or C; R represented A or G). Homologous searches revealed more than 96% pairwise similarity cut-off between PORT2 and *Microbulbifer* type strains especially *M. elongatus* (**Table 3.1**).

Table 3.1. The 16S rRNA pairwise similarity between PORT2 and *Microbulbifer* type strains

Rank	Name	Strain (Type)	Accession	Pairwise Similarity (%)	Authors
1	*M. elongatus*	DSM 6810	AF500006	99,5	Yoon et al. 2003
2	*M. salipaludis*	SM-1	AF479688	98,0	Yoon et al. 2003
3	*M. agarilyticus*	JAMB A3	AB158515	97,8	Miyazaki et al. 2008
4	*M. hydrolyticus*	DSM 11525	AJ608704	97,8	González et al. 1997
5	*M. aestuariivivens*	GHTF-23	KX982847	97,3	Park et al. 2017
6	*M. mangrovi*	DD-13	LZDE01000120	97,1	Vashist et al. 2013
7	*M. celer*	ISL-39	EF486352	96,2	Yoon et al. 2007
8	*M. yueqingensis*	CGMCC 1.10658	jgi.1076136	96,2	Zhang et al. 2012

The maximum likelihood tree showed a bootstrap value of 100 % indicated a strong monophyletic relationship between PORT2 and *M. elongatus* spp. (**Figure 3.4**).

Other analysis methods such as neighbor-joining and maximum parsimony also produced almost similar tree topology.

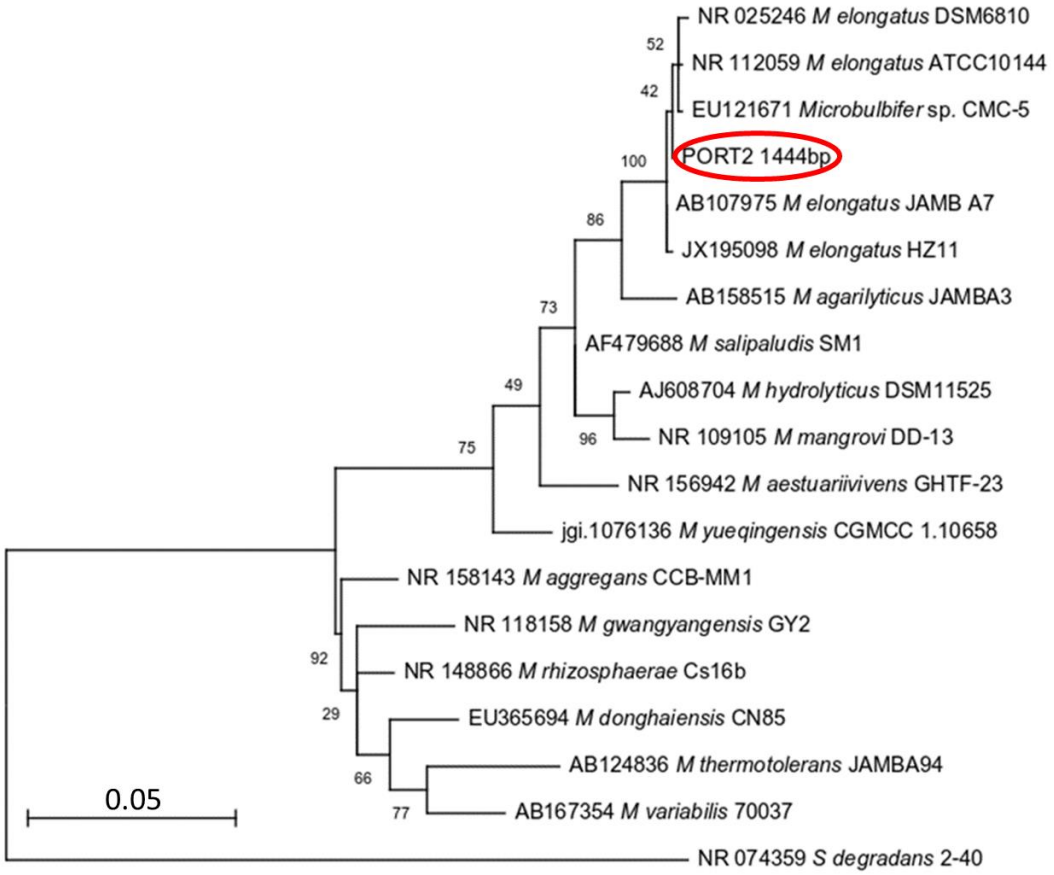

Figure 3.4. Maximum likelihood phylogeny tree of PORT2 based on partial 16S rRNA gene sequence. Numbers at branch points indicate the bootstrap value (%) of 1000 replications. *Saccharophagus degradans* 2-40 (Accession number NR074359) was used as an outgroup. The branch length indicates the expected number of nucleotide substitutions per 100 nucleotides.

Genome sequencing of PORT2 obtained 2.9 Mio raw reads with fragment sizes 300-304 bp. The assembly resulted in a draft genome sequence with a size of 4,156,734 bp in 59 contigs or scaffolds and GC content of 57.6 % without any extrachromosomal element. The N50 value was 197,941 bp. The genome completeness was 99% with 0.9% contamination assessed by CheckM analysis (Parks et al. 2015). It consisted of 3598 coding sequences (CDSs), a single set of gene operon 16S-23S-5S rRNA, 44 tRNAs for all standard amino acids, and 11 additional RNAs. These values were still feasible for genome annotation using the Microscope platform (Microscope team, personal communication).

PORT2 draft genome was also used to delineate the speciation more precisely. ANIblast+ analysis showed that PORT2 had 96.43% similarity to *M. elongatus*

DSM6810^T (not yet published); 85.66% to *M*. HZ11 and less than 80% to other *Microbulbifer* and agarolytic bacteria. *In silico* DNA-DNA hybridization (isDDH) also showed a higher similarity between PORT2 and *M. elongatus* DSM6810^T (68.9 to 93.2%) with a G+C% difference of 0.07 (**Table 3.2**).

Table 3.2. ***In silico*** **DNA-DNA hybridization between PORT2 and other agarolytic bacteria (Meier-Kolthoff et al. 2014)**

Microorganism	DDH Estimation (%) of PORT2			G+C % Difference
Reference	Formula 1	Formula 2*	Formula 3	
Microbulbifer donghaensis CGMCC_1.7063 ^{T}	12.5-18.9	19.7-24.4	13-18.4	2.13
Microbulbifer thermotolerans DSM19189 ^{T}	11.5-17.7	18.4-23.1	12.1-17.3	1.05
Microbulbifer variabilis 70037^T	10.8-16.9	19.1-23.8	11.5-16.7	8.73
Microbulbifer yueqingensis CGMCC_1.10658 ^{T}	12.3-18.7	19.4-24.1	12.9-18.2	4.45
Microbulbifer mangrovi DD131 ^{T}	20.9-27.9	20.6-25.3	20.1-26	0.42
Microbulbifer marinus CGMCC_1.10657 ^{T}	12.7-19.1	19.6-24.3	13.2-18.7	2.18
Microbulbifer agarilyticus S89	22.7-29.7	20.3-25	21.4-27.3	0.75
Microbulbifer HZ11	74.9-82.3	28.1-33	61.3-67.9	0.87
Microbulbifer elongatus DSM6810^T	87.6-93.2	**68.9-74.7**	87.5-92.4	**0.07**
Microbulbifer salipaludis Q7	24.7-31.7	21.1-25.8	23.1-29.1	0.79
Saccharophagus degradans 2-40	9.9-15.8	32.9-37.8	10.6-15.7	11.74
Zobellia galactanivorans DsiJ	9.8-15.8	16-20.5	10.6-15.6	14.79
Catenovulum agarivorans YM01	9.8-15.8	29.4-34.3	10.6-15.7	17.53

* Formula 1: length of all HSPs divided by total genome length
Formula 2: the sum of all identities found in HSPs divided by overall HSP length (Recommended for incomplete or draft genome)
Formula3: the sum of all identities found in HSPs divided by total genome length

A functional assignment of putative CDS was obtained from COG analysis (Tatusov et al. 2000). From 3598 CDS within the PORT2 genome, at least 2083 genes were classified into one Cluster of Orthologous Groups (COG) class. The CDSs overrepresented certain COG classes such as group E (Amino acid transport and metabolism), K (Transcription), C (Energy production and conversion), G (Carbohydrate transport and metabolism), M (Cell wall/membrane/envelope biogenesis), and P (Inorganic ion transport and metabolism). Seven percent of the CDSs on PORT2 were classified within group S for unknown function (**Figure 3.5**). The AgaE86, AgaF16 was positioned within clusters U and G, respectively. On the other hand, the other agarases AgaA50, AgaB50, AgaC50, and AgaD86 were not clustered into any COG categories of the COG database.

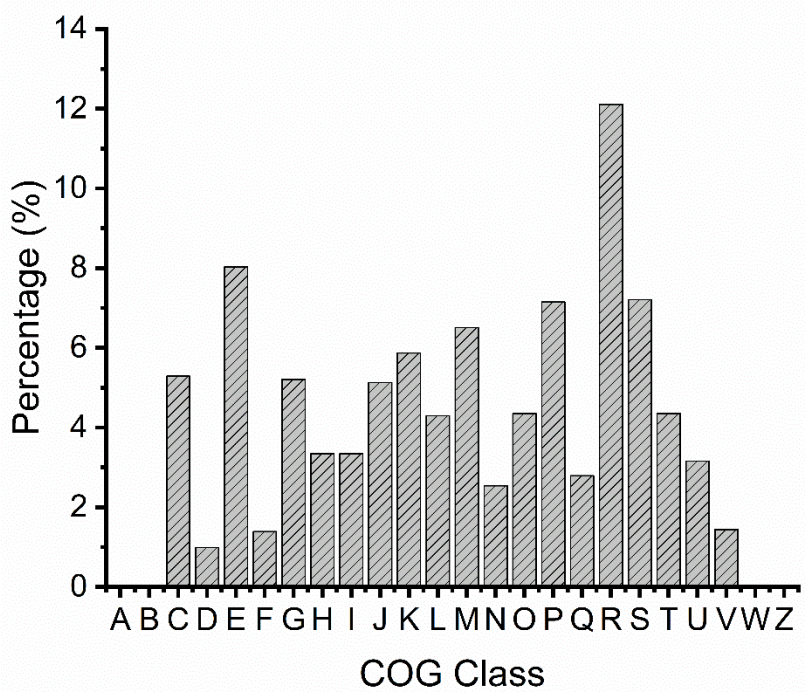

Figure 3.5. Distribution of PORT2 coding sequences (CDS) in each Cluster of Orthologous Groups (COG) to delineate genes function. COG categories: A (RNA processing and modification), B (Chromatin structure and dynamic), C (Energy production and conversion), D (Cell cycle control, division, chromosome partitioning), E (Amino acid transport and metabolism), F (Nucleotide transport and metabolism), G (Carbohydrate transport and metabolism), H (Coenzyme transport and metabolism), I (Lipid transport and metabolism), J (Translation, ribosomal structure, and metabolism), K (Transcription), L (Replication, recombination, and repair), M (Cell wall/membrane/envelope biogenesis), N (Cell motility), O (Posttranslational modification, protein turn over, chaperones), P (Inorganic Ion transport and metabolism), Q (Secondary metabolites biosynthesis, transport, and catabolism), R (General function only), S (Function unknown), T (signal transduction mechanisms), U (Intracellular trafficking, secretion, and vesicular transport), V (Defense mechanisms), W (Extracellular structures).

Genome annotation delineated central carbohydrate metabolism pathways in PORT2. The pathways consisted of the tricarboxylic acid cycle (TCA), pentose phosphate, glyoxylate, De-Ley Doudoroff, and Embden-Meyerhof-Parnas pathways. The Entner-Doudoroff (ED) pathway was assigned as a galactose metabolism pathway in PORT2. Concomitantly, carbohydrate transportation systems such as the phosphotransferase system, ATP-dependent ABC-type sugar transport system, the permease system, and H^+ symport mechanisms were also recognized. Type II and Type V secretion systems for protein transport from the cytoplasm to other compartments or environment or cells were also depicted. The bacterium also encoded genes for aerobic respiration and anti-oxidative stress, such

as glutathione reductase (GoR), superoxide dismutase (SOD), catalase (CAT), and peroxidase (POD).

Moreover, candidate genes for nutrient acquisition in the marine environment were also found. Sulfur assimilation was indicated by sulfatases and sulfate reduction I pathway. An acid phosphatase pathway regulation was depicted for phosphate acquirement during oxidative stress and/or from the phosphate-salvage environment. Osmolyte production was indicated by the ectoine biosynthesis pathway. The annotation also displayed PORT2 capability to degrade marine polysaccharides such as chitin, carrageenan, porphyran, and agarose.

3.2. Discussion

The coastal area provides various niches for a wide range of heterotrophic bacteria, from marine to freshwater species. Most agarolytic activities have been derived from marine bacteria or their symbionts but soil and gut bacteria also can acquire the capability through horizontal gene transfer (Hehemann et al. 2010; Temuujin et al. 2012). Native marine bacteria can be distinguished from others due to their specific nutrient requirements and adaptation.

PORT2 genome annotation reveals the presence of several genes that regulate specific adaptation capability to the marine environment. Metabolic pathways such as osmolyte biosynthesis, cell protection against the UV radiation and complete pathway for adaptation to sulfate, low iron, and phosphate availability are depicted (Zhao et al.. 2019; Perez et al. 2017; de Villegas 2007; Yoseph et al. 2010; Hide and Kong 2010; Tostevin et al. 2014). Basic metabolism and physiological functions of PORT2 as marine bacterium are also indicated by COG clusters. The high percentage of putative functional genes belong to the amino acid transport and metabolism (E), carbohydrate transport and metabolism (G) and inorganic ions transport and metabolism (P) classes may suggest the innate competition and survival capacities of PORT2 in the marine environment (Lauro et al .2009; Cobo-Simón and Tamames 2017).

However, most agarase families such as GH50 and GH86 families have not been classified into any COG categories within the COG database, except for GH16 that is classified to G category for carbohydrate transport and metabolism. The classification of AgaE86 into category U (Intracellular trafficking, secretion, and

vesicular transport). The categorization of a gene or protein into a COG is derived from pairwise sequence similarity of at least three different lineages that show a consistent pattern of best hit (BeT) (Tatusov et al. 1997). Indeed, carbohydrate-active enzymes include agarases have huge diversities and most of them have not been accommodated or included in the COG database.

Moreover, PORT2 demonstrates growth in minimal media made from seawater and has clear sodium and potassium dependency. The requirements confirm the identity of PORT2 as a native marine bacterium. In agreement with these results, Mac Leod et al. (1954) have found that marine bacteria are distinguishable from other bacteria due to their capacity to survive and grow in seawater. Sodium and potassium are required by marine bacteria to maintain cell wall structure and nutrient transport while Ca^{2+} and Mg^{2+} can be optional. Sodium-membrane transporter allows marine organisms to grow faster within ecological pressures (Hobbie 1988).

PORT2 shows phenotype and biochemical characteristics typical of marine gram-negative bacteria. Considering the absence of chemotaxonomy data, the classification of PORT2 based on morphological taxonomy is quite challenging. Meanwhile, species conception in bacteria delineates < 97% of 16S rRNA homology similarity and DNA reassociation value < 70% (Stackebrandt and Goebel 1994). Therefore, the 16S rRNA of PORT2 was sequenced as the initial step to infer the taxonomy identity of PORT2. The 16S rRNA cladogram demonstrates a monophyletic relationship between PORT2 and *Microbulbifer elongatus*, which indicated a common ancestry. Moreover, PORT2 draft genome size and GC content also fall within the range of *Microbulbiferaceae* (Genome size 4.1 - 4.8 Mb; GC content 57.1±0.8%) (Sun et al. 2014; Imran et al. 2017). The results become more evident when comparing the PORT2 genome to the available *Microbulbifer* genomes. *In silico* ANI and DDH reveal the same species relationship between PORT2 and *Microbulbifer elongatus* DSM6810. However, subtle differences for PORT2 are recognized such as immotility, higher salt tolerance, and the inability to use gelatin or produce H_2S. Biochemical characteristics of isolate PORT2 in comparison with other *Microbulbifer* type strains are summarized in **Appendix 2**. Hence, all results suggest PORT as new sub-species of *M.elongatus* with detailed classification: **Domain**: Eubacteria; **Phylum**: Proteobacteria; **Class**: Gammaproteobacteria; **Ordo**: Cellvibrionales;

Family: Microbulbiferaceae; **Genus**: *Microbulbifer;* **Species**: *Microbulbifer elongatus* strain PORT2.

Previously, three strains of *M. elongatus* had been reported; JAMB-A7; CMC-5, and HZ11. They are isolated from various niches such as deep-sea, seaweed decomposition, seawater, and capable to degrade marine polysaccharides (Ohta et al.. 2004b; Jonnadula 2011; Sun et al.. 2014). Formerly, *Microbulbifer elongatus* was designated as *Pseudomonas elongate* by having typical *Pseudomonad* phenotypes: gram-negative, motile with polar flagella, aerobic, rod-shaped and classified as a member of *Pseudomonads* subgroup V. An extensive study involving several approaches: polyphasic, chemotaxonomy, DNA-DNA hybridization, 16S rRNA analysis reclassified *P.elongata* into a new species namely *Microbulbifer elongatus* with type strain species ATCC 10144^T /$DSM6810^T$ /$LMG2182^T$ (Anzai et al. 2000; Yoon et al. 2003).

Microbulbifer is copiotroph marine Gammaproteobacteria that occupy nutrient-rich niches such as marine snows. Copiotroph bacteria are polymer degraders with feast and famine lifestyles (Spring et al.. 2005; Arnosti 2010; Wakabayashi et al.. 2012; Arnosti 2014). In correlation with the lifestyle strategy, most of the characterized *Microbulbifer* including PORT2 display cell cycle pleomorphism by adjusting cell shape/size ratio. Pleomorphism has been considered as a particular bacterial adaptational strategy during nutritional or environmental change or stress (Huang et al.. 2008; Nishijima et al.. 2009; Wakabayashi et al.. 2012). Even though *Microbulbifer* genus is known as polymer degraders, their carbohydrate-active enzyme capabilities differ. *M. donghaiensis, M. yueqingensis, M. aggregans, M. marinus,* and *M. variabilis* are non-agarolytic and unable to degrade agar (Nijishima et al.. 2009; Zhang et 2012; Moh et al.. 2017). On the contrary, *M. elongatus*, *M. salipaludis, M. mangrovi, M agarilyticus*, *M. pacificus* LD25, and PORT2 can degrade and utilize agar as a carbon source (Yoon et al.. 2003; Imran et al.. 2017; Oh et al.. 2011; Chen at al 2015).

The PORT2 substantial capability in agar degradation marks with liquefaction activity. PORT2 can utilize not only agar but also a wide range of complex marine polysaccharides as a sole carbon source. Experimentally, PORT2 shows a preference for rich-nutrient media for higher agarase production. The agarolytic activity was considerably high in the second phase of biphasic growth indicates that

agar probably is not the main carbon source for the bacterium at the rich-nutrient condition and the agarase system is inducible. A similar result also has been observed by Furusawa et al. (2017). They have found that *Persicobacter* sp. CCB-QB2 also exhibits diauxic growth in the presence of tryptone and agar. The bacterium also displays high agarolytic activity at the second growth phase. Different from *Persicobacter* sp. CCB-QB2, PORT2 prefers yeast extract than tryptone for triggering higher agarase synthesis or activity.

The inducibility of the agarase system is proposed by Van der Meulen and Harder (1976). They observe that the casamino acids trigger higher agarase synthesis in *Cytophaga flevensis*. In particular, agar oligosaccharides induce consecutive agarase production while galactose and glucose repress it. Their experiment also reveals that *C. flevensis* produces a perpetual extracellular agarase at basal metabolism.

Overall, it can be concluded that PORT2 is a new strain of *M. elongatus*. It is the first agarolytic marine bacterium from the Indonesian coastal area that has been isolated and characterized further. The *in silico* exegesis of the PORT2 agarolytic system will be explained further in the next chapter.

4. Genome Profiling for *In Silico* Elucidation of the Agarolytic System

4.1. Results

Agarases Annotation and *In Silico* Characterization

In recent years, computational approaches have been used extensively for *in silico* identification of key genes and gene clusters involved in certain metabolism pathways. The generated data establish a starting point for investigating gene functionality experimentally.

The annotation of the draft genome of PORT2 indicated the presence of six agarase genes located at two different contigs in PORT2. BLASTp analysis against protein structure database (PDB) and non-redundant protein database (nr) at NCBI informed gene similarity and the possible identity of each gene (**Table 4.1**). The annotation also depicted other putative genes encoded hypothetical proteins, sugar transporter and regulatory system, D-galactose, and 3,6 α-anhydro-L-galactose utilization in the vicinity of agarase genes (**Figure 4.1**).

The analysis specified the agarase genes into three different glycoside hydrolase (GH) families; GH16, GH50, and GH86. Two agarase genes encoded GH50 agarases at contig 34 were designated as 341 or agaA50 and 342 or agaB50. The agaA50 was separated from agaB50 by 443 bp of nucleotides. The other four agarase gene were located at contig 45. One agarase gene was designated as 451 or agaC50 also encoded GH50. Two other genes encoded GH86 agarases were designated as 452 or agaD86 and 453 or agaE86. The last gene was designated as 454 or agaF16 encoded GH16 agarase.

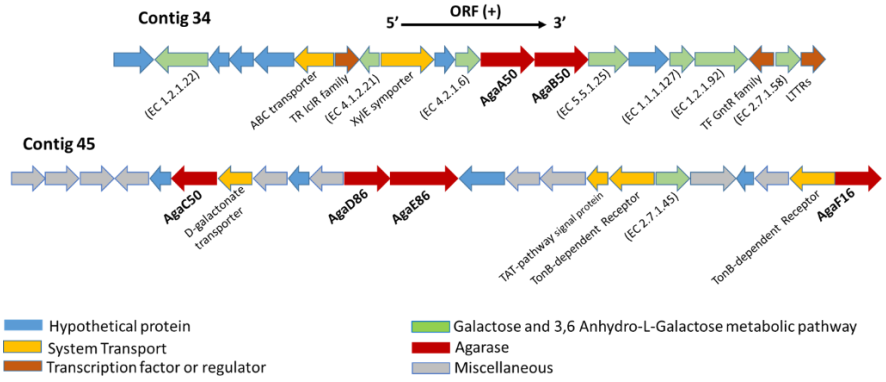

Figure 4-1. **Schematic agarase genes and the intervening genes within the *M. elongatus* PORT2 genome**. Agarase (*red); c*ell transport system (*beige*); galactose and 3,6-α-L-anhydrogalactose metabolism (pale *pink*); hypothetical protein (*gold*); miscellaneous functions (*blue*).

SignalP and Protparam analysis predicted the physical and chemical properties of PORT2 agarases (**Table 4.1**). The enzymes showed theoretical pI between 4.37-4.99; GC content of 53 to 59%; aliphatic index (AI) between 63.07 to 74.08 and instability index (II) between 24.40 to 39.39. AgaF16 showed the lowest II value 24.40 and AgaE86 had the highest II value 39.39.

Table 4.1. Theoretical properties of PORT2 agarases

Protein (aa/bp)	Signal Peptide		CAZY Family	Protparam analysis	Similarity (NCBI-PDB)
	I	II			
AgaA50 (802)	-	√ (aa29-30)	GH50	Theoretical size: 89.9 kDa pI: 4.8 GC (%): 55 Start Codon: ATG Stop Codon: TGA Aliphatic index: 71.66 Instability index: 31.31 (stable)	Aga50D *Saccharophagus degradans* 2-40 (E-val=0.0; Query cover: 92%; % identity: 55%)
AgaB50 (769)	-	√ (aa31-32)	GH50	Theoretical size: 82.5 kDa pI: 4.84 GC (%): 57.4 Start Codon: GTG Stop Codon: TGA Aliphatic index: 71.86 Instability index: 33.59 (stable)	Aga50D *Saccharophagus degradans* 2-40 (E-val=0.0; Query cover: 91%; % identity: 45%)
AgaC50 (781)	-	√ (aa20-21)	GH50	Theoretical size: 87.7 kDa pI: 4.99 GC (%): 53 Start Codon: ATG Stop Codon: TAA Aliphatic index: 74.08 Instability index: 33.69 (stable)	Aga50D *Saccharophagus degradans* 2-40 (E-val=0.0; Query cover: 93%; % identity: 52%)
AgaD86 (809)	-	√ (aa21-22)	GH86	Theoretical size: 87.7 kDa pI: 4.99 GC (%): 54.9 Start Codon: ATG Stop Codon: TAA Aliphatic index: 74.08 Instability index: 33.69 (stable)	GH86 *Bacterides uniformis* (E-val=0.0; Query cover: 93%; % identity: 52%)

Table 4.1. Theoretical properties of PORT2 agarases (continued)

Protein (aa/bp)	Signal Peptide		CAZY Family	Protparam analysis	Similarity (NCBI-PDB)
	I	II			
AgaE86 (1369)	√ (a29-30)		GH86	Theoretical size: 147.4 kDa pI: 4.37 GC (%): 56.4 Start Codon: ATG Stop Codon: TAA Aliphatic index: 63.07 Instability index: 39.39 (stable)	GH86 β porphyranase *Bacterides plebeieus* (E-val=1e-35; Query cover: 49%; % identity: 23.6%)
AgaF16 (597)	√ (aa19-20)	-	GH16	Theoretical size: 63.9 kDa pI: 4.52 GC (%): 59 Start Codon: ATG Stop Codon: TGA Aliphatic index: 66.35 Instability index: 24.40 (stable)	Chain A- agarase *Microbulbifer thermotolerans* JAMB-A94 (E-val=0.0; Query cover: 46%; % identity: 86.8%)

The putative agarases exhibited varied gene modularity from simple to complex (**Figure 4.2**). The GH50 agarases depicted simple gene structures consisted of a lipoprotein signal peptide II (SPII) and an agarase domain. The SPII was located at the beginning of the N terminus with glycine at position +2 before amino acid terminal cysteine at the cleavage site. In contrast, agaE86 and agaF16 presented modular complexities by having a signal peptide I (SPI), agarase domain, and more than one carbohydrate-binding modules (CBMs) interconnected by a glycine-serine linker with different length. The SPIs were also located at the beginning of the N terminus and showed a conserved motif of (A-X-A) at position -3 and -1 from the cleavage site. While agaD86 complexity laid in between by having an SP II and an agarase domain fused with an unknown domain.

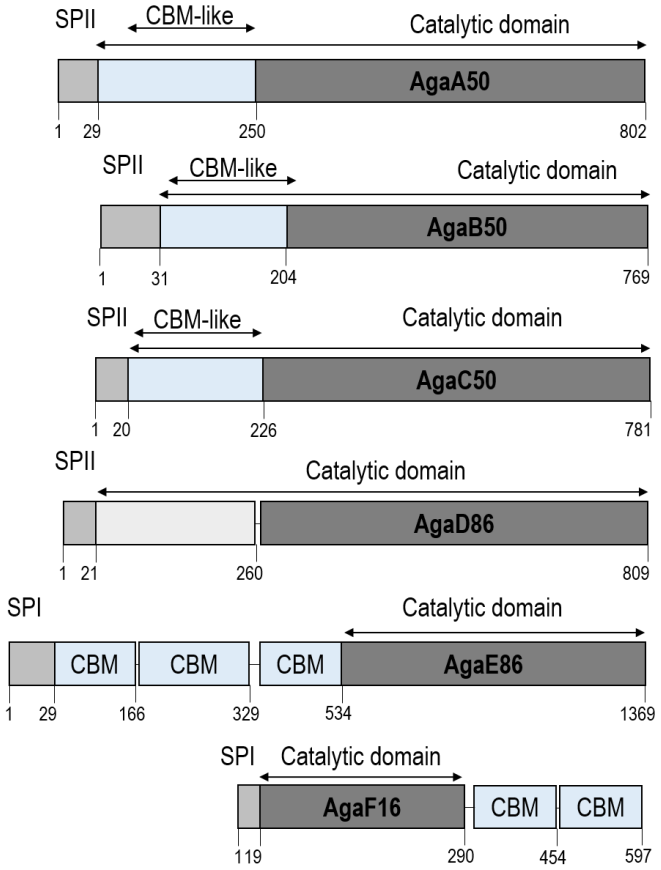

Figure 4.2. Agarase genes modularity in *M. elongatus* PORT2. Agarase domain (*dark gray*); carbohydrate-binding module (CBM) (*light blue*); signal peptide I or II (SPI or SPII) (*medium gray*). The numbers below represent nucleotides.

The agaA50 and agaF16 had a unique motif upstream of the genes. Three-adenine preceded the putative Shine-Dalgarno motif (ACGAG) of the agaA50 gene. This motif had been proposed to stipulate stronger ribosomal protein S1 binding on the ribosomal binding site (RBS). The agaF16 had an adenine cytosine-rich region preceding the Shine–Dalgarno motif (AGGAG). Both motifs indicated a high protein translation event (Boni et al 1991; Laursen et al 2005).

Among PORT2 agarases, only agaB50 had more than one possible functional agarase ORFs. CLC software 7.3 identified several possible start codons and RBS. Some start codons were canonical (AUG, GUG, UUG) and one was not (AUU). A contiguous putative signal peptide II-agarase domain modularity was determined using the longest ORF (**Figure 4.3.**).

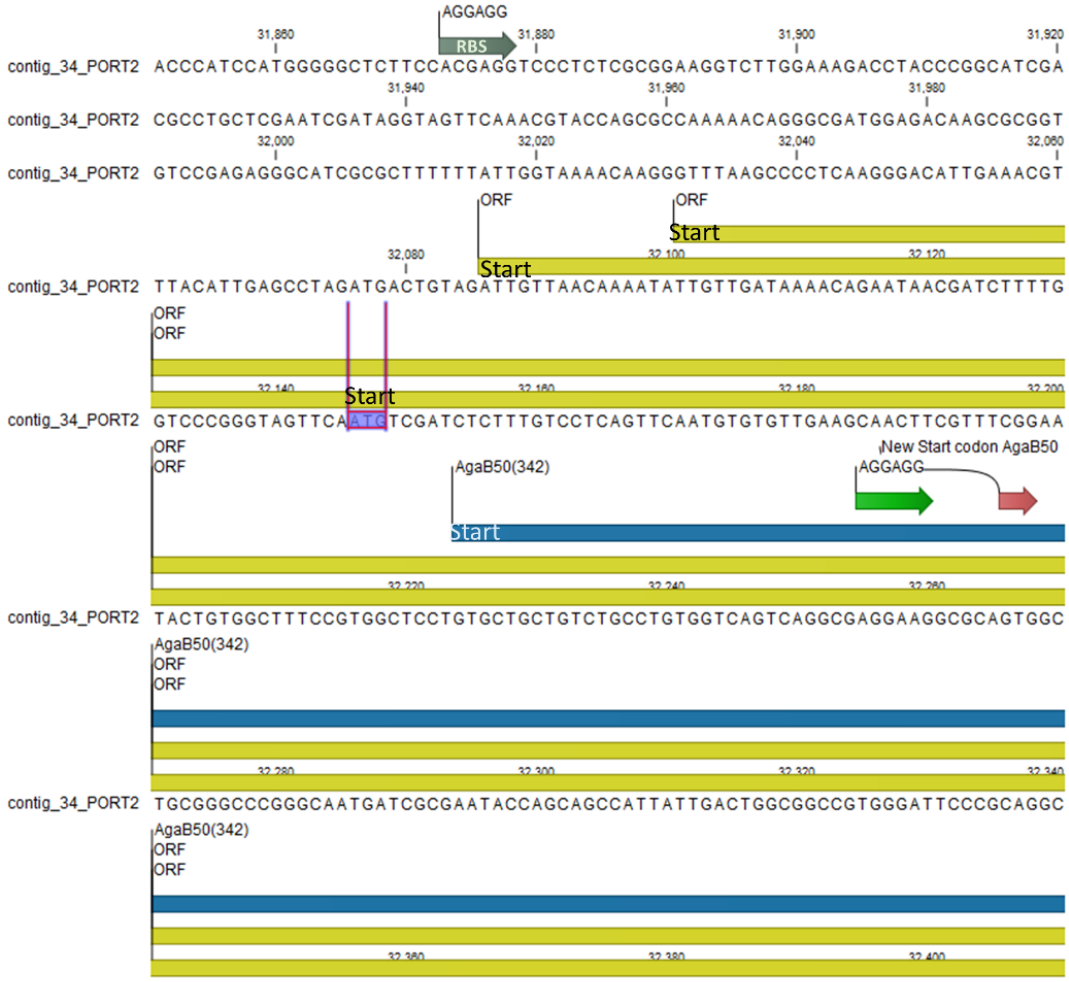

Figure 4.3. **Open reading frame (ORF) analysis of agaB50**. Annotated agaB50 on CLC Main Workbench 7 (*yellow bar*); RAST genome annotation (*Blue bar*); ribosomal binding site (RBS) (*green arrow*).

Carbohydrate Active Enzymes (Cazymes) Abundance

The dbCan analysis suggested the presence of other putative carbohydrate-active enzymes within the genome of PORT2. Besides agarases families, the bacterium also encoded 66 carbohydrate-binding modules (CBMs) and other 151 carbohydrate-active enzymes (cazymes) families consisted of 56 glycoside hydrolases (GHs), 26 glycoside transferases (GTs), 24 polysaccharide lyases (PLs), 28 carbohydrate esterases (CEs), and 17 redox enzymes with auxiliary activities (AAs). The analysis also indicated that PORT2 and other agarolytic *Microbulbifers* encoded more glycoside hydrolases and polysaccharide lyase than non-agarolytic *Microbulbifer*. In comparison to other agarolytic Gammaproteobacteria such *as Catenovulum agarivorans* YM01 and *Saccharophagus degradans* 2-40, genus *Microbulbifer* spp. showed fewer cazymes abundance (**Figure 4.4.**).

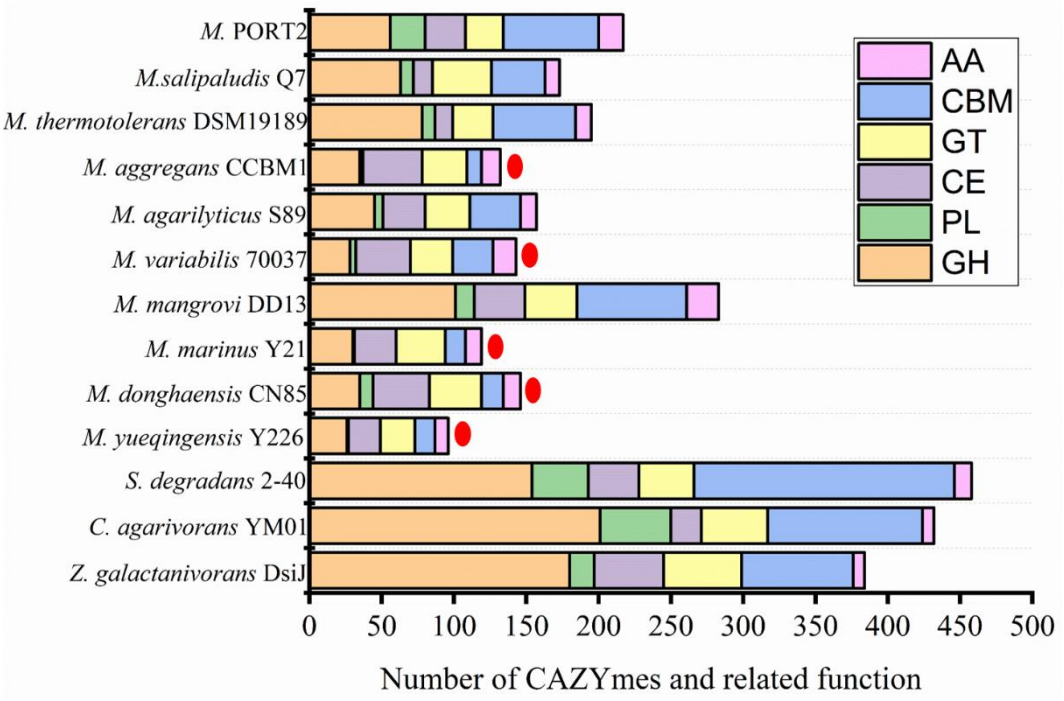

Figure 4.4. Cazymes abundance within *M. elongatus* PORT2 and other marine agarolytic bacteria. Non-agarolytic *Microbulbifer* (*red dot*). (abbreviations: CBM=carbohydrate binding module; AA=auxiliaries activity: CE=carbohydrate esterase; PL=polysaccharide lyase; GT=glycoside transferase; GH=glycoside hydrolase; C. represents *Catenovulum*; Z for *Zobellia*; S for *Saccharophagus*; and M for *Microbulbifer*.

Some glycoside hydrolase (GH) indicated prevalent occurrence in every *Microbulbifer* species such as GH6, GH13, GH16, GH19, GH23, GH28, GH31, and GH103 (**Table 4.2**). On the other hand, some GH indicated species-specificity regardless of the agarolytic capability (**Table 4.3**). In particular, two β-agarases families, GH50 and GH86, existed only in agarolytic *Microbulbifer*. Commonly, agarolytic bacteria also encode GH96 or GH117 for the cleavage of α-glycosidic bonds in agar. However, gene synteny comparison did not reveal the presence of any GH96 or GH117, neither in PORT2 nor in other *Microbulbifer* spp. (**Figure 4.5**).

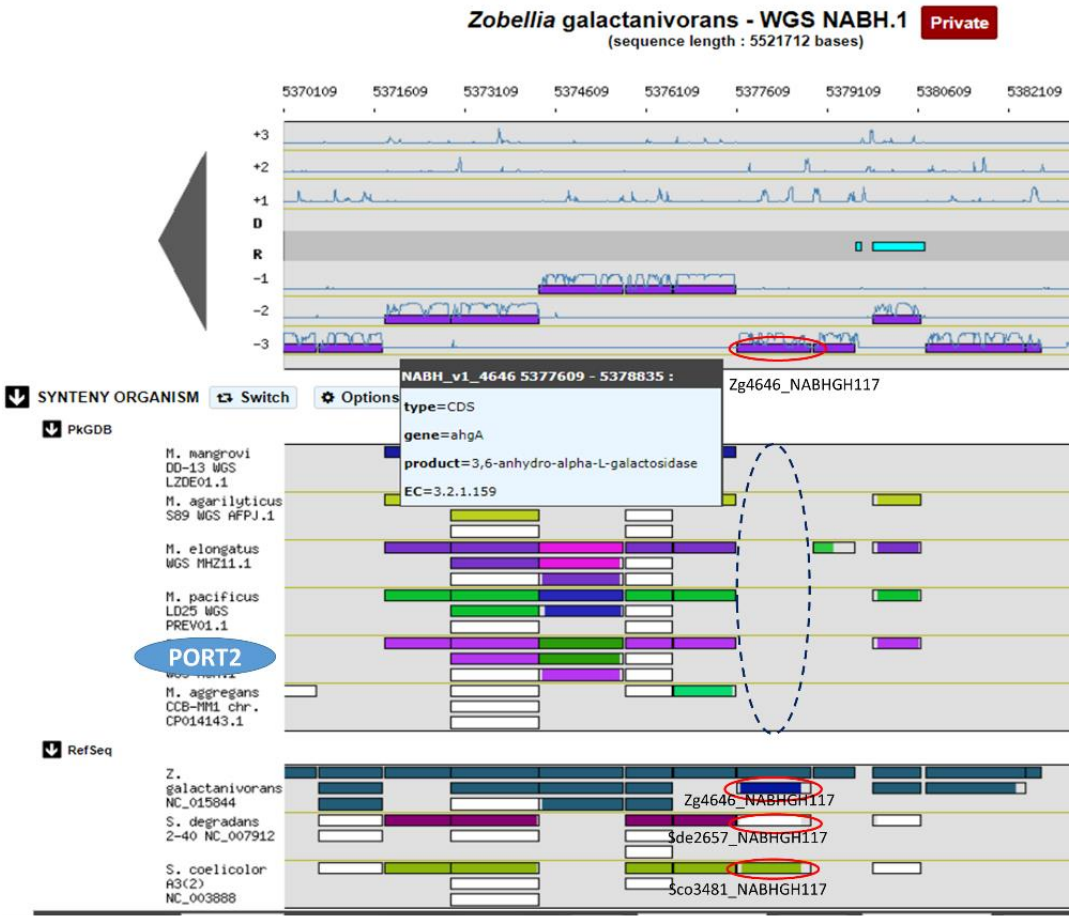

Figure 4.5. Gene synteny comparison for localization of neoagarobiose hydrolase (NABH-GH117) in *M. elongatus* PORT2. Reference genomes (*red ellipse*): *Zobellia galactanivorans* (Zg); *Saccharophagus degradans* (Sd); *Streptomyces coelicolors* (Sco); PORT2 and other *Microbulbifer* species (*dark blue ellipse*).

Table 4.2. Prevalent glycoside hydrolases in genus *Microbulbifer* spp. and other agarolytic bacteria

No	Species	Source of isolate	Common GH								Reference
			GH6	GH13	GH16	GH19	GH23	GH28	GH31	GH103	
1.	M.*pacificus* LD25	Hot saltspring	endoglucanase	α-amylase	xyloglucanase, etc	chitinase	lysozyme	α-L-rhamnosidase	α-galactosidase	Peptidoglycan lytic trasnglycosilase	Chen et al (2015)
2.	*M. salipaludis* Q7	Sea cucumber									Yang et al (2018)
3.	*M. agarilyticus* S89	Deep-sea									Oh et al (2011)
4.	*M. mangrovi* DD3	Mangrove sediment									Imran et al (2017)
5.	*M. thermotolerans* DSM19189	Deep sea									Miyazaki et al (2008)
6.	*M.* PORT2	Seawater									This study
7.	*M. marinus* CGMCC1.10657	Sediment bay									Zhang et al (2012)
8.	*M. yueqingensis* CCGMC 1.10658	Sediment bay									Zhang et al (2012)
9.	*M. aggregans* CCBM1	Estuarine sediment									Moh et al (2017)
10.	*M. variabilis* 70037	Surface of algae									Imamura et al (2019)
11.	*S.degradans* 2-40	Surface of salt marsh									Ekborg et al (2005)
12.	*C. agarivorans* YM01	Seawater									Yan et al (2011)
13.	*Z.galactanivorans* Dsij	Surface of algae									Barbeyron et al (2001)

M. = Microbulbifer
S. degradans = Saccharophagus degradans
C. agarivorans = Catenovulum agarivorans
Z. galactanivorans = Zobellia galactanivorans

Table 4.3. Specialized glycoside hydrolases (GH) in genus *Microbulbifer* spp. and other agarolytic bacteria

No	Species	Source of Isolate	GH family														
			4	16**	26	30	32	46	50*	64	81	86*	95	109	115	130	145	146
1.	*M.pacificus* LD25	Hot saltspring																
2.	*M. salipaludis* Q7	Sea cucumber																
3.	*M. agarilyticus* S89	Deep sea																
4.	*M. mangrovi* DD3	Mangrove sediment																
5.	*M. thermotolerans* DSM19189	Deep sea																
6.	*M.* PORT2	Seawater																
7.	*M. aggregans* CCBM1	Estuarine sediment																
8.	*M. variabilis* 70037	Surface of algae																
9.	*M. marinus* CGMCC1.10657	Sediment bay																
10	*M. yueqingensis* CCGMC 1.10658	Sediment bay																
11.	*S.degradans* 2-40	Surface of salt marsh																
12.	*C. agarivorans* YM01	Seawater																
13.	*Z.galactanivorans* Dsij	Surface of algae																

* Glycoside hydrolase family for ß-agarase from Gammaproteobacteria (*red*)

** Glycoside hydrolase family in which ß-agarase is one of the members (GH16-16) (*dark gray*)

Specialized GH present only in: one sample species (*brown*); two samples species (*blue*)

M. = Microbulbifer

S. degradans = Saccharophagus degradans

C. agarivorans = Catenovulum agarivorans

Z. galactanivorans = Zobellia galactanivorans

4.2. Discussion

This chapter describes *in silico* identification and characterization of *M.elongatus* PORT2 agarolytic pathways. PORT2 genome profiling reveals the presence of a ß-agarolytic system consisted of six ß-agarases genes from three agarases families: GH16, GH50, and GH86. The agarases are proposed to be stable in a test tube indicating by the instability index (II) values that are less than 40 and the high aliphatic indexes (AIs) (Guruprasad et al. 1990; Ikai 1980). The II and AI values also can indicate the possibility of soluble overproduction for the recombinant agarases. Idicula-Thomas and Balaji (2005) have reported that soluble recombinant proteins overexpressed in *E.coli* demonstrate high AI and low II values.

Protein synthesis is known to occur in the cytoplasm. A signal peptide will destine a protein to enter the secretory pathway and translocate into the periplasm or the extracellular space. Commonly, the SPII will direct the protein to a cytoplasmic or outer membrane localization. A sorting signal, the amino acid residue at the +2 position from terminal cysteine at the cleavage site will define the exact location. If it is aspartic acid, the protein will anchor to the inner membrane plasma and orient toward the outer membrane (Roosmalen et al. 2004). PORT2 agarases were identified to carry a signal peptide either I or II. In this study, it is proposed that the GH50s and AgaD86 in PORT2 are membrane-bound agarases as they carry signal peptide II (SP II) at their N terminus.

On the other hand, AgaF16 and AgaE86 are considered to be extracellular agarases. Those agarases have a signal peptide I (SPI) at their N terminus. Generally, SPI signalizes extracellular transport of an unfolded protein that will immediately fold-up after release outside the cell (Gennity and Inouye 1991; Matsuyama et al.1995). Moreover, the agarase domain in AgaF16 and AgaE86 were associated with carbohydrate-binding modules (CBMs). It is known that the CBM increases the substrate affinity of endo-glycoside hydrolases and enhances the catalytic efficiency (Abbott et al. 2014). Thus, the CBM is supporting their presence as extracellular agarases. The CBM was connected to the agarase domain or signal peptide by a glycine-serine linker.

The glycine-serine linker had different locations and lengths in AgaD86, AgaE86, and AgaF16. The differences indicate structural flexibility and conceivably affect

enzyme activity or substrate specificity. Studies on cellulases have revealed that the presence of glycine-serine linkers allows proper orientation between domains and stabilizes protein conformations. They have observed that the linker length is vital not only for enzyme functionality and processivity but also for the adaptation to the different substrates (Black et al. 1996; Sammond et al. 2012; Ruiz et al. 2016). Moreover, the length of the linker influences solvent accessibility suggesting that a longer linker makes the protein more hydrophilic and accessible by the solvent (George and Heringa 2002).

In this work, *in silico* abundance of cazymes in PORT2 was also investigated and compared to other agarolytic bacteria. The exploration shows that among the analyzed genomes, glycoside hydrolases are the most abundant cazymes followed by CBMs. Additionally, it is important to highlight that some polyspecific GHs such as GH16, GH13, GH19, GH23, GH31, and GH 103 most possibly, serve as core glycoside hydrolases. Conversely, some GHs indicate species-specificity. Moreover, among 10 *Microbulbifer* genomes that have been published publicly, the presence of GH16 does not always indicate agarolytic capability. Only the occurrence of GH50 and GH86 families confirm the ability in *Microbulbifer*. Together, these findings emphasize that glycoside hydrolases (GHs) are distributed among species that have a close phylogeny correlation. Relevant to the results, Davies et al. (2005), Berlemont and Martiny (2016) have reported that GHs substantially diverge mostly in a small cluster of relatives at the genus or species level with an average gene abundance of at least 2.4%.

This study used agarolytic *S.degradans* 2-40 and *Zobellia galactanivorans* Dsij as models. Both models indicate two-stage agarolytic pathways. The first stage is the hydrolysis of agar polymer into oligomers such as neoagarohexaose (NA6) and neoagarotetraose (NA4) by endo-β-agarase(s). Occasionally, this step also generates the smallest repeating unit, neoagarobiose (NA2). Otherwise, exo-β-agarases continue the oligomer degradation into NA2. The second stage is monomerization of agar disaccharide. The GH117 or α-neoagarobiose hydrolase (NABH) cleaves NA2 further into D-galactose and 3,6 α-anhydro-L-galactose. The differences between those models are the agarase machinery and the workplace. *S. degradans* 2-40 agarases system involves extracellular endo-β-agarase GH16, membrane-bound exo-β-agarases GH50 and GH86, and intracellular GH117. In

contrast, *Z.galactanivorans* employs only extracellular endo-β-agarases GH16 and several GH117s.

The first-stage agarolytic pathway in PORT2 shows similarity to *S. degradans* 2-40. Genome annotation and comparative analysis show the presence of putative extracellular GH16, GH86, and membrane-bound GH50 and GH86 in *M. elongatus* PORT2. Furthermore, it also informs the evident absence of GH117 or α-agarase GH96 not only in PORT2 but also in other agarolytic *Microbulbifer*. The non-occurrence of the enzymes thus suggesting an incomplete agarolytic system that is contradictory to the availability of D-galactose and 3,6 α-anhydro-L-galactose degradation pathways and the ability of the bacterium to utilize agar as a sole carbon source.

Genome profiling successfully elucidates the presence of the ß-agarolytic system in *M. elongatus* PORT2. Multiple β-agarases genes from the same family either GH50 or GH86 could reflect substrate and product specificities. Interestingly, even though PORT2 is a mesophilic bacterium, *in silico* gene characterization points out possible thermostable characteristics of its agarases. Thermostability particularly is looked for in agarase industrial applications due to the gelling properties of the substrate. Up to date, characterized thermostable agarases have been isolated from unique environments such as a deep-sea, saltwater hot spring, and soils. Most of them are GH16 family, three are GH50, and none is GH86 (Park et al. 2020). Indeed, the *in silico* characterization has provided a starting point for designing an experimental elucidation of the PORT2 agarases functionality in the next chapter.

5. Recombinant Agarases from *Microbulbifer elongatus* PORT2

5.1. Results

In silico characterization detected the presence of six β-agarases genes within genome PORT2. The genes were mined from the genomic DNA (gDNA) by PCR amplification and cloned into *E. coli* DH5α by using the restriction enzyme ligation method. The native signal peptides were omitted in gene cloning for intracellular heterologous expression in *E.coli*. The recombinant plasmids and the encoded agarases were designated as pME1 (AgaA50), pME2 (AgaB50), pME3 (AgaC50), pME46 (AgaD86T), pME6 (AgaE86) and pME9 (AgaF16A). The plasmids contained the gene inserts ranging from 0.86 to 2.9 kb (**Appendix 3**). Notably, pME46, pME6, and pME9 carried only the catalytic domain of each agarase because carbohydrate-binding module-containing plasmids were either can not be cloned or expressed.

The plasmids were transformed into *E.coli* BL21 (DE3) for overexpression. AgaA50, AgaB50 AgaC50, and AgaF16A were overproduced as soluble proteins except for AgaD86T and AgaE86 (the GH86s). The GH86s insolubility could be caused by incorrect protein folding during the overexpression. Lowering the expression temperature can enhance proper protein folding and increase solubility (Schein 1989). Therefore, the *E.coli* Artic Express was used to overcome the expression problem in AgaD86 and AgaE86. The system is designated for heterologous expression of the targeted protein that is assisted by Cpn60 to enhance proper protein folding at low temperatures (<15 °C). AgaD86T was probably expressed as a soluble protein. The ambiguity was derived from molecular weight closeness between AgaD86T (53 kDa) and Cpn60 (58 kDa). On the other hand, AgaE86 was inexpressible in Artic Express. The expression problem of AgaE86 could be caused by poor codon utilization in *E.coli*. The Codon adaptation index (CAI) of AgaE86 was 0.75 to 0.78 which is lower than the ideal index (0.8-1), indicating potential poor heterologous expression (Selleck and Tan 2008).

All recombinant agarases were partially purified using a nickel–nitrilotriacetic acid-immobilized metal affinity chromatography (Ni-NTA IMAC) system. The obtained proteins were desalted and concentrated using centrifugal ultrafiltration before characterized further. The expression and purification results were observed using SDS PAGE (**Figure 5.1**).

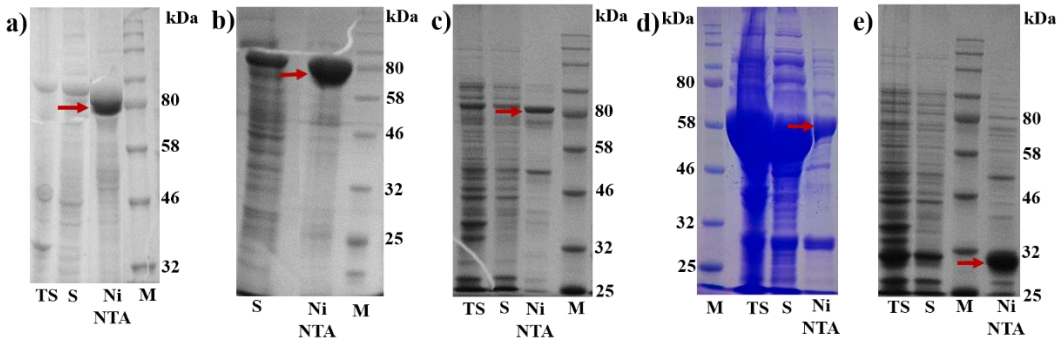

Figure 5.1. SDS PAGE of recombinant agarases PORT2 expression in *E .coli* (*black arrows*). Total protein (TS); soluble protein fraction (S); flow-through (FT); elution fraction from Ni-NTA IMAC (Ni-NTA); color prestained protein marker NEB (M).

The agarases activities were qualitatively screened using agarose and artificial substrates (β-*p* nitrophenyl galactopyranoside (β-*p*npg) and α-*p* nitrophenyl galactopyranoside (α-*p*npg)). All recombinant agarases were active on β-*p*npg but not on α-*p*npg indicating β-glycosidase activity. Only AgaB50 and AgaF16A showed distinct agarase activities by forming a clear zone on the agarose plate (**Figure 5.2**). Therefore, these two agarases were characterized by firstly.

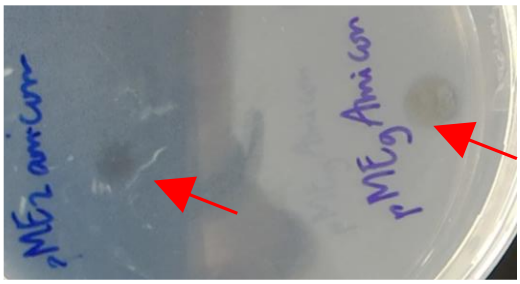

Figure 5.2. Qualitative test of 1 µL recombinant agarases on 1% w/v agarose plate: AgaB50 (pME2) and AgaF16A (pMe9). The agarolytic activity is indicated by clear zones formation (*red arrows*).

Endo-β-agarases AgaB50 and AgaF16A

Biochemical Properties of AgaB50

The agaB50 had a size of 2232 bp nucleotides encoding 743 amino acid residues with a calculated molecular mass of 82.5 kDa and pI of 4.84. The gene had GTG

and TGA as start and stops codons, respectively. The AgaB50 showed a molecular weight of around 82 kDa on SDS PAGE gel (**Figure 5.1.b**). The protein resembled 45% sequence identity to Aga50D, an exo-β agarase from *Saccharophagus degradans* 2-40, and β-agarase from *Agarivorans gilvus*.

The activity of AgaB50 on agarose was measured over the pH range of 4 to 10 at 50 °C. The enzyme exhibited agarase activity at a wide pH profile from pH 6 to 9. It displayed maximum activity at pH 7 and maintained more than 60% of its activity at pH 6 to 7.5 (**Figure 5.3.a**). AgaB50 was also active at a wide-temperature range between 6.5 to 70 °C. It displayed a maximum activity at 50 °C at pH 8 (**Figure 5.3.b**). A 1 h heat treatment between 20-40 °C did not affect the activity. The enzyme lost 20% of its activity after 1 h preincubation at 50 °C. The activity diminished at a higher incubation temperature (**Figure 5.3.c**). The specific activity of AgaB50 on agarose with assay condition of pH 7; 50 °C was 242 U/mg.

AgaB50 was sensitive to all tested chemicals. It lost 50% of its activity in the presence of 1 mM thiol reagents such as β-mercaptoethanol (BME), dithiothreitol (DTT), and inorganic salts ions such as Na^+ and Ca^{2+} (10 and 0.5 mM). Other chemicals, Mg^{2+} (5 and 10 mM), and EDTA (1 mM) also reduced almost 60% of the enzyme activity. Glycerol (2.5% v/v) and SDS (1 mM) were detrimental to AgaB50 activity (**Figure 5.3.d**).

Biochemical Properties of AgaF16A

The size of the agaF16A was 837 bp nucleotides encoding 279 amino acid residues with a calculated molecular mass of 31.4 kDa and pI of 4.85. The AgaF16A was predicted as the catalytic domain of AgaF16. Neither AgaF16 nor AgaF16A contained cysteine residue. AgaF16A shared identities of 86.7% with β-agarase *Microbulbifer thermotolerans* JAMB A94 and 53.7% with β-agarase B from *Zobellia galactanivorans* DsiJ. The expressed protein had a size of around 31 kDa on SDS PAGE gel (**Figure 5.1.e**).

AgaF16A activity on agarose was examined over a wide pH range from 4 to 10 at 50 °C. The enzyme was active at a pH range from 6 to 9 with maximum activity at pH 7 (**Figure 5.3.a**). The enzyme also showed activity at a wide temperature between 6.5 to 70 °C at pH 8 and reached a maximum of 50 °C (**Figure 5.3.b**). Indeed, AgaF16A retained more than 90% of its activity even after preincubation

for 1 h at 50°C. However, preincubation at a higher temperature diminished the activity (**Figure 5.3.c**). The presence of SDS (1 mM) and salts ion Na^+ (150 mM) did not affect the activity of AgaF16A to any practical extent, except for Ca^{2+} (5 mM), which decreased almost 40% of the activity. The addition of some chemicals at a concentration of 1 to 10 mM such as Mg^{2+}, EDTA, BME, DTT, and 10% (v/v) glycerol even enhanced the activity of AgaF16A at least one fold (**Figure 5.3.d**). The specific activity of AgaF16A on agarose at pH 8, 50 °C was 772 U/mg.

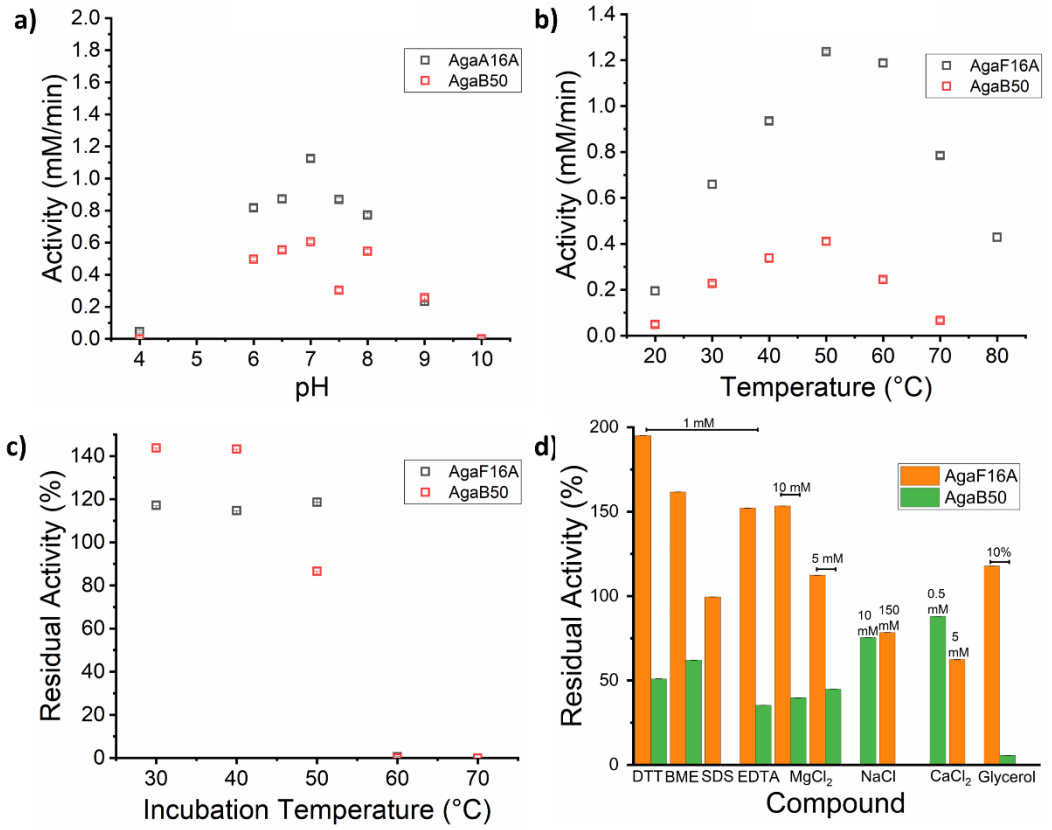

Figure 5.3. Biochemical characteristics of AgaB50 and AgaF16A on agarose 0.2% w/v: **a**) the effect of pH on enzyme activity at 50 °C, **b**) the effect of temperature on enzyme activity at pH 8, **c**) enzyme stability measurement at 50 °C at pH 7 (AgaB50) and pH 8 (AgaF16A) after 1 h preincubation at a certain temperature, **d**) the effect of various ions and reagents on enzyme activity at 50 °C, pH 7 (AgaB50) and pH 8 (AgaF16A). All data are measured in three replicates and presented as the mean value of triplicates. Abbreviation: β-mercaptoethanol (BME), dithiothreitol (DTT), sodium dodecyl sulfate (SDS), ethylenediaminetetraacetic acid (EDTA).

Endo β-Agarase Action

The qualitative assay on artificial substrates indicated the agarase activities of AgAB50 and AgaF16A. A time series-agarose-degradation of each enzyme was evaluated to determine the action mode.

AgaB50 displayed a gradual product formation on time-series agarose hydrolysis. TLC analysis showed product patterns with retention times similar to neoagarooligosaccharides (NAOS) markers (**Figure 5.4.a.**). Product specificity was also verified using HPLC-RID. The HPLC analysis displayed more clearly the gradual degradation pattern and continuously released of NAOS with different lengths. The result showed that AgaB50 converted agarose into neoagarotetraose (NA4) (20.9 min) as a major product and a lesser extent of neoagarohexaose (NA6) (16.9 min) and neoagarobiose (NA2) (28 min). Interestingly, the HPLC depicted a depletion of the released products; NA6, NA4, and NA2 at 4 h reaction (**Figure 5.4.b.**).

The ability of AgaB50 to utilize NAOS as substrate was examined individually by using endpoint enzymatic reaction with an excess amount of enzyme. The result showed that AgaB50 degraded substrate larger than NA2. Notably, AgaB50 only generated a prominent amount of NA2 from NAOS (**Figure 5.4.c.**).

Similar to AgaB50, AgaF16A also produced multi-size products from agarose. The product retention times showed similarity to NA4 (20.9 min) and NA6 (16.9 min) on TLC and HPLC-RID analysis. However, the time-course reaction showed more rapid final-size product formation than AgaB50 with NA4 as the major product followed by NA6 (**Figure 5.5.a** and **5.5.b**).

Different from AgaB50 which took NA4 as the smallest substrate and always produced a single product size when hydrolyzed NAOS, AgaF16A was unable to use NA4. The enzyme also can utilize neoagarooligosaccharides with NA6 as the smallest substrate and hydrolyzed it into NA4 and NA2. Indeed, AgaF16A showed a clear endo-β-catalytic pattern different from AgaB50.

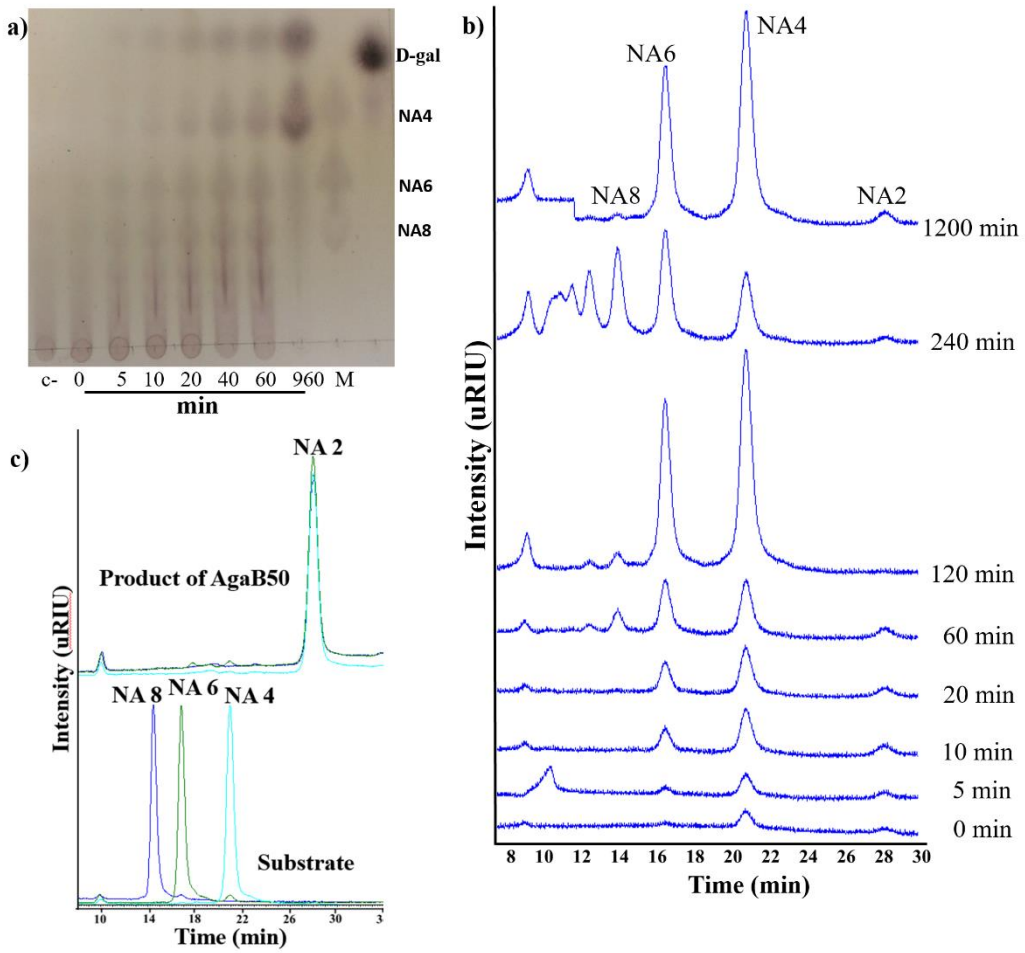

Figure 5.4. Product specificity of AgaB50. Time series reaction on 0.2% w/v agarose in ultrapure water monitored by **a)** TLC, **b)** HPLC-RID, **c**) the smallest substrate specificity test monitored by HPLC-RID (each substrate: 0.5 mg/mL in ultrapure water; endpoint enzymatic reaction at 50 °C; 800 rpm). Abbreviations: neoagarooctaose (NA8); neoagarohexaose (NA6); neoagarotetraose (NA4); neagarobiose (NA2); and D-galactose (D-gal). The retention times (Rt) of neoagarooligosaccharide standards are: 14.6 min (NA8); 16.9 min (NA6); 20.9 min (NA4); 28 min (NA2) and 33.7 min (D-galactose).

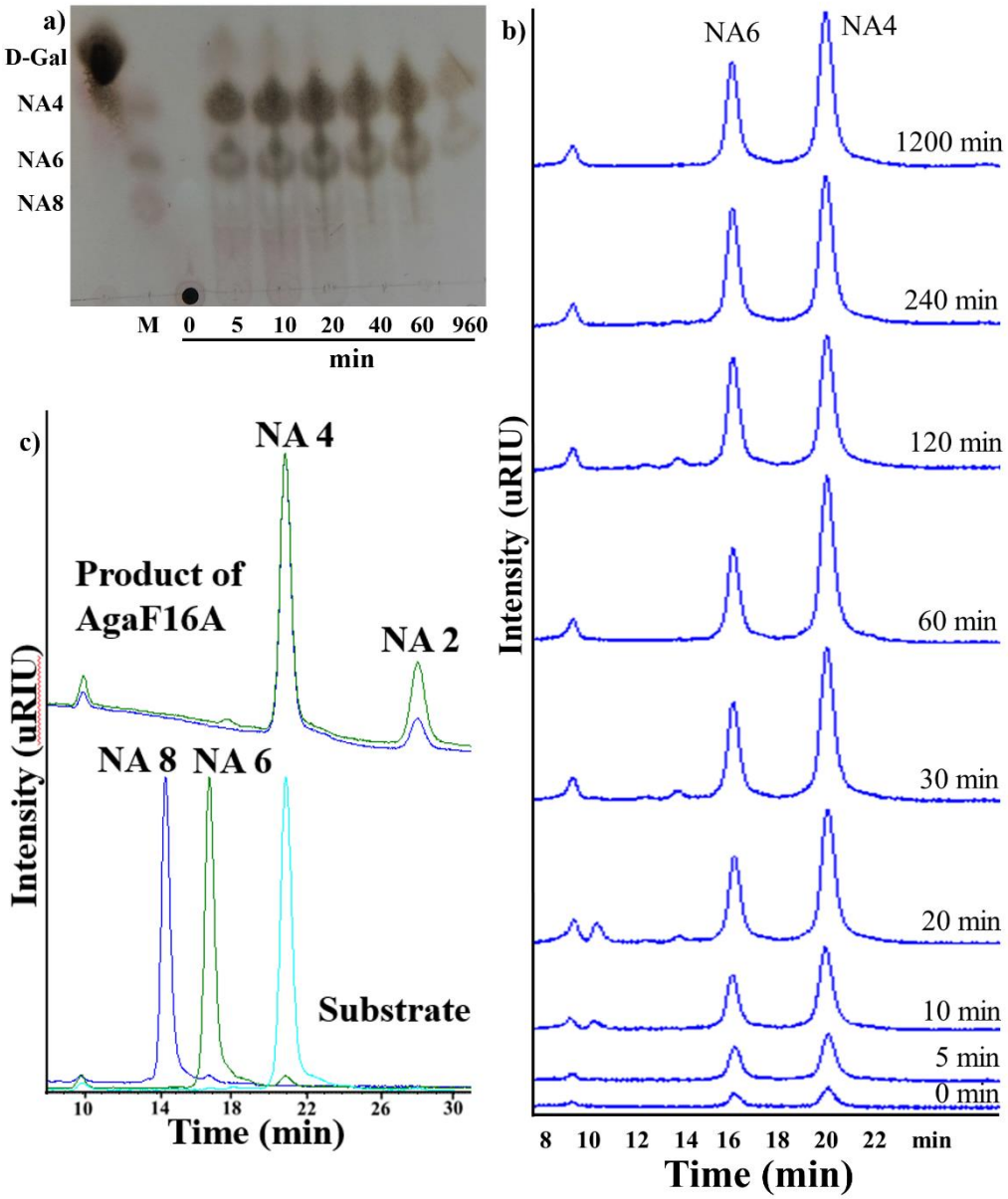

Figure 5.5. Product specificity of AgaF16A. Time series reaction on 0.2% w/v agarose in ultrapure water monitored by **a)** TLC, **b)** HPLC-RID, **c**) smallest substrate specificity test monitored by HPLC-RID (each substrate: 0.5 mg/mL in ultrapure water; endpoint enzymatic reaction at 50 °C; 800 rpm). Abbreviations: neoagarooctaose (NA8); neoagarohexaose (NA6); neoagarotetraose (NA4); neagarobiose (NA2); and D-galactose (D-gal). The retention times of neoagaroligosaccharide standards are: 14.6 min (NA8); 16.9 min (NA6); 20.9 min (NA4); 28 min (NA2) and 33.7 min (D-galactose).

Biochemical characterization of AgaA50, AgaC50, and AgaD86T was performed using β-*p*npg, a common artificial substrate for a hydrolytic enzyme. This chromogen can be used in either discontinuous or continuous assay at an elevated temperature (Lieshout 2007). Indeed, the activity on an artificial substrate only approximates the hydrolytic efficiency of natural substrates.

Exo-β-agarases GH50

PORT2 encoded three GH50 agarases, AgaA50, AgaB50, and AgaC50. All of them showed more than 40% of sequence similarity to Aga50D, an exo-agarase GH50 from *S. degradans* 2-40 indicating similar protein folding and function. Notably, the AgaB50 showed the lowest similarity and distinct endo-exo-β-agarase activity. On the other hand, AgaA50 and AgaC50 did not show any clear activity on agar or agarose during the qualitative assay. The product formation was below the detection limit of the DNS reagent.

The agarolytic of AgaA50 and AgaC50 was detected using HPLC analysis. AgaA50 showed clear agarolytic activity on NAOS. AgaA50 hydrolyzed NA4, NA6, or NA8 and released a prominent amount of NA2 (**Figure 5.6.a**). In contrast, AgaC50 depicted a subtle or very specific agarase activity by taking only NA4 as a substrate and hydrolyzed it into NA2 (**Figure 5.6.b**). Similar to SdAga50D, both enzymes released a single-size product indicating an exo-β-agarase action that hydrolyzes the glycosidic bond from the end chain of the substrate.

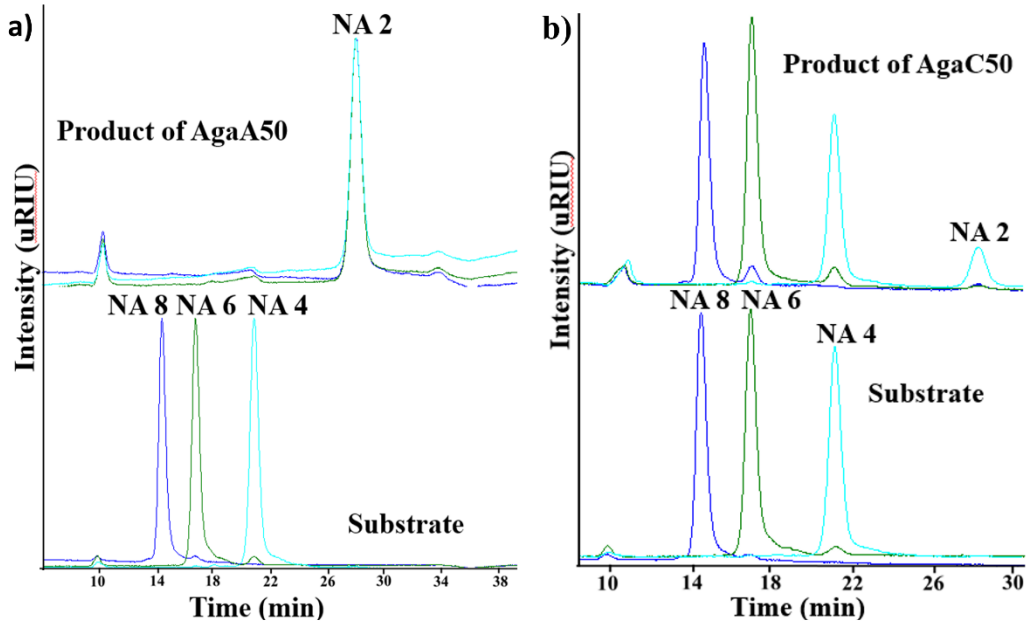

Figure 5.6. Exo-agarolytic activity on neoagarooligosaccharides monitored by HPLC-RID a) AgaA50, b) AgaC50. Endpoint enzymatic reaction at 50 °C, 800 rpm, substrate concentration: 0.5 mg/mL in ultrapure water. Abbreviations: Neoagarooctaose (NA8); neoagarohexaose (NA6); neoagarotetraose (NA4) and neagarobiose (NA2). The retention times of standards are: 14.6 min (NA8); 16.9 min (NA6); 20.9 min (NA4); 28 min (NA2).

Biochemical Properties of AgaA50

The agaA50 consisted of 2313 bp nucleotides encoding 770 amino acids with calculated pI 4.74 and a molecular weight of 86.6 kDa. AgaA50 showed 55% sequence identity to Aga50D, an exo-β agarase from *S. degradans* 2-40. The purified Ni-NTA protein showed a size of around 80 kDa on the SDS-PAGE gel (**Figure 5.1.a**).

AgaA50 activity on β-pnpg was measured over a pH range of 5.6 to 9.1 at 40 °C. The enzyme displayed activity at a pH range from 6 to 9 and reached a maximum at pH 6.5 (**Figure 5.7.a**). The activity was also tested at wide range temperatures between 30 to 80 °C at pH 7. AgaA50 demonstrated more activity at a temperature higher than 50 °C and achieved maximum at 60 °C (**Figure 5.7.b**). The enzyme still maintained more than 70% of its activity after 1 h preincubation at 50 °C but was inactivated by higher preincubation temperature (**Figure 5.7.c**). Monovalent ions Na^+ and K^+ (1 and 10 mM), glycerol (2.5% v/v), and DTT, Ni^{2+} and Fe^{3+} (each 5 mM) slightly decreased the AgaA50 activity. SDS (0.5% v/v) and EDTA (2.5 mM) affected the AgaA50 activity negatively. In contrast, divalent ion Ca^{2+} (10 mM) or Mg^{2+} (1 mM) enhanced the activity of AgaA50 (**Figure 5.7.d**). AgaA50 showed Michelis-Menten behavior on β-*p*npg with K_m value 1.26 mM and V_{max} 0.028 mM/min.

Biochemical Properties of AgaC50

AgaC50 was the third GH50 agarase carried by PORT2. The gene consisted of 2346 bp nucleotides encoding 781 amino acid residues. AgaC50 had a calculated molecular weight of 87.7 kDa and pI 4.99 with 52% sequence identity to Aga50D, an exo-β agarase from *S. degradans* 2-40. Recombinant AgaC50 showed a smaller size (around 86 kDa) on the SDS PAGE gel due to the signal peptide exclusion for heterologous expression in *E.coli* (**Figure 5.1.c.**).

The activity of AgaC50 on β-pnpg was measured over a pH range of 5.6 to 9.1 at 50 °C. The enzyme showed a wide range of activity from pH 5.6 to 9.1 with a sharp maximum at pH 7.5 (**Figure 5.7.a**). AgaC50 also displayed activity at a temperature range from 30 to 80 °C and a maximum at 60°C at pH 7.5 (**Figure 5.7.b**). It retained more than 70% of its activity after 1 h preincubation at 40°C but less than 40% after preincubation at a higher temperature (**Figure 5.7.c.**). Divalent and monovalent

ions such as $Na^+$and K^+ (1 and 10 mM) did not affect the activity negatively except Ca^{2+}. Other chemicals such as EDTA (2.5 mM), SDS (0.5% v/v), Glycerol (2.5% v/v), Fe^{3+} and DTT (5 mM) significantly reduced the enzyme activity. Monovalent ion Mg^{2+} (1 mM) enhanced the activity (**Figure 5.7.d)**. AgaC50 also showed Michelis Menten's behavior on β-*p*npg but the kinetic parameters were lower than AgaA50 by having K_m and V_{max} values 0.62 mM and 0.00096 mM/min, respectively.

Hence, four recombinant agarases had been successfully characterized. Despite action similarity as endo-β agarases, AgaB50 and AgaF16A displayed distinct biochemical characteristics such as temperature stability and resistance to some inorganic ions, chemicals, or reagents. The most pronounced differences were indicated by their substrate-products specificity.

On the other hand, AgaA50 and AgaC50 displayed an exo-agarase action. Indeed, biochemical characterization also depicted AgaA50 and AgaC50 differences. AgaA50 was more thermostable and efficient than AgaC50. Both enzymes indicated a metal-dependent characteristic which depicted the function of Ca^{2+} and Mg^{2+} as the enzyme activator, respectively. The characteristics of PORT2 recombinant agarases were summarized in **Table 5.1**.

Table 5.1. Biochemical chemical properties of PORT2 recombinant agarases

Enzyme	Size* (kDa)	Biochemical Properties**			Product
		pH	T (°C)	Feature	
AgaA50	86.6	6.5	60	Ca^{2+}	NA2
AgaB50	82.5	7	50	-	NA6, NA4, NA2
AgaC50	87.7	7.5	60	Mg^{2+}	NA2
AgaF16A	31.2	7	50	Mg^{2+}, EDTA, DTT/BME	NA6, NA4

* calculated molecular weight
** for maximum activity

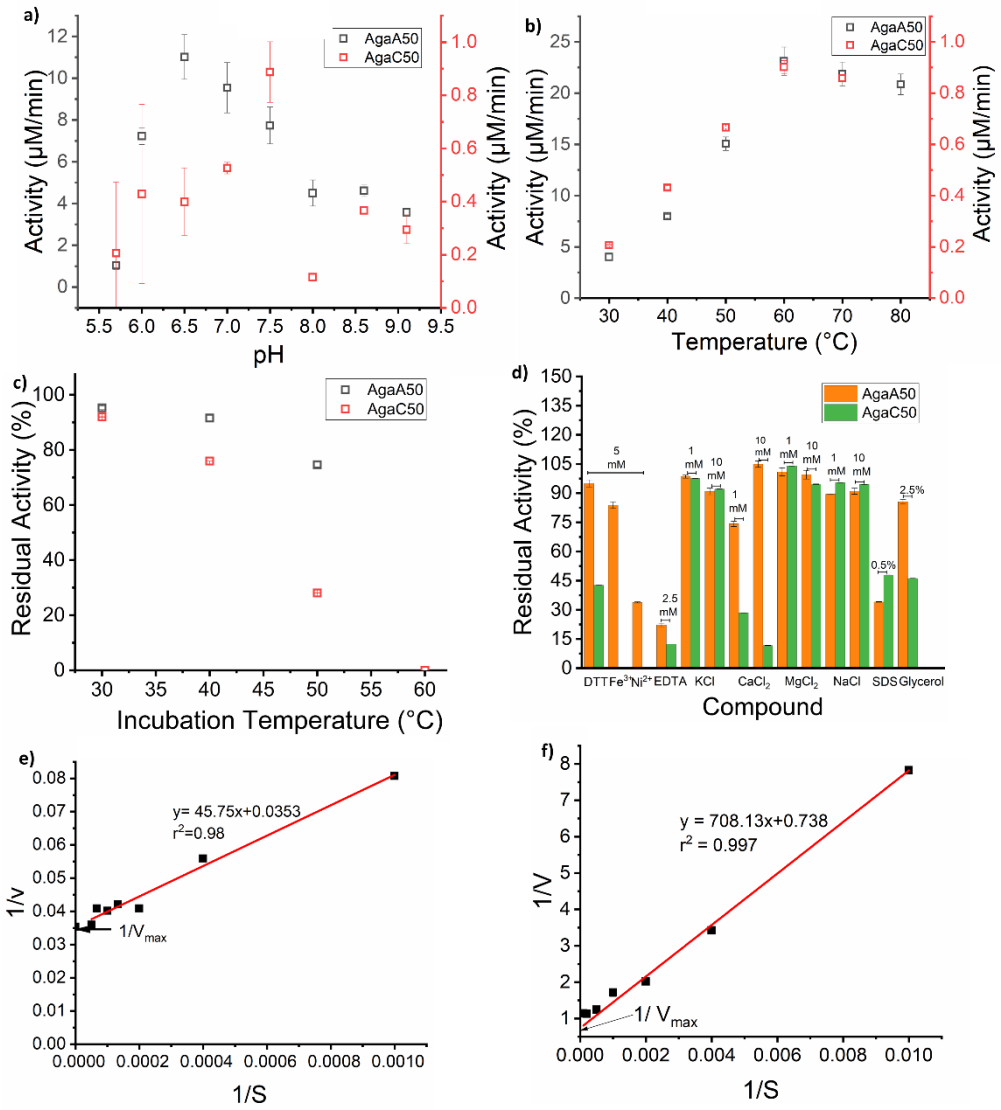

Figure 5.7. **Biochemical characteristics of AgaA50 and AgaC50 on β-pnpg**: **a**) effect of pH on enzyme activity at 40 °C (AgaA50) and 50 °C (AgaC50), **b**) effect of temperature on enzyme activity at pH 7 for AgaA50 and pH 7.5 for AgaC50, **c**) enzyme stability measurement at 60 °C, pH 7 for AgaA50 and pH 7.5 for AgaC50 after 1 h preincubation at a certain temperature, **d**) effect of ions & chemicals on the enzyme activity at temperature 60 °C, pH 7 for AgaA50 and pH 7.5 for AgaC50, **e**) Lineweaver Burk plot of AgaA50, **f**) Lineweaver Burk plot of AgaC50. All data are measured in three replicates and presented as the mean value of triplicates. Error bars represent the deviation of triplicates.

Due to biochemical properties and mode of action differences, structural information of PORT2 recombinant agarases was inferred by using the protein modeling approach. The analysis requires a minimum sequence length of 150 amino acids with 40% identity. The accuracy of modeling improves if the template for generating a model belongs to the same protein family (Wilson et al. 2000; Jabeen et al. 2018).

PORT2 GH50s showed more than 40% sequence identity to Aga50D from *S. degradans* 2-40. The structure of Aga50D had been experimentally elucidated, thus increasing the possibility of getting accurate models for PORT2 GH50s.

Protein models of PORT2 GH50s were automatically built up by SWISS model from a monomeric state of exo-β agarase Aga50D chain A from *S.degradans* 2-40 (PDB id: 4BQ4.A) (SdAga50D) (Waterhouse et al. 2018). Therefore, the generated models also showed a monomeric state. Indeed, SdAga50D itself has tetrameric structures (Pluvinage et al. 2013). Hence, the protein models did not indicate the original quaternary structures of PORT2 GH50s.

Structure comparison between the models and template resulted in root mean square deviation (RMSD) values < 1 Å indicated that SdAga50D was a sufficient template for homology modeling (Fiser 2010; Jabeen et al. 2018). The modeling parameters indicated a reliable model prediction (**Table 5.2**). Multiple sequence alignments between the template and models indicated sequence modifications in PORT2 GH50s (**Figure 5.8.**) and (**Table 5.2**).

SdAga50D showed a homotetrameric structure, each consisted of C-terminus $(\alpha/\beta)_8$ barrel fused to N-terminus a β-sandwich CBM-like domain by a coil-α helix-coil linker (**Figure 5.9.a**). The protein had an end-blocked tunnel substrate-binding site typical for an exo-glycoside hydrolase with a retaining mechanism (**Figure 5.9.b and c**). A partial part of the CBM-like domain formed a roof covering the substrate-binding tunnel and contributed some substrate-binding residues (**Figure 5.9.d**). SdAga50D (E534Q) mutant in complex with NA8 displayed the binding sub sites of -2, +1, +3 for 3,6-anhydro-L-galactose and D-galactose at -1 and +2 (**Figure 5.9.d**) (Pluvinage et al. 2013).

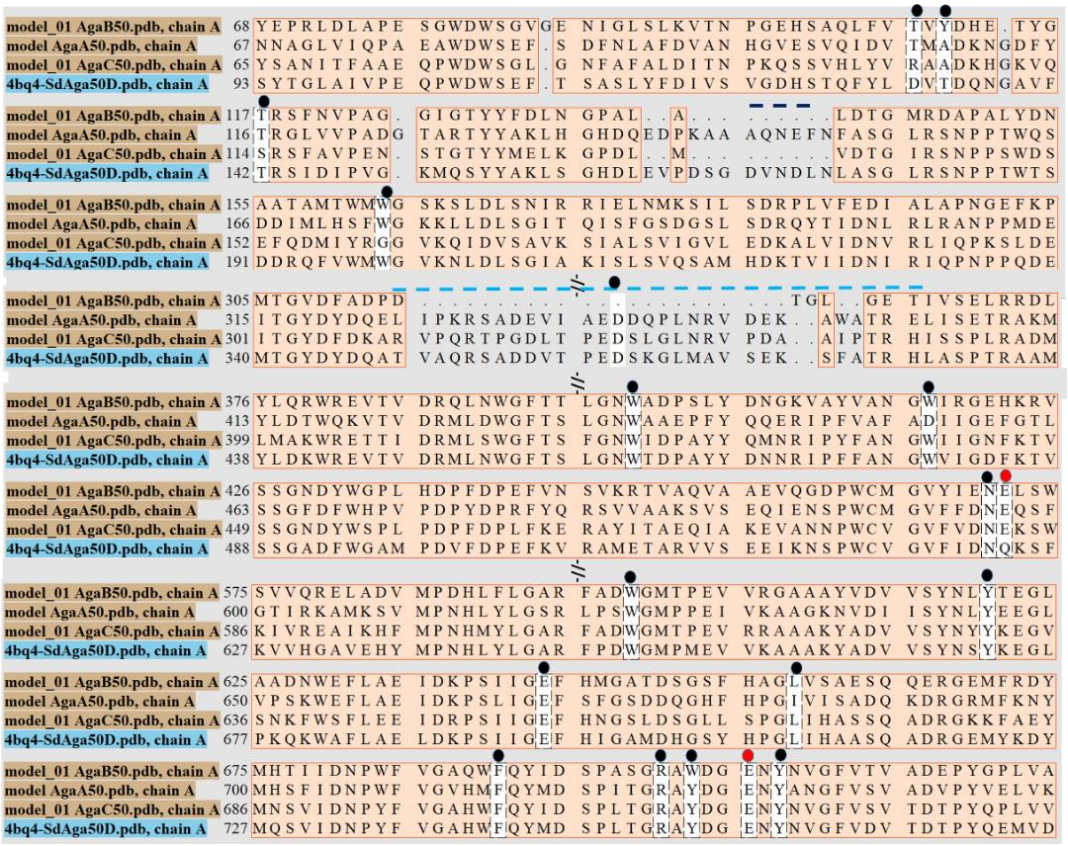

Figure 5.8. Multiple alignments of PORT2 GH50s with the template PDB id: 4BQ4.A (SdAga50D), *black dots* are substrate-binding residues; *red dots* are the catalytic residues; the *black dashed line* is a part of the CBM-like domain, the *blue-dashed line* is the end-loop of active site tunnel.

Table 5.2. Comparison of PORT2 GH50s to SdAga50D (PDB id: 4BQ4.A)

Parameter	**SdAga50D**	**AgaA50**	**AgaB50**	**AgaC50**
Model Quality (Benkert et al. 2011):				
GMQE	Template	0.80	0.76	0.79
QMEAN Z score		-0.65	-1.12	-0.75
Template similarity (%)	100	55.89	46.13	53.65
Substrate-binding site modifications (Pluvinage et al. 2013):				
CBM-like	W199; T142; T134; D132	W174; T116; **A**108; **T**106	W163; T117; **Y**110; **T**108;	**G**160; **S**114; **A**106; **R**104
$(\alpha/\beta)_8$ barrel	D362 L710 W479	D337 **I**683 **D**454	deletion deletions W417	D323 deletions W440
Tunnel shape modifications (Pluvinage et al. 2013):				
Tunnel roof	E165-N176	E140-N151	deletions	deletions
End Tunnel	A351- M367	**P**326- **N**342	deletions	**P**312- **M**328

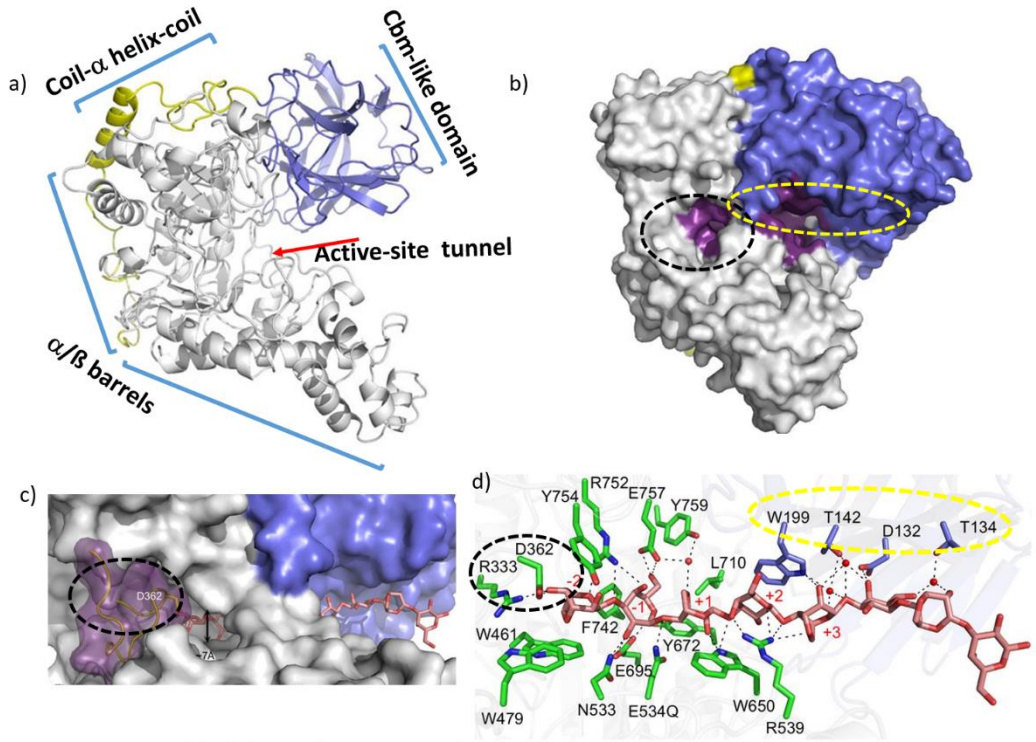

Modified from Pluvinage et al. J. Biol. Chem. 2013;288:28078-28088

Figure 5.9. Features of Aga50D from *S. degradans* 2-40. a) ribbon representation comprising N-terminus CBM-like domain (*blue*); coil-α helix-coil linker (*yellow*) and C-terminus $(\alpha/\beta)_8$ barrel (*white*), **b**) surface display; substrate-binding site (*purple*); blocked-end tunnel (*black-dashed ellipse*), CBM-like domain roof (*yellow-dashed ellipse*), **c**) surface of the substrate-binding site; the end tunnel contributes Asp362 for substrate binding (*black-dashed ellipse*), **d**) amino acid residues of substrate-binding sub sites (-2 to +3) form direct hydrogen bonds complex with NA8 (*magenta sticks*) or via water molecules (*red dot*), subsite residues from $(\alpha/\beta)_8$ barrel (*green sticks*) and CBM-like domain (*blue sticks*).

Among the generated models, the AgaA50 model resembled the template closely (**Figure 5.10.a)**. AgaA50 model displayed similar substrate-binding site topology, a blocked-end tunnel with the CBM-like domain formed a roof covering the tunnel (**Figure 5.10.b and c**). The alignment between the model and template postulated a substrate-binding site in AgaA50 with E509 and E668 as the catalytic residues located 5.4 Å apart (**Figure 5.10.a**).

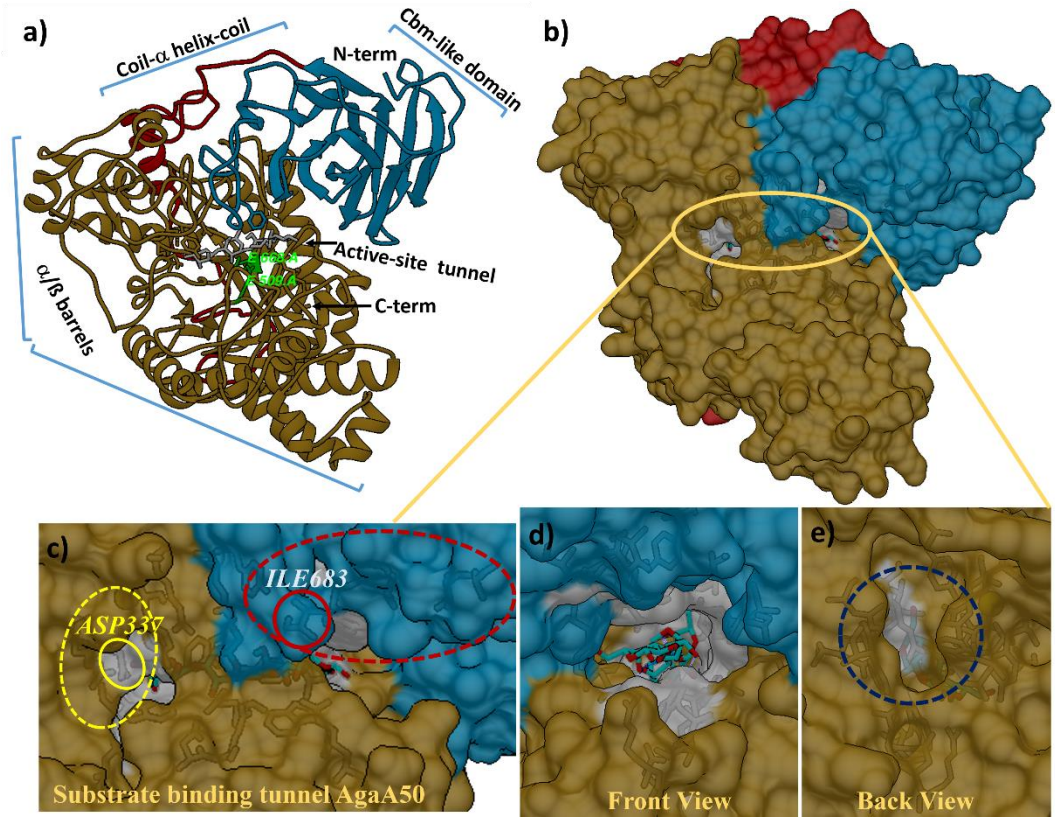

Figure 5.10. **AgaA50 model**: **a**) The cartoon of secondary structure; N-terminus CBM-like domain (*blue*), coil-α helix-coil linker (*red*) and C-terminus $(\alpha/\beta)_8$ barrel domain (*brown*); and catalytic residues E509 and E668 (*green*), **b**) surface of AgaA50, **c**) views of substrate binding site topology (*light gray*) is visualized with an NA4 as the substrate (*blue-red stick*); end-block tunnel (*yellow dashed ellipse*); CBM-like roof (*red dashed ellipse*); substrate binding residue that also blocks the end tunnel (D337, *yellow cycle*); and substrate binding residue that forms roof covering the tunnel (I683, *red cycle*) **d**) front view of substrate binding tunnel **e**) closed-end of substrate binding tunnel (blue dashed circle).

The AgaB50 model also displayed an N-terminus CBM-like domain fused by a coil-α-helix-coil linker to C-terminus $(\alpha/\beta)_8$ barrel domain (**Figure 5.11.a**). However, the superposition of the template and model showed deletions at the end-blocked tunnel (Val351- Ala367, according to SdAga50D amino acid position) and the CBM-like domain roof visualizing an open-end short tunnel substrate-binding site (Glu165-Asn176, according to SdAga50D amino acid position) (**Figure 5.11. b to e**). Two putative catalytic residues of AgaB50 were E472 and E643 located around 5 Å apart. (**Figure 5.11.a**).

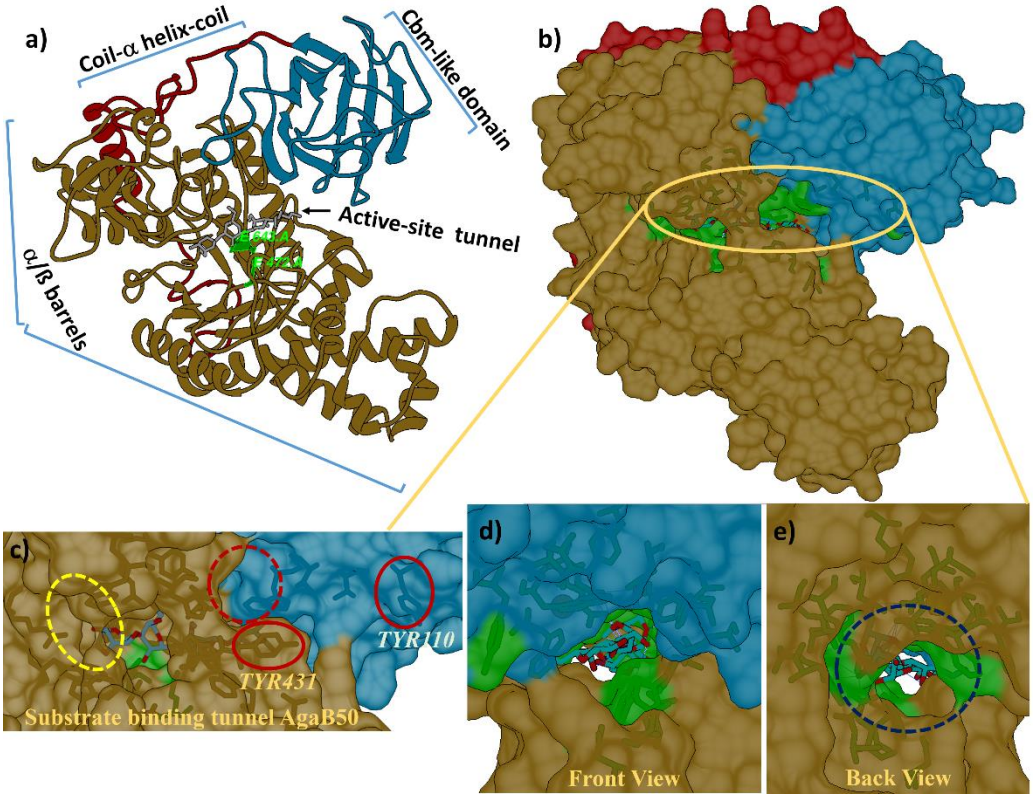

Figure 5.11. **AgaB50 model**: **a**) Secondary structure cartoon; N-terminus CBM-like domain (*blue*), coil-α helix-coil linker (*red*); C-terminus $(\alpha/\beta)_8$ barrel domain (*brown*) and catalytic residues E472 and E643 (*green*) **b**) the AgaB50 (*surface*) displays a short tunnel substrate-binding site (*green*); **c**) the deletions at the end-blocked tunnel loop (*yellow dashed ellipse*) and the CBM-like domain roof (*red dashed ellipse*); substrate-binding residues that are mutated, F431Y and T110Y, (*red ellipse*); an NA4 in the substrate-binding site (*blue-red sticks*). **d**) Front view of substrate binding tunnel **e**) opened-end of substrate binding tunnel (*blue dashed ellipse*).

The AgaC50 model also displayed structure similarity to SdAga50D. Two putative catalytic residues glutamic acids, E495 and E654 located 5.4 Å apart within the substrate-binding tunnel (**Figure 5.12.a)**. Template-model superposition concealed deletion at the CBM-like domain of AgaC50 (Asp165-Asn176, according to SdAga50D amino acid position) (**Figure 5.12.b and c**). Furthermore, substrate-binding residues within the CBM-like domain of AgaC50 also showed mutation events in comparison to the template, chain A of SdAga50D (PDB id 4BQ4.A) (**Table 5.2**). Significantly, the aromatic tryptophan 160 was substituted by small residue glycine (W160G), nucleophilic threonine was replaced by small alanine (T106A), and acidic aspartic acid was mutated into basic arginine (D104R) (**Figure 5.12.d**).

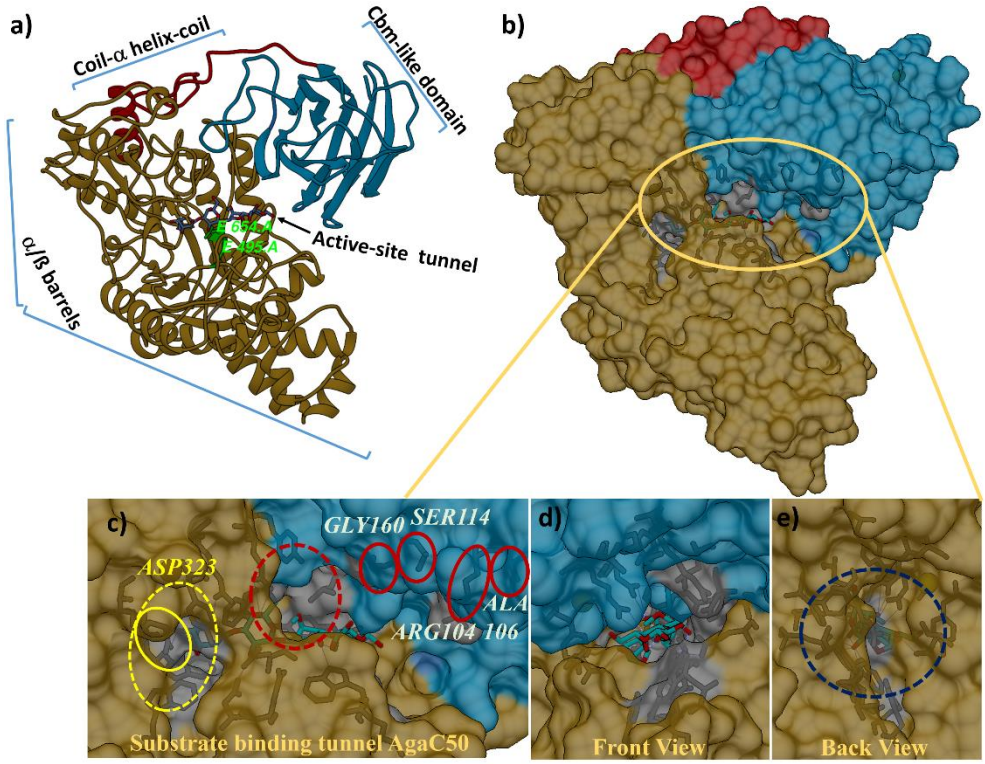

Figure 5.12. **AgaC50 model**: **a**) Cartoon AgaC50; N-terminus CBM-like domain (*blue*), coil-α helix-coil linker (*red*), C-terminus $(\alpha/\beta)_8$ barrel domain (*brown*), catalytic residues E654 and E495 (*light green*), **b**) the AgaC50 (*surface*) shows substrate binding sites (*gray*), **c**) the end-blocked tunnel loop (*yellow dashed ellipse*), D323, the substrate-binding residue at the end of the closed tunnel (yellow ellipse), the deletion of residues which are responsible for closing the tunnel roof from CBM-like domain (*red dashed ellipse*); mutated substrate-binding residues (red ellipse); an NA4 in the substrate-binding tunnel (*blue-red sticks*), **d**) front view of substrate binding tunnel, **e**) closed-end of substrate binding tunnel (blue dashed ellipse).

Homology modeling was also performed for AgaA16A to visualize the substrate-binding site and mode of action. The best template was generated from a catalytic domain of thermostable endo β-agarase AgaA *Microbulbifer thermotolerans* JAMB A94 (PDB id: 3WZ1.1.A) (MtAgaA). AgaF16A showed 87% identity to the template with GMQE score: 0.98 and QMEAN Z-score: -0.09 indicating a reliable model. Different from AgaB50, the AgaF16A model displayed two antiparallel β-sheet jelly rolls formed a concave cleft active-site typical for the GH16 family (**Figure 5.13.a**). The AgaF16A was also superposed to the crystal structure of mutant AgaAE131S (PDB id: 1URX.A) from *Zobellia galactanivorans* DsiJ (ZgAgaAE131S), to visualize the substrate-binding site (**Figure 5.13b**). All those templates are monomeric endo β-agarases from the GH16 family with retaining mechanism (Takagi, et al. 2015; Allouch et al. 2003)

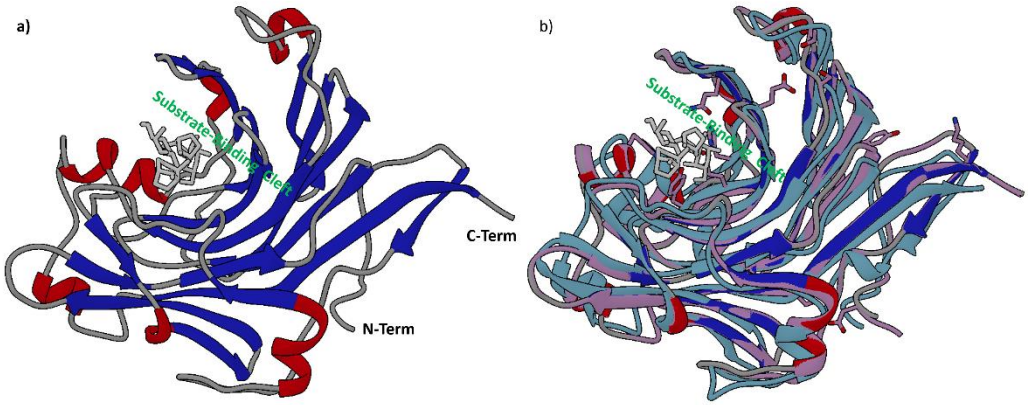

Figure 5.13. **AgaF16A model**. **a**) cartoon of secondary structure and predicted substrate-binding cleft, the jelly roll-β-sheets (*blue*); α-helix (*red*); loops (*gray*) **b**) Structures superposition among ZgAgaA (*sky blue*), MtAgaA (*light purple*) and model AgaF16A (*dark blue*); neoagarotetraose (NA4) (*white stick*s).

The multiple sequence alignments displayed catalytic residues conservation among AgaF16A and the templates. Substrate-binding residues in AgaF16A were more similar to MtAgaA than to ZgAgaA with a conserved β-bulge motif, EXDXXE. The sequence motif in AgaF16A was E^{127}[I]D[V][I]E^{132} with E127 and E132 as putative catalytic residues. (**Figure 5.14**). AgaF16A had neither a loop bridge nor a second substrate-binding site that was present in AgaB, a GH16 agarase from *Z. galactanivorans* DsiJ (ZgAgaB).

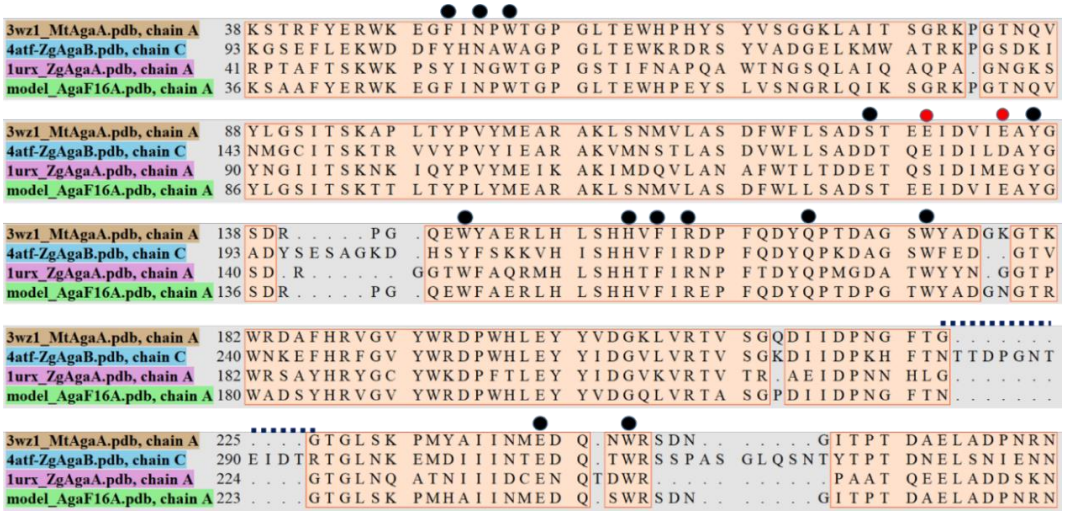

Figure 5.14. **Multiple sequence alignments of AgaF16A with templates from β-agarase GH16.** MtAgA (PDB id: 3WZ1) (*brown*), ZgAgaB E189D (PDB id: 4ATF.chain C) (*light blue*), ZgAgaA E131S (PDB id: 1URX.chain A) (*purple*), and AgaF16A (*light green*): catalytic residues (*red dots*); substrate-binding sites (*black dots*); loop bridge of dimer ZgAgaB (*black-dashed*).

The SdAga50D and ZgAgaB proteins showed multisubunit quaternary structures. Therefore, quaternary structures of PORT2 GH50 and AgaF16A were also

evaluated using blue native polyacrylamide gel electrophoresis (BN-PAGE) (**Figure 5.15**). AgaF16A showed migration of protein with molecular weight twice of the calculated size indicating a dimeric state. Meanwhile, AgaA50 and AgaB50 migrated to the position with smaller sizes than the calculated size indicating a compact globular structure. Some bands with higher molecular weight along the lines could indicate a multimeric state but probably also some impurities which were indicated by SDS PAGE (**Figure 5.1**).

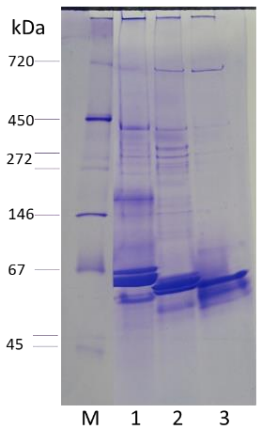

Figure 5.15. Blue native polyacrylamide gel electrophoresis (BN-PAGE) of PORT2 recombinant agarases. Lane M is a protein standard for blue native gel (SERVA, Germany), Lane 1. AgaA50 Lane 2. AgaB50 and Lane 3. AgaF16A.

AgaD86T

AgaD86T was predicted as a C-terminus agarase domain of AgaD86 and overproduced in *E.coli* Artic Express. The AgaD86T had 1416 bp nucleotide encoding 472 amino acid residues with calculated pI 4.49 and molecular weight 53.2 kDa. A qualitative activity assay on agarose and neoagarooctaose (NA8) was performed to ensure that the protein was not the Cpn60 from *E.coli* Artic Express. AgaD86T displayed a subtle activity on NA8 by releasing a small amount of neoagarohexaose (NA6), and neoagarobiose (NA2) (**Figure 5.16.a**) but did not show clear agarolytic activity on agarose or other agar polymers (**Figure 5.16. b**). The enzyme was also active on β-pnpg.

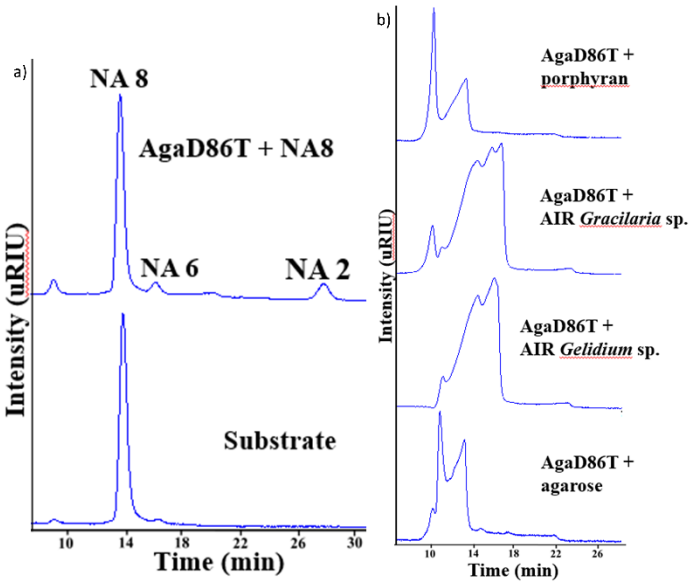

Figure 5.16. **AgaD86T activity monitored by HPLC-RID. a) on neoagarooctaose 0.5 mg/mL in ultrapure water b) on agar polymers.** Endpoint enzymatic reactions at 40 °C, 24 h, 800 rpm, excess enzyme amount.

Considering the presence of subtle agarase activity in AgaD86T, the influence of pH and temperature was also characterized using artificial substrate β-*p*npg to infer some basic information that probably could reflect the biochemical properties of AgaD86. The enzyme displayed an activity at wide pH from 5 to 9 and a maximum at pH 6 at 40 °C (**Figure 5.17.a**). It also showed a wide range of temperature activity between 30 to 80 °C and maximum at 60 °C; pH 6 (**Figure 5.17.b**). Interestingly, the activity was increased significantly after 1 h preincubation at a temperature between 30 to 50 °C. However, a 1 h preincubation at 60 °C reduced 50% of the activity (**Figure 5.17.c**). The enzyme showed a distinct measurement deviation which could indicate that β-*p*npg probably was not the proper substrate.

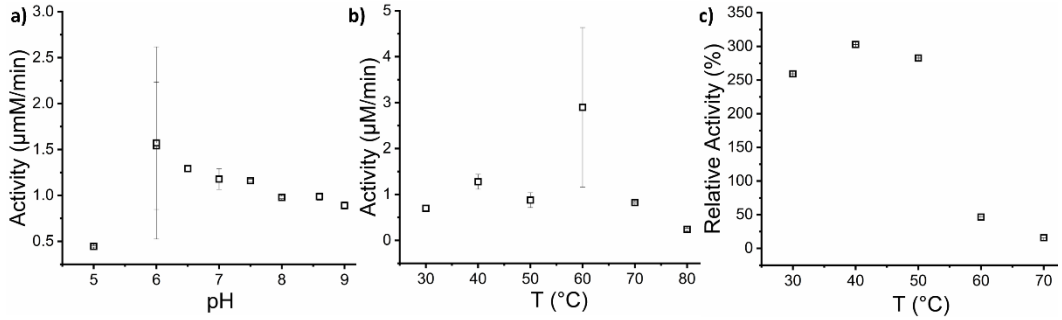

Figure 5.17. **Biochemical characteristics of AgaD86T on β-pnpg**.: **a**) effect of pH on enzyme activity at temperature 40 °C, **b**) effect of temperature on enzyme activity at pH 6 **c**) measurement of enzyme stability at pH 6, 50 °C after 1 h preincubation at a certain temperature. All data are mean values from triplicates. Error bars represent the standard deviation of triplicates.

AgaD86T had 35% sequence identity to a β-porphyranase GH86 from *Bacteroides plebeius* and 44.6% identity to β-agarases GH86 from *Bacteroides uniformis*. The crystal structures from both proteins had been elucidated (Hehemann et al. 2012c; Pluvinage et al. 2018). A protein model was generated to evaluate the poor performance of AgaD86T and to visualize the substrate-binding site. The model of AgaD86 was generated from the template BuGH86E322Q (PDB id: 5TAO chain A). The model had a GMQE value of 0.75 and QMEAN Z-score -3 indicating a reliable model structure (**Figure 5.18. a**). The template BuGH86E322Q is an endo-β-agarase GH86 mutant (E322Q) from *Bacteroides uniformis* in complex with five sugars of the neoagarooctaose (NA8). It has a structure consisted of a $(\alpha/\beta)_8$ barrel core with two Ig-like domains. The enzyme had a crater substrate-binding site topology (**Figure 5.18. b)** that accommodated D-galactose residue at -3 and -1 sub sites and a neoagarobiose at +1 and +2 sub sites (**Figure 5.18. d)** (Pluvinage et al. 2018).

Structure comparison to the template showed that the AgaD86T model resembled an incomplete α/β barrel core with two Ig-like domains. Some β-barrels chain surrounds the substrate-binding site were missing (**Figure 5.18. c**). Thus, only some important residues within the substrate-binding site were still available such as nucleophile E64, which was equivalent to the catalytic residue of BuGH86E322Q (**Figure 5.18.d**). Thus, the model clearly explained the subtlety activity of AgaD86T on NA8 or agar polymers (**Figure 5.16**).

Combining *in silico* and experimental characterization, this study demonstrated that mesophilic *M. elongatus* PORT2 encoded a thermostable β-agarolytic system for agar conversion into NA2. Regrettably, the function of GH86s was unable to verify properly.

The *in silico* characterization did not inform the presence of any GH117 or GH96 in PORT2. Both enzymes are responsible for hydrolyzing α-glycosidic bonds in agar or agar oligosaccharides. Nevertheless, D-galactose, and 3,6-α-anhydro L-galactose catabolic machinery, some sugar transporters, and regulatory system were clustered in the vicinity of β-agarases genes (**Figure 4.1**).

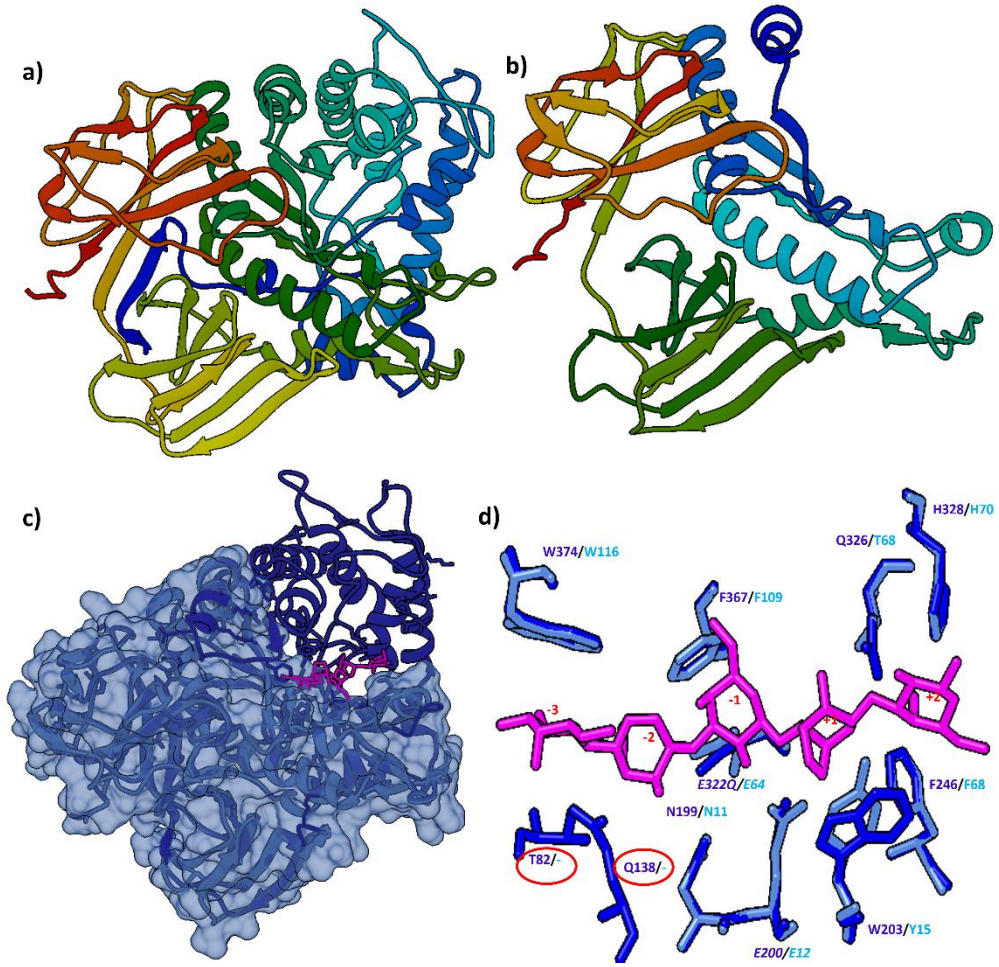

Figure 5.18. AgaD86T model. Rainbow Cartoons of **a**) model AgaD86T **b**) template BuGH86E322Q: N-terminus (*blue)*, C-terminus (*red*), **c**) surface of AgaD86T (*cyan*) superposes with BuGH86E322Q (*grey*) in complex with neoagarooligosaccharides (*magenta*), d) superposition of substrate binding residues (-3 to +2) in AgaD86T (*skyblue*) to BuGH86E322Q (*blue*), neoagaroocta/-pentaose (*magenta*), missing residues in AgaD86T (*red ellipse*).

M.elongatus PORT2 displayed a diauxic growth in a medium containing proteinous substrate and agar. Therefore, PORT2 was proposed to deploy a consecutive basal amount of extracellular endo-β-agarase(s) (such as AgaF16) to sense the presence of agar and hydrolyze it into a variety of NAOS such as NA6 and NA4. The cells recognized the presence of NAOS as inducers for the cognate exo-β-agarases (AgaA50, AgaB50, AgaC50). The enzymes then hydrolyzed the available NAOS into NA2 (**Figure 5.19**.). Hence, the second agarolytic pathway for NA2 assimilation and monomerization in PORT2 was constructed hypothetically. Presumably, the NA2 was then taken up by the cell using the available TonB-dependent or other sugar transporters. Inside the cytosol, NA2 was converted into

D-galactose and 3,6-α-anhydro L-galactose by an unknown neoagarobiose hydrolase (NABH)-like enzyme for cell energy feedstock (**Figure 5.19**.).

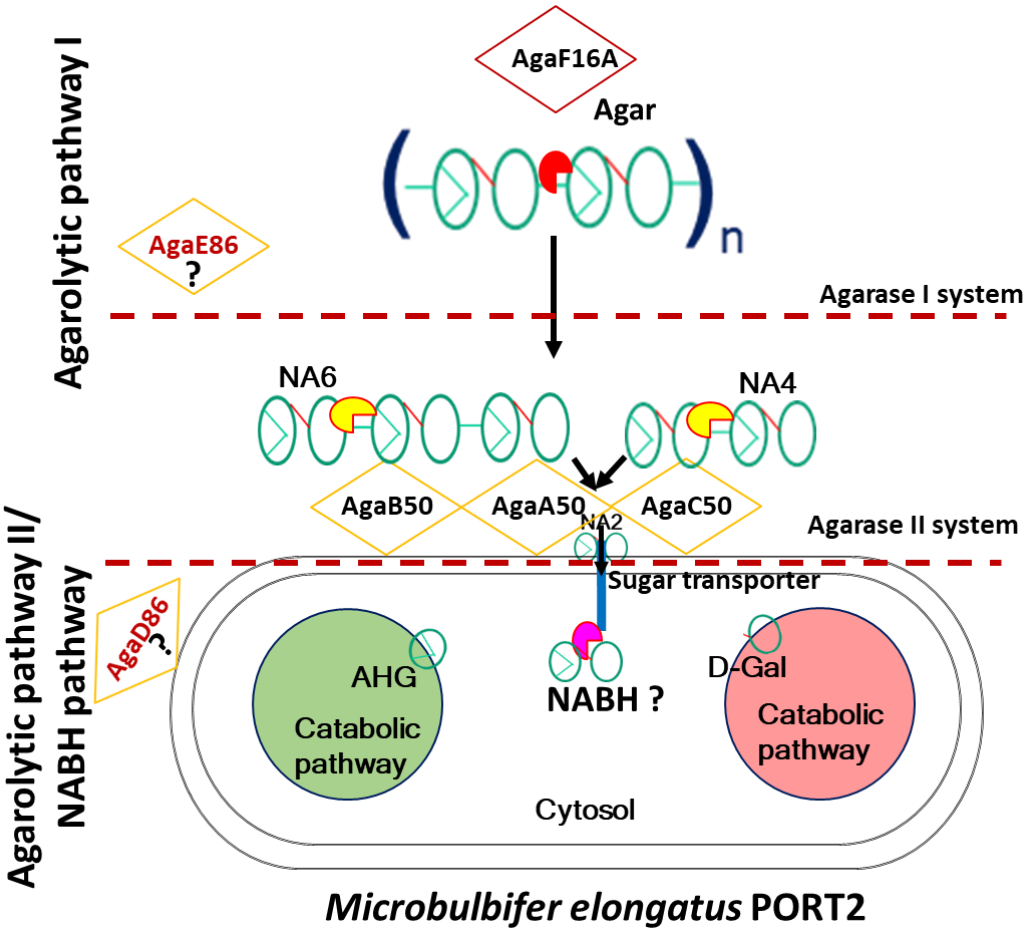

Figure 5.19. **Reconstruction of thermostable agarolytic pathways in *Microbulbifer elongatus* PORT2.** The first-stage of agarolytic pathway employs consecutive expression of endo-agarase such as AgaF16 (*red packman*) to sense the presence of agar polymer. When the substrate is available, AgaF16 produces mixtures of agar oligosaccharides (neoagarohexaose (NA6); neoagarotetraose (NA4)) to induce the production of cognate exo-and/or exo-endo-agarases (*yellow packman*) such as AgaA50, AgaB50, and AgaC50. Those agarases convert longer agar oligosaccharides to neoagarobiose (NA2). Hypothetically, the cell starts the second-stage pathway by transporting NA2 into the cytosol through available sugar transporter. An unknown α-neoagarobiose hydrolase (NABH)-like enzyme (*magenta packman*) is produced to degrade NA2 further into 3,6-α-anhydro L-galactose (AHG) and D-galactose (D-Gal). The monomers then enter each of its catabolic pathways to be converted into energy for cell maintenance and growth. The role of AgaD86 and AgaE86 are still unknown but their *in silico* properties indicate endo-agarase capability.

Conversion of Indonesian Agars into Neoagarooligosaccharides

The ability of the recombinant agarases to use various agar types was tested on different macro algae polysaccharides include agars from Indonesia. Those polysaccharides had different cold-water solubility and gelling properties which

could affect the agarase activity and product (**Table 5.3**). The absence of NAOS in the substrate before the enzymatic reaction was verified using HPLC-RID (**Figure 15.20**). Notably, a small content of glucose was detected in AIR *Gelidium* sp.

Table 5.3. Agar polysaccharides for substrate specificity test

Agar Polysaccharide	Macro alga Producer	Source	Cold Water Solubility	Gelling Property* (T< 40 °C)
Agarose	Unknown-red alga	VWR	Insoluble	Gel-Agar
Agar kobeI	Unknown-red alga	Roth	Insoluble	Gel-Agar
κ-carrageenan	*Kappaphycus* sp.	Sigma	Insoluble	Gel-Non agar
Sodium alginate	Unknown-brown alga	Sigma	Insoluble	Gel-Non agar
AIR *Gelidium* sp.	*Gelidium* sp.	Indonesia	Insoluble	Gel-Agar
AIR *Gracilaria* sp.	*Gracilaria* sp.	Indonesia	Insoluble	Weak Gel
AIR *Ulva* sp.	*Ulva* sp.	Indonesia	Soluble	Non-Agar
Porphyran	*Porphyra* sp.	Carbosynth	Soluble	Non-Agar
Laminarin	*Laminaria* sp.	Sigma	Soluble	Non-Agar

AIR: Alcohol Insoluble Residues

*Gelling property was defined by dissolving the insoluble substrate in hot water followed by cooling down at room temperature,

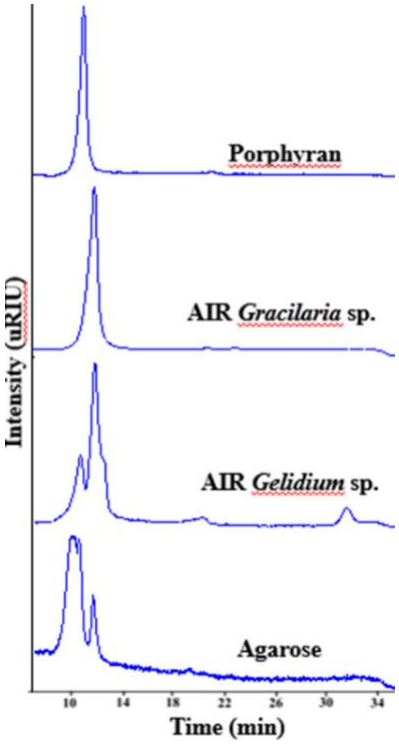

Figure 5.20. **Analysis of different agar polymers substrates (0.2% w/v in ultrapure water) monitored by HPLC-RID**. Each substrate is incubated without any enzyme addition at 50 C °C; 800 rpm for 24 h. Peaks at migration time < 14 min could indicate mixtures of soluble polymers and probably also high molecular weight of neo-or agarosaccharides (>NA10). A small peak appearance after 30 min in AIR *Gelidium* sp. indicates glucose.

The endo-β-agarase AgaB50 preferred gelling-agar substrates such as agarose and AIR *Gelidium* sp. than AIR *Gracilaria* sp. or porphyran (**Figure 5.21.a**). The enzyme showed no activity on non-agar substrates. It released products from AIR *Gelidium* sp. and agarose with similar retention time to NA4 and NA2 standards. Larger NAOS was also released from AIR *Gelidium* sp and AIR *Gracilaria* sp. The products of AIR *Gracilaria* sp. or porphyran showed slightly different retention times from NA4 and NA2 indicating the presence of an additional side-chain group within the sugar backbone (**Figure 5.21.a**).

AgaF16A released products with higher intensities than AgaB50 indicating a more efficient degradation process (**Figure 5.21.b**). The enzymatic products of agarose and AIR *Gelidium* sp. had similar retention times to NA6 and NA4. The enzyme also produced NAOS from porphyran and AIR *Gracilaria* sp. which also showed slightly different retention times to NA4 and NA2.

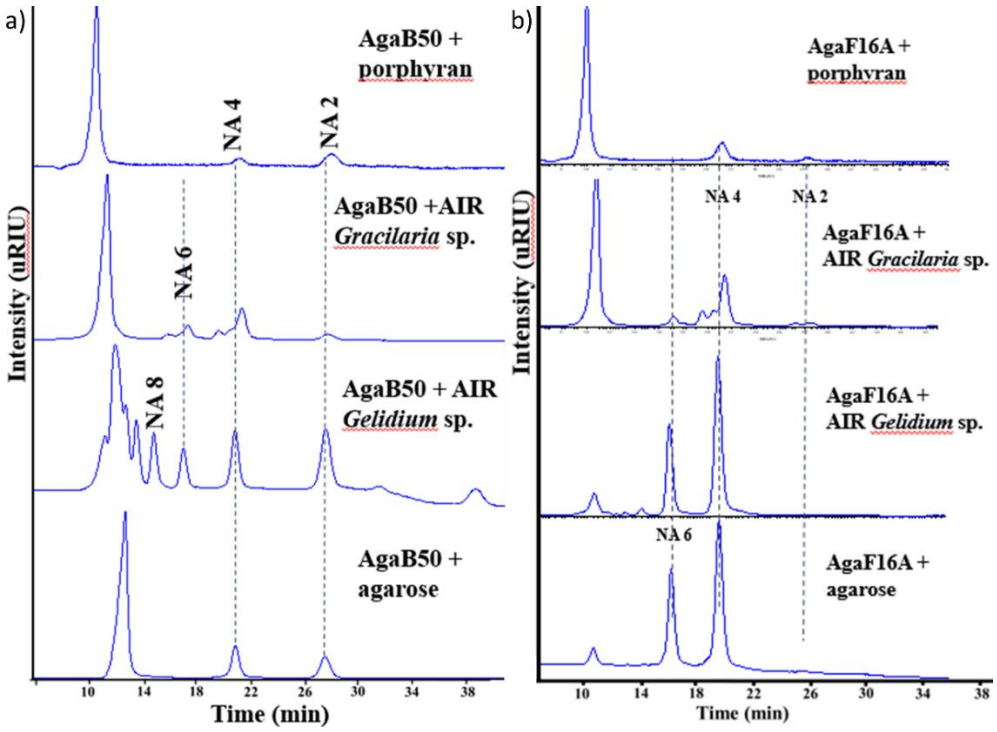

Figure 5.21. **Instrumental analysis of the PORT2 endo-β-agarases activities on different agar polymers 0.2% w/v in ultrapure water, monitored by HPLC-RID**: **a**) AgaB50 produces neagarotetraose (NA4) and neoagarobiose (NA2) from agarose and AIR *Gelidium* sp.; modified NA4 and NA2 from porphyran and AIR *Gracilaria* sp., **b**) AgaF16A releases neoagarohexaose (NA6) and NA4 from agarose and AIR *Gelidium* sp.; modified NA4 and NA2 from porphyran and AIR *Gracilaria* sp. Enzymatic reaction: 24 h, 50 °C, 800 rpm, endpoint measurement. The retention times of neoagaroligosaccharide standards are: 14.6 min (NA8); 16.9 min (NA6); 20.9 min (NA4); 28 min (NA2) and 33.7 min (D-galactose).

AgaA50 also preferred gelling-agar substrates, AIR *Gelidium* sp. and agarose. The enzyme produced a single product with a retention time similar to NA2. It showed no activity on AIR *Gracilaria* sp. and porphyran (**Figure 5.22.a**). However, AgaC50 was unique compared to two other GH50s. It showed no activity on any macroalga polysaccharides that were tested. (**Figure 5.22.b**).

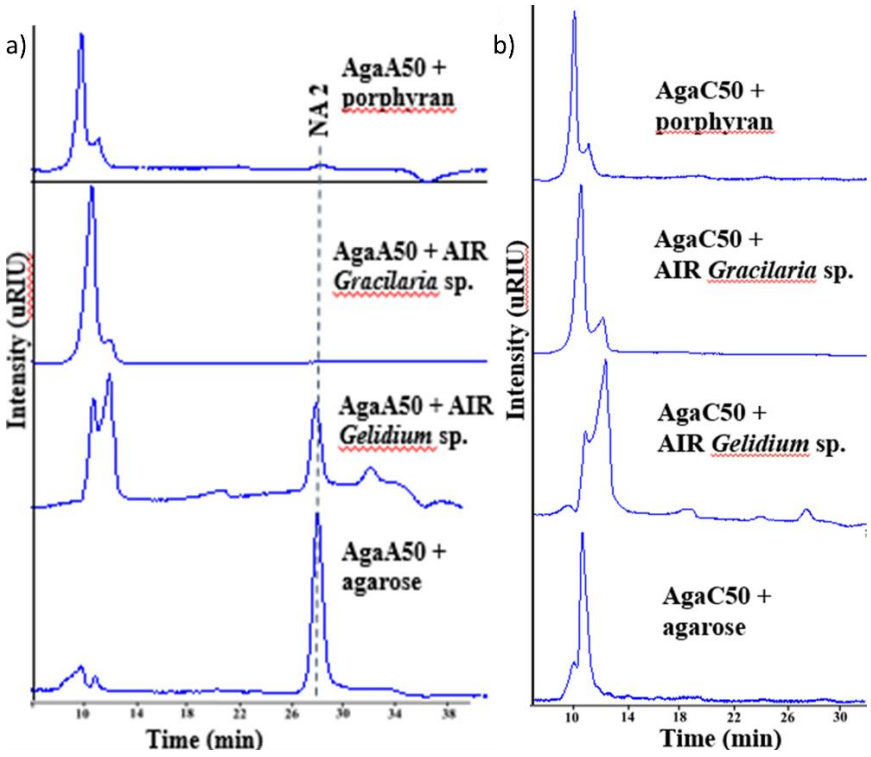

Figure 5.22. **Instrumental analysis of the PORT2 exo-agarases on different agar polymers 0.2% w/v in ultrapure water, monitored by HPLC-RID**; **a**) AgaA50 releases neoagarobiose (NA2) from agarose and AIR *Gelidium* sp., **b**) the absence of AgaC50 activity. Enzymatic reaction 24 h, 50 °C, 800 rpm, endpoint measurement. The retention times of neoagaroligosaccharide standards are: 14.6 min (NA8); 16.9 min (NA6); 20.9 min (NA4); 28 min (NA2) and 33.7 min (D-galactose).

Cascade reaction for Indonesian Agar Conversion

The experiments indicated the potential application of PORT2 recombinant agarases for NAOS production from Indonesian agar. It was substantiated by the preparation of NA2 using a cascade reaction of AgaF16A and AgaA50. In general, the reaction achieved higher NA2 conversion than a single enzymatic action of AgaA50. However, AIR *Gracilaria* sp was less converted than AIR *Gelidium* sp. Nevertheless, AIR *Gracilaria* sp conversion released shouldered NA2 different from NA2 of AIR *Gelidium* sp. that could indicate chemical structure variation (**Figure 5.23.**).

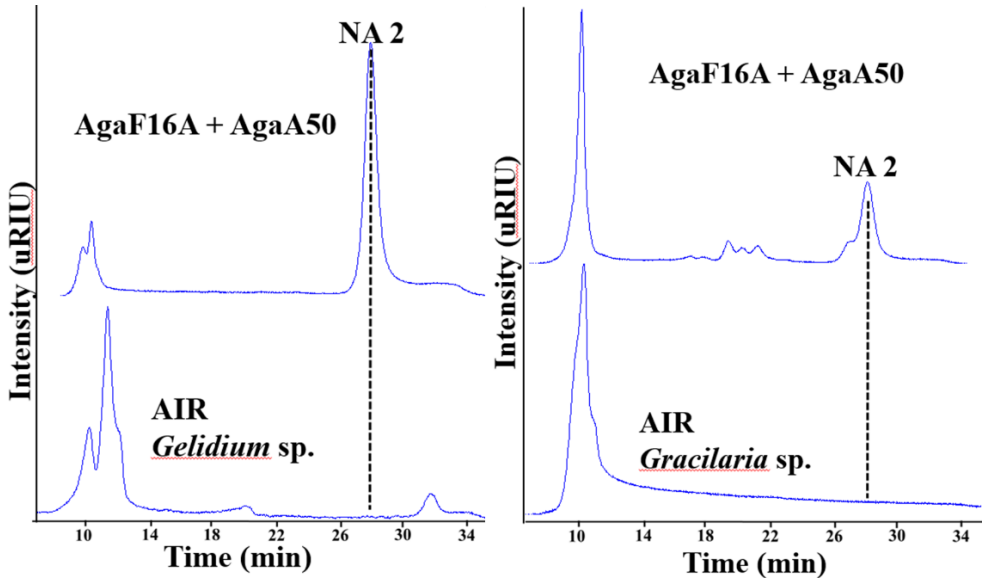

Figure 5.23. Instrumental analysis of cascade reaction products of AgaAF16A and AgaA50 with substrate concentration of 0.2% in ultrapure water at 40 °C, 24 h monitored by HPLC-RID. The cascade reaction releases neoagarobiose from AIR *Gelidium* sp. and modified neoagarobiose from AIR *Gracilaria* sp. The retention times of standards are: 14.6 min (NA8); 16.9 min (NA6); 20.9 min (NA4); 28 min (NA2).

The substrates and products from the cascade reaction were analyzed further to infer the occurrence of chemical structure modification using Fourier transform infrared spectroscopy (FTIR). FTIR qualitatively detected the presence of typical functional groups of agar backbone and the presence of additional side chains. FTIR spectra of substrates agarose and Kobe I (representing AIR *Gelidium* sp.) showed pattern similarity that was subtly different from AIR *Gracilaria* sp. (**Figure 5.24.a)**. A shouldered peak absorbance attributed to L-galactose-6-sulfate, a repeating unit of porphyrobiose in porphyran at 820 cm^{-1} was absent in all samples (Lahaye 1986).

All samples showed absorption bands around 930 and 850 cm^{-1} indicated the presence of 3,6-anhydro-linkage and axial sulfate ester at C4 of D-galactose, respectively (Lahaye 1986). The spectra between 2940-2890 cm^{-1} with a maximum peak of 2920 cm^{-1} attributed to the vibration of CH and CH_2 groups from total sugar content. The absorption bands at 1370 and 1410 cm^{-1} indicated sulfate ester (Lahaye 1986). Indeed, the cascade reaction products showed spectra with higher absorption intensity than their substrates. The AIR *Gracilaria* sp and its enzymatic product displayed a shouldered band around 1465 cm^{-1} indicating the presence of CH_2 and CH_3 groups (**Figure 5. 24.b)**.

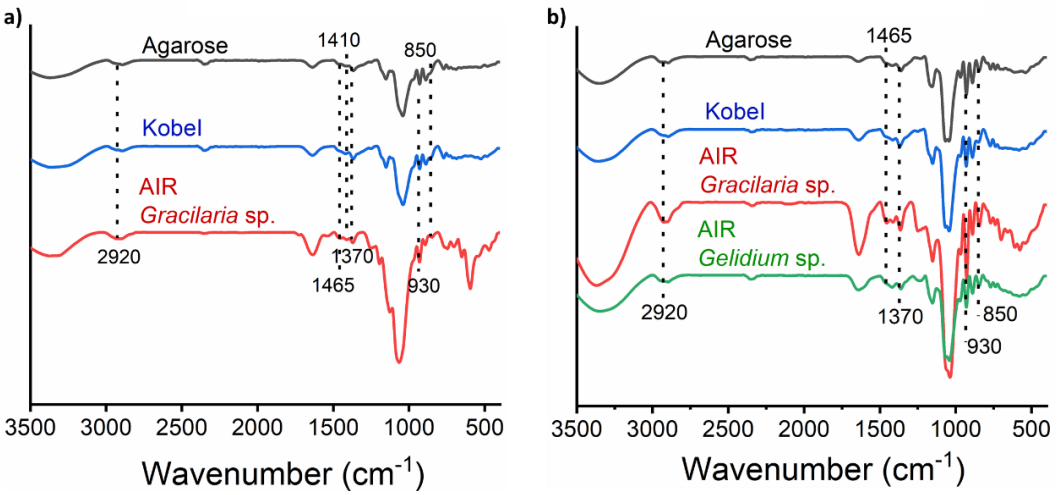

Figure 5.24. **FTIR spectra** a) substrates, b) products of cascade reaction AgaF16A and AgaA50. Enzymatic products of agarose, Kobe I and AIR *Gelidium* sp showed profiles similarities that are dfferent from AIR *Gracilaria* sp, especially at wavenumber between 500-1500 cm^{-1}. The absorption band indicated the presence : 3,6-anhydro-linkage (930 cm^{-1}); axial sulfate ester at C4 of D-galactose (850 cm^{-1}); the vibration of CH and CH_2 groups from total sugar content (2940-2890 with a maximum peak of 2920) cm^{-1}; sulfate ester (1370 and 1410) cm^{-1}; CH_2 and CH_3 groups (shouldered band at 1465 cm^{-1}).

5.2. Discussion

The previous chapter describes *in silico* characterization of six putative β-agarases in PORT2. Five of them have been successfully overexpressed in the *E. coli* system and characterized. This chapter reports the characterization and potential application of those recombinant agarases.

Two recombinant agarases, AgaB50 and AgaF16A qualitatively displayed activity on an agarose gel. During the characterization, both enzymes demonstrate an endo-β-1,4-agarolytic activity by performing internal cleavage that is indicated by the formation of mixed-size products. However, AgaB50 and AgaF16A show distinct product patterns indicating not only a different endo-action but also probably their cellular role (Arnal et al. 2019).

Even though AgaF16A has slightly fewer hydrophobic tryptophan residues than AgaB50 within the substrate-binding site, it shows a rapid final-size product formation since the beginning of the reaction indicating an endo-processive action in which the enzyme maintains substrate attachment during the subsequent reaction to increasing conversion efficiency. This assumption is contradicting to Matsuzawa et al. (2014) and Arnal et al. (2019) that have found the increasing number of

hydrophobic residues tryptophan positively correlates with endo-processivity of xyloglucanase GH74 from *Geotrichum* sp. and *Paenibacillus* KM21. A substrate topology that is adapted to a longer substrate may contribute to better processivity of AgaF16A.

The presence of SPI and 2 CBMs in AgaF16 (AgaF16A) suggests extracellular localization and indicates cell wall-targeting function. Therefore, AgaF16 (AgaF16A) is proposed as substrate-sensing machinery to upregulate the interrelated agarases system in PORT2. Besides, the processivity of AgaF16A enables the initial rapid release of highly diffusible NA6 or NA4 from agar. Those oligosaccharides act as signal inducers to up-regulate the cognate agarases and switch on the agarolytic concert (Van der Meulen and Harder 1976; Arnal et al. 2019).

The possible cognate agarases are AgaA50, AgaC50, and AgaB50. The N-terminus lipoprotein signal peptide (SPII) indicates their presence as membrane-bound proteins. The negative effect of anionic detergent on their activities also possibly signalize their membrane-bound characteristics (Gennity and Inouye 1991; Walker 2009; Finnegan and Percival 2015). They share similar actions as an exo-β agarase. This mode of action performs a glycosidic cleavage from the end chain of the substrate which releases a single product size. In particular, AgaB50 depicts a conditional exo-endo-β-agarase action. The enzyme probably also has a transglycosylation activity depends on the substrate size.

Homology modeling has been used to visualize theoretical structures of PORT2 recombinant agarases for the identification of key amino acid residues involved in different agarolytic action. Even though this technique is not as accurate as experimental X-Ray crystallography, it has been highlighted as a viable method for predicting the structural and molecular function of an unknown protein. In general, PORT2 GH50s structures resembled the template SdAga50D, especially AgaA50. AgaA50 and AgaC50 displayed an end-blocked substrate-binding tunnel and needed a divalent metal ion as a cofactor. Yet, AgaA50 and AgaC50 show higher temperature activity and stability at 50 °C than the template (Kim et al. 2010).

Studies on conserved amino acid mutations within enzymes have suggested that alteration of those residues does not always decimate the enzyme activity but

probably only modifies the wild-type mechanisms. The type of enzyme and amino acid substitution define the effect of the mutation (Peracchi 2001; Betts and Russel 2003). The AgaC50 displays substantial amino acid mutations within the substrate-binding site. The mutated residues showed different properties and chemical reactivity that can affect their interaction with water and substrate. The effect of mutation is exemplified by tryptophan mutation into glycine. The tryptophan is responsible for hydrophobic interaction with the 3,6 anhydro-α-L-galactose at the +3 subsite (Pluvinage et al. 2013). The AgaC50 also displays amino acid deletions at the tunnel roof formed by the CBM-like domain. Thus, the tunnel becomes more opened and shorter. Together, those modifications probably disrupt enzyme-substrate interactions and contribute to feeble activity and extreme substrate specificity of AgaC50.

Indeed, AgaC50 is not the only weak glycosidase in the GH50 family, BpGH50 (β-agarase from *Bacteroides plebeius)* also displays deficient agarase or porphyranase activity even though the catalytic site remains conserved. Notably, BpGH50 is lacking the CBM-like domain, therefore some substrate-binding residues within this part are not available. Nevertheless, they have proposed that the enzyme might need a hybrid structure of substrates such as porphyrobiose-agarobiose which has not been produced yet by any porphyranase or agarase (Giles et al. 2017). Indeed, AgaC50 and BpGH50 instantiate the important role of the CBM-like domain to support the catalytic activity.

Different from AgaC50, the AgaB50 model specifies structure modification vindicates the exo-endo-action capability. Some amino acids at the end-blocked of the substrate-binding tunnel and the CBM domain-like forming the tunnel-roof have been deleted. Notably, the aspartic acid that is located at the tunnel end and responsible for hydrophobic interaction with 3,6 anhydro-α-L-galactose at -2 subsite (Pluvinage et al. 2013). These modifications may create an open-end short tunnel topology that possibly augments binding affinity for the longer substrate. As a consequence, the activity mode of AgaB50 is modified drastically from a pure exo- into exo-endo-agarase. In this context, it is indispensable to highlight that probably not only a mode of action that is altered but also the hydrolysis/transglycosylation equilibrium indicated by the increase/decrease of

product formation (NA4 and NA2) at a certain time reaction frame (between 4 to 5 hours reaction).

Another recombinant agarase, AgaD86T represents the partial part of AgaD86. The model-template superposition indicated that AgaD86T probably typifies an endo-β-agarase with a concave active site topology. This assumption is attributed to the presence of similar substrate-binding residues in AgaD86T except for two missing residues homologous to T82 and Q138 from BuGH86E322Q.

Homology modeling also indicates the oligomerization possibility of the quaternary structures of PORT2 agarases. The BN-PAGE has been developed for the characterization of protein oligomerization properties while retains protein functionality. Protein migration on BN-PAGE reflects not only the size but also its conformation. The BN-PAGE displays significantly smaller sizes of AgaA50 and AgaB50. Those proteins probably have an oligomeric state with compact monomeric conformation that allows higher mobility than on denaturing SDS PAGE (Niepmann 2007). Therefore, their sizes are smaller than the calculated sizes. In contrast, AgaF16A mobility only indicates a dimeric state at the size of around 62 kDa.

Enzymatic saccharification needs to consider the physicochemical properties of agar. Solid agar particles are dispersed continuously in the water phase at sol state temperature (>43 °C). When the temperature cools down, the agars enter the gel state by forming continuous polymer networks that entrap water in each cavity. Generally, the sol state provides more access for agarases to hydrolyze the polymer (Kim et al. 2017). Therefore, agarases with high-temperature activity or with high thermostability are preferred for industrial applications (Chi et al. 2019; Park et al. 2020).

Up to date, only three thermostable agarases are from the GH50 family, none is from Aga86 and the rest are members of GH16 such as Raga7 from deep-sea *Microbulbifer* JAMB A7 or AgaA from *Microbulbifer thermotolerans* JAMBA94. The Raga7 and AgaA work optimum at 55 °C. They produce NA4 as the main product. Thiol reagents, SDS 2%, EDTA 100 mM, or metal ions that commonly present in seawater do not affect their activity (Ohta et al. 2004). (Park et al. 2020).

Moreover, most of them have been isolated from organisms that adapt to unique niches such as AgaA from a deep-sea *Microbulbifer thermotolerans* JAMBA94 (Ohta et al. 2004) and AgaL4 from saltwater hot spring *Microbulbifer pacificus* LD25 (Chen et al. 2019). Thermostable agarase originates from a mesophilic organism is an exception, such as AgaW from *Cohnella* sp LGH and AgaB-4 from *Paenibacillus agarexedens*. Indeed, both of them are mesophilic soil bacteria representing a unique niche for agarases (Li et al. 2015; Chen et al. 2018).

Notably, deriving from a mesophilic marine bacterium, PORT2 recombinant agarases demonstrate thermostable characteristics. They are active at a high temperature between 50-60°C and maintain more than 75% of activity after 1 h incubation at 50 °C except for AgaC50. AgaF16A characteristics are comparable to Raga7 from deep-sea *Microbulbifer* JAMB A7 or AgaA from *Microbulbifer thermotolerans* JAMBA94. However, the AgaL4 from *M. pacificus* LD25 is still superb among known thermostable GH50 agarases includes PORT2 GH50s.

The effects of different metal ions and additives on PORT2 recombinant agarases were also tested to elucidate their potential for industrial applications. The AgaA50 and AgaC50 demonstrate activity enhancement by divalent ion Ca^{2+} and Mg^{2+}, respectively, while EDTA negatively affects the activities, thus corroborating their metal-dependent-protein characteristics (Klebe 2013; Pereira et al. 2017). Meanwhile, AgaF16A shows tolerance to SDS and metal ions normally present in seawater. Specifically, DTT or β-mercaptoethanol increases the enzymatic activity of AgaF16A two-folds. Different from AgaF16A, in other cases, the increase is due to the protection of thiol groups within the enzyme structure by the reducing agents. Exemplary are β-agarase RAgaA7 from *Microbulbifer* sp. JAMB A7 and rHZ2 from *Agarivorans* sp. HZ105 (Ohta et 2004; Lin et al. 2012). Hence, how the thiol reagent could positively affect AgaF16A activity in the absence of thiol or cysteine is still unclear. In contrast, AgaB50 is sensitive to all tested metal ions and chemicals. Specifically, Ni^{3+} inhibits the activities of AgaA50 and AgaC50. Despite having different nickel ion states, Ni-NTA purification probably could affect the enzymes negatively. Therefore, other purification methods should be considered for further work.

Agar-derived-oligosaccharides have been seen as potential feedstock for seaweed-based biofuels (Park et al. 2020). Moreover, many potential bioactivities of agar-

derived saccharides also have been elucidated and confirmed to be non-toxic and generally recognized as safe (GRAS) (Hong et al.2017). A mixture of NA4 and NA6 remarkably shows anti-obesity and anti-diabetic effects (T2DM) (Hong et al. 2017). NAOS mixture is also proven as a potential immunomodulator (Park et al. 2014; Kang et al. 2017; Lee et al. 2017; Wang et al. 2017). Individually, NA4 and NA6 indicate convincing anti-inflammatory and anti-tumor activities in the mouse model (Wang et al. 2017; Park et al. 2014 Lee et al. 2017). NA4 also exhibits a potent hydroxyl radical scavenging activity and a higher moisturizing power than glycerol and hyaluronic acid (Kobayashi et al. 1997). A potential application of NA4 as a prebiotic or hepatic-recovery agent is also reported (Zhang et al. 2017). NA2 shows potential anti melanogenesis activity for a skin-whitening agent (Kobayashi et al. 1997; Lee et al. 2008; Yun et al. 2013). The influence of sulfate content on the biological activities of marine macro algae polysaccharides also has been reported (Pomin et al. 2008; Patel 2012). Indeed, nutrient availability, hydrodynamic condition, producing-species, harvesting period, and method of extraction affect the characteristics of agar and its derived saccharides (Usov 2011; Sousa et al. 2013).

The performance of PORT2 recombinant agarases for Indonesian agar conversion into agar derived sugars is substantiated using AIR *Gelidium* sp. and *Gracilaria* sp. Qualitatively, AIR *Gelidium* sp shows more gel strengths characteristics than AIR *Gracilaria* sp. In general, the PORT2 agarases prefer less side-chain masking substrate indicated by stronger gelling properties. Indeed, the FTIR analysis indicates more pronounced sulfate and methyl masking in AIR *Gracilaria* sp. and its enzymatic products than in AIR *Gelidium* sp. The agarases hydrolyze AIR *Gelidium* sp into NA6; NA4; and NA2, and AIR *Gracilaria* sp hydrolysis results in modified NA6 and NA4. Among recombinant agarases PORT2, AgaF16A characteristic and mode of action show compatibility to AgaA50. A cascade reaction of AgaF16A and AgaA50 converts AIR *Gelidium* sp into NA2 and AIR *Gracilaria* sp into modified NA2. The NAOS from Indonesian agars indicates enrichment of sulfate and methyl, promising the possibility of new potential biological activity. Notably, the kinetic parameters of those enzymes need to be redefined for the appropriate application.

The complex structure of agar requires concerted agarases for efficient depolymerization. Thus, several agarases are commonly found within an agarolytic organism. The presence of GH50 and GH86 in PORT2 shows gene duplication. Maintaining the duplication is a costly event since it may cause higher energy consumption and reduce the organism's fitness significantly (Wagner 2005; Qian and Zhang 2008). Indeed, the characterization of the PORT2 GH50s depicted structural and functionality divergence. Hence, apart from the potential application perspective, each agarase enzyme indicates a different role for the ecological fitness of PORT2.

In general, agarolytic bacteria use two-steps agar degradation pathways. The first pathway is responsible for cleaving agar polymer into the smallest repeating unit, neoagarobiose or agarobiose. The second pathway converts the agar disaccharides into D-galactose and 3,6-α-anhydro L-galactose for cell growth and maintenance. In particular, the 3,6-α-anhydro L-galactose is an unfavorable carbon source for general microorganisms. Only agarolytic organisms can utilize this unique sugar. This study has elucidated the first-step agar degradation pathway in PORT2. The pathway employs a concert of extracellular thermostable β-agarases. However, genome profiling is unable to unveil the presence of canonical enzyme machinery responsible for the second pathway, such as α-neoagarobiose hydrolase (NABH) or α agarase. On the other hand, the genome profile depicts the presence of putative 3,6-α-anhydro L-galactose degradation pathway. Moreover, some hypothetical proteins with unknown functions present in the vicinity of agarase genes and putative genes for 3,6-α-anhydro L-galactose degradation, suggesting possible availability of unknown NABH-like enzyme(s). Indeed, the ability of PORT2 to use agar as a sole carbon source signalizes the existence of a complete agar degradation system.

6. Conclusions and Outlooks

Agar is a marine heteropolysaccharide with repeating units consists of 3,6-α-anhydro-L-galactopyranose and D-galactopyranose linked by α-(1,3) and β-(1,4) linkages. Agar-derived saccharides have been promoted as a prospective replacement for petroleum-based feedstock. Some studies have revealed their biological activity emphasizing their potential not only as biofuels feedstock but also for other applications.

Agar-producing macro algae are one of Indonesia's national commodities. However, high added-value products from the agars are rarely developed in Indonesia. Enzymatic biotransformation of agar offers high specific product generation and more environmentally friendly than chemical hydrolysis. The development of industrial biotechnology for producing added-value products from the agars demands infrastructure and research efforts. One crucial part of the research needs to establish is bio agents, the organism, and/or the enzyme.

Agarases are glycoside hydrolases for catalyzing the cleavage of agar into sugar derivatives via an inverting or retaining mechanism. The enzymes differentiate into β- and α-agarase with endo-or exo-catalytic action. They are classified into several families. Up to date, more β-agarases has been characterized and structurally elucidated than α-agarase. The GH16-16, GH50, and GH86 are families for retaining β-agarase. The only inverting β-agarase family is GH118. Known α-agarases have an inverting mechanism. GH96 is the endo-α-agarase and GH117 is an exo-α-agarase family.

A mesophilic gram-negative marine bacterium had been isolated from Batu Karas seawater, Pangandaran, West Java, Indonesia. Biochemical and molecular identification classify this bacterium as a new strain of *Microbulbifer elongatus*. Notably, this species is known as agarolytic bacteria and plays a role as marine polymers degrader. The bacterium is designated as *Microbulbifer elongatus* PORT2. PORT2 encodes a β-agarolytic pathway. It consists of AgaF16 from GH16; AgaA50, AgaB50, and AgaC50 from GH50; AgaD86 and AgaE86 from GH86.

Two agarases, AgaF16 and AgaE86 signalize their presence as extracellular agarases showing complex modularity by having signal peptide, agarase domain, and more than one carbohydrate-binding domain (CBMs). On the other hand, the GH50 and AgaD86 structure consist of an agarase domain and a signal peptide which indicates membrane-bound characteristics.

The AgaF16A, GH50s, and AgaD86T have been successfully expressed in *E.coli* and further characterized. AgaF16A shows endo-β-agarase activity releasing NA4 and NA6 from agarose and NAOS larger than NA6. Without any cysteine residues, AgF16A shows distinct stability upon reducing agents. Remarkably, the GH50 agarases display profound *in silico* structure modification explaining the mode of action divergent and substrate-product specificity. AgaB50 displays endo-exo-β agarase action. It releases NA6, NA4, and NA2 from agarose but only NA2 from NAOS larger than NA2. In contrast, AgaA50 and AgaC50 show pure exo-β-agarase actions and release NA2 as a product. Regrettably, the functionality of GH86 in PORT2 could not be elucidated in this study.

Despite originating from a mesophilic bacterium, PORT2 recombinant agarases display comparable characteristics to the known 50 °C thermostable agarases. Except for AgaB50, the activity of all the characterized recombinant agarases from PORT2 is enhanced by an appropriate concentration of Ca^{2+} or Mg^{2+}. The agarases releases not only typical agar-derived saccharides neagarohexaose (NA6), neoagarotetraose (NA4), neoagraobiose (NA2) but also the modified ones from Indonesian natural agar which promising potential novel bioactivity. In particular, the cascade reaction of AgaF16A and AgaA50 resulted in a higher conversion of Indonesian agar into NA2 or modified NA2.

Generally, a β-agarolytic organism encodes two-stage agar degradation pathways. The first pathway hydrolyzes agar polymer into the smallest repeating unit neoagarobiose (NA2). The second pathway breaks down of α-glycosidic bonds of the NA2 to release agar monomers, D-galactose, and 3,6 α-anhydro-L-galactopyranose. The first agarolytic pathway of PORT2 is a β-agarase system similar to other agarolytic *Gammaproteobacteria* such as *Saccharophagus degradans* 2-40 and *Catenovulum agarivorans* YM01. Comparative genome analysis indicates GH50 and GH86 as protein markers for agarolytic *Gammaproteobacteria*.

However, PORT2 and other agarolytic *Microbulbifer* species lack any α-agarase, either GH117 or GH96. PORT2 probably could have an alternative pathway or machinery to substitute the second agarolytic pathway or the canonical role of GH117. This hypothesis is based on the experimental evidence of agar utilization as a sole carbon source while either GH96 or GH117 is absent and also the presence of hypothetical proteins in the vicinity of agarases genes clusters of the bacterium.

This research contributes mainly to establish a basic knowledge of the agar degradation system in PORT2 that can represent other agarolytic *Microbulbifer*. It becomes preliminary results for agar biotechnology development in Indonesia and also generates a bait for the discovery of new neoagarobiose hydrolase-like enzymes.

Future experiments need to be oriented in some directions to support the valorization of agar-based research in Indonesia. Functional elucidation of GH86s and characterization of modified NAOS bioactivity will enlarge the potential application of PORT2 agarases and its agar-derived saccharides. The absence of GH117 provides the opportunity for discovering new enzyme substitute(s). The development of enzyme immobilization technology will improve the efficiency of conversion cycles and ease the downstream process handling. Finally, bioprocess engineering will provide great assistance in assessing the feasibility of an industrial application for agar-derived saccharides production.

References

Abbott, D.W., and van Bueren, A.L. (2014). Using structure to inform carbohydrate binding module function. *Curr. Opin. Struct*. Biol. 28, 32–40.

Alderkamp A.C., Rijssel M.V., Bolhuis H. (2007). Characterization of marine bacteria and the activity of their enzyme systems involved in degradation of the algal storage glucan laminarin. *FEMS Microbiol. Ecol.* 59 108–117. Doi: 10.1111/j.1574-6941.2006.00219.x.

Allouch, J., Jam., M., Helbert, W., Barbeyron, T., Kloareg., B., Henrissat, B., Czjzek, M. (2003). The three-dimensional structures of two β-agarases. *J. Biol. Chem*. 278, 47171–47180.

Allouch, J., Helbert, W., Henrissat, B., Czjzek, M. (2004). Parallel substrate binding sites in a β-agarase suggest a novel mode of action on double-helical agarose. *Structure* 12, 623–632.

Anzai Y., Kim H., Park J.Y., Wakabayashi H., Oyaizu H.(2000). Phylogenetic affiliation of the *Pseudomonads* based on 16S rRNA sequence. *Int J Syst Evol Microbiol*.;50: 1563–1589. 10.1099/00207713-50-4-1563.

Armisén, R. (1991). Agar and agarose biotechnological applications. *Hydrobiologia* 221, 157–166. doi:10.1007/BF00028372.

Arnal, G., Stogios, P. J., Asohan, J., Attia, M.A., Skarina, T., Viborg, A.H., Henrissat, B., Savchenko, A., Brumer, H. (2019). Substrate specificity, regiospecificity, and processivity in glycoside hydrolase family 74. *The Journal of Biological Chemistry*, *294*(36), 13233–13247. doi:10.1074/jbc.RA119.009861.

Arnosti C. (2010). Microbial extracellular enzymes and the marine carbon cycle. *Ann. Rev. Mar Sci.* 3 401–425. doi:10.1146/annurev-marine-120709-142731.

Arnosti C. (2014). Patterns of microbially driven carbon cycling in the ocean: links between extracellular enzymes and microbial communities. *Adv. Oceanogr.* 2014 1–12. doi:10.1155/2014/706082.

Attia, M. A., Nelson, C. E., Offen, W. A., Jain, N., Davies, G. J., Gardner, J. G., Brumer, H. (2018). *In vitro* and *in vivo* characterization of three *Cellvibrio japonicus* glycoside hydrolase family 5 members reveals potent xyloglucan backbone-cleaving functions. *Biotechnol. Biofuels* 11, 45.

Baker D.C., Defaye J., Horton D., Hounsell E.F., Kamerling J.P., Serianni A.S. (1997). Nomenclature of Carbohydrates. *Carbohydrate Research*. 297 (1): 1. doi:10.1016/S0008-6215(97)83449-0.

Barbeyron T., L'Haridon S., Corre E., Kloareg B., Potin P. (2001). Zobellia galactanivorans gen. nov., sp. nov., a marine species of *Flavobacteriaceae* isolated from a red alga, and classification of *Cytophaga uliginosa (ZoBell* and *Upham* 1944*)* Reichenbach 1989 as *Zobellia uliginosa gen. nov., comb. nov. Int J Syst Evol Microbiol.* 51 (Pt 3): 985–97. doi*:*10.1099/00207713-51-3-985

Barcelos M.C.S., Lupki F.B., Campolina G.A., Nelson D.L., Molina G. (2018). The colors of biotechnology: general overview and developments of white, green, and blue areas. *FEMS Microbiol Lett*. 365(21):230–39.

Benkert, P., Biasini, M., Schwede, T. (2011). Toward the estimation of the absolute quality of individual protein structure models. *Bioinformatics* 27, 343-350.

Berlemont, R., Martiny, A.C. (2015). Genomic potential for polysaccharide deconstruction in bacteria. *Applied and environmental microbiology*, 81(4), 1513–1519. doi:10.1128/AEM.03718-14.

Bertoni, M., Kiefer, F., Biasini, M., Bordoli, L., Schwede, T. (2017). Modeling protein quaternary structure of homo- and hetero-oligomers beyond binary interactions by homology. *Scientific Reports* 7.

Betts, M.J., Russell, R. B. (2003). Amino acid properties and consequences of substitutions. *In* M. R. Barnes, & I. C. Gray (Eds.), *Bioinformatics for geneticists.* pp. 289-316.

Bharathi P.A.L., Nair S., Chandramohan D. (2001). Marine microbiology-a glimpse of the strides in the Indian and the global arena (Chapt. 14) *in* The Indian Ocean: a Perspective. Vol 2; p: 495-538. ISBN 90 5809 224 0.

Black G.W., Rixon J.E., Clarke J.H., Hazlewood G.P., Theodorou M.K., Morris P., Gilbert H.J. (1996). Evidence that linker sequences and cellulose-binding domains enhance the activity of hemicellulases against complex substrates. *Biochem J*. 319:515–520.

Biasini, M., Bienert, S., Waterhouse, A., Arnold K., Studer G., Schmidt T., Kiefer F., Cassarino T.G., Bertoni M., Bordoli L., Schwede T. (2014). SWISS-MODEL: Modelling protein tertiary and quaternary structure using evolutionary information. *Nucleic Acids Research*. 42. W252–W259.

Boni, I.V., Isaeva, D.M., Musychenko, M.L., Tzareva, N.V. (1991). Ribosome-messenger recognition: mRNA target sites for ribosomal protein S1. *Nucleic acids research*, *19*(1), 155 -162. doi:10.1093/nar/19.1.155.

Burke, C., Steinberg, P., Rusch, D., Kjelleberg, S., Thomas, T. (2011). Bacterial community assembly based on functional genes rather than species. *Proc Natl Acad Sci USA*. 108(34), 14288–14293. doi:10.1073/pnas.1101591108.

Camacho C.L., Coulouris G., Avagyan V., Ma N., Papadopoulos J., Bealer K., Madden T.L. (2009). BLAST+: architecture and applications. *BMC Bioinformatics.* 10:421.

Chen Z.W., Lin H.J., Huang W.C., Hsuan S.L., Lin J.H., Wang J.P. (2018). Molecular cloning, expression, and functional characterization of the β-agarase AgaB-4 from *Paenibacillus agarexedens*. *AMB Express* 8(1):49.

Chen Y.P., Wu H.T., Wang G.H., Wu D.Y., Hwang I.E., Chien M.C., Pang H.Y., Kuo J.T., Liaw L.L. (2019). Inspecting the genome sequence and agarases of *Microbulbifer pacificus* LD25 from a saltwater hot spring. *J Biosci Bioeng* 127(4):403–410.

Chi, W.J., Chang, Y.K., Hong, S.K. (2012). Agar degradation by microorganisms and agar-degrading enzymes. *Appl. Microbiol. Biotechnol.* 94, 917 – 930.

Cobo-Simón, M., & Tamames, J. (2017). Relating genomic characteristics to environmental preferences and ubiquity in different microbial taxa. *BMC genomics*, *18*(1), 499. doi:/10.1186/s12864-017-3888-y.

Correc G., Hehemann J.H., Czjzek M., Helbert W. (2011). Structural analysis of the degradation products of porphyran digested by *Zobellia galactanivorans* β-porphyranase A. *Carbohydr. Polym*.;83:277–283. doi: 10.1016/j.carbpol.2010.07.060.

Cottrell M.T., Kirchman D.L. (2016). Transcriptional control in marine copiotrophic and oligotrophic bacteria with streamlined genomes. *Appl EnvironMicrobiol* 82:6010–6018. doi:10.1128/AEM.01299-16.

Czech, L., Hermann, L., Stöveken, N., Richter, A. A., Höppner, A., Smits, S., … Bremer, E. (2018). Role of the Extremolytes Ectoine and Hydroxyectoine as Stress Protectants and Nutrients: Genetics, Phylogenomics, Biochemistry, and Structural Analysis. *Genes*, *9*(4), 177. doi:10.3390/genes9040177.

David, B., Irague, R., Jouanneau, D., Daligault, F., Czjzek, M., Sanejouand, Y..H., Tellier, C. (2017). Internal water dynamics control the transglycosylation/hydrolysis balance in the agarase (AgaD) of *Zobellia galactanivorans*. *ACS Catal.* 7: 3357– 3367. doi: 10.1021/acscatal.7b00348.

Davidson A.L., Chen J. (2005). Structural biology. Flipping lipids: is the third time the charm?. *Science* .308 (5724); 963-5.

Davies G., Henrissat, B. (1995). Structures and mechanisms of glycosyl hydrolases. *Structure* 3, 853–859.

Davies G. J., Wilson, K. S., Henrissat, B. (1997). Nomenclature for sugar-binding subsites in glycosyl hydrolases. *The Biochemical journal*. 321 (Pt2) (Pt2). 557–559. doi:10.1042/bj3210557.

Davies G.J., Gloster T.M., Henrissat B. (2005). Recent structural insights into the expanding world of carbohydrate-active enzymes. *Curr. Opin. Struc. Biol*. 15: 637–645. doi: 10.1016/j.sbi.2005.10.008.

Davies G.J., Williams S.J. (2016). Carbohydrate-active enzymes: sequences, shapes, contortions, and cells. *Biochem. Soc. Trans*. 44: 79–87.

Day D.F., Yaphe W. (1975). Enzymatic hydrolysis of agar: purification and characterization of neoagarobiose hydrolase and p-nitrophenyl alpha- galactoside hydrolase, *Can. J. Microbiol*. 21 1512–1518.

Delattre, C., Michaud, P., Courtois, B., Courtois, J. (2005). Oligosaccharides engineering from plants and algae applications in biotechnology and therapeutics. *Minerva Biotec*. 17: 107-117.

De Long E.F., Karl D.M. (2005). Genomic perspectives in microbial oceanography. *Nature* 437(7057):336–342.

De Villegas M.E.D. (2007) Biotechnological Production of Siderophores. In: Varma A., Chincholkar S.B. (eds) Microbial Siderophores. Soil Biology, vol 12. Springer, Berlin, Heidelberg.

Dong Q., Ruan L., Shi H. (2016). A β-agarase with high pH stability from *Flammeovirga* sp. *SJP92*. *Carbohydr Res*.;432:1–8. doi: 10.1016/j.carres.2016.05.002.

Edgar, R.C. (2004). MUSCLE: multiple sequence alignment with high accuracy and high throughput. *Nucleic Acids Research*. 32(5), 1792-97.

Ekborg, N.A. (2005). The agarase system of *Saccharophagus degradans* 2-40: Analysis of the Agarase System and Protein Location. *Dissertation*. University of Maryland.

Enke T.N., Datta M.S., Schwartzman J., Cermak N., Schmitz D., Barrere J., Pascual-García A., Cordero O.X. (2019). Modular assembly of polysaccharide-degrading marine microbial communities. *Curr Biol*. 29:1528–1535. doi:10.1016/j.cub.2019.03.047.

Ekborg N.A., Gonzalez J.M., Howard M.B., Taylor L.E., Hutcheson S.W., Weiner R.M. (2005). *Saccharophagus degradans* gen. nov., sp. nov., a versatile marine degrader of complex polysaccharides. *Int. J. Syst. Evol. Microbiol.* 55 1545–1549. 10.1099/ijs.0.63627-0.

Elkahlout K., Alipour S., Eroglu I., Gunduz U., Yucel M. (2017) Long-term biological hydrogen production by agar immobilized *Rhodobacter capsulatus* in a sequential batch photobioreactor. *Bioprocess Biosyst Eng* 40(4):589–599.

Fiala, G. J., Schamel, W. W., & Blumenthal, B. (2011). Blue native polyacrylamide gel electrophoresis (BN-PAGE) for analysis of multiprotein complexes from cellular lysates. *Journal of visualized experiments: JoVE*, (48), 2164. doi:10.3791/2164.

Ferdouse F., Holdt S.L., Smith R., Murúa P., Yang Z. (2018). The global status of seaweed production, trade, and utilization – FAO.Volume 124.

Finnegan, S., Percival, S. L. (2015). EDTA: An Antimicrobial and Antibiofilm Agent for Use in Wound Care. *Advances in wound care*. 4(7). 415–421. doi:10.1089/wound.2014.0577.

Fiser, A. (2010). Template-based protein structure modeling. *Methods in Molecular Biology*. 673, 73–94.

Furusawa, G., Lau, N. S., Suganthi, A. and Amirul, A.A.A. (2017) Agarolytic bacterium *Persicobacter* sp. CCB-QB2 exhibited a diauxic growth involving galactose utilization pathway. *MicrobiologyOpen* 6.

Gennity, J. M. and Inouye, M. (1991) The protein sequence responsible for lipoprotein membrane localization in *Escherichia coli* exhibits remarkable specificity. 266, 16458–16464.

The Authors and Curators of CAZypedia. Glycoside Hydrolase Family 16. (2019, September 25). *CAZypedia, © 2007-2019* Retrieved 17:02, January 4, 2020 from http://www.cazypedia.org/index.php?title=Glycoside_Hydrolase_Family_16&oldid=14289.

Genicot-Joncour, S., Poinas, A., Richard, O., Potin, P., Rudolph, B., Kloareg, B., Helbert, W. (2009). The cyclization of the 3,6-anhydro-galactose ring of iota-carrageenan is catalyzed by two D-galactose-2,6-sulfurylases in the red alga Chondrus crispus. *Plant physiology*, *151*(3), 1609–1616. doi:10.1104/pp.109.144329.

George, R. A., Heringa, J. (2002). An analysis of protein domain linkers: their classification and role in protein folding. *Protein Engineering, Design and Selection, 15(11), 871–879.* doi:10.1093/protein/15.11.871.

Giles, K. , Pluvinage B., Boraston A.B. (2017). Structure of a glycoside hydrolase family 50 enzyme from a subfamily that is enriched in human gut microbiome *Bacteroidetes*. *Proteins*. 85: 182–187.

Goris J., Konstantinidis K.T., Klappenbach J.A., Coenye T., Vandamme P., Tiedje J.M.(2007). DNA-DNA hybridization values and their relationship to whole-genome sequence similarities. *Int J Syst Evol Microbiol*.57.(Pt 1):81-91.

Guerrero C., Vera C., Serna N., Illanes A. (2017) Immobilization of *Aspergillus oryzae* β-galactosidase in an agarose matrix functionalized by four different methods and application to the synthesis of lactulose. *Bioresour Technol*. 232:53–63

Guiseley K.B. (1970). The relationship between methoxyl content and gelling temperature of agarose. *Carbohydr. Res*. 13: 247–256.

Guruprasad, K., Reddy, B.V.B. and Pandit, M.W. (1990) Correlation between stability of a protein and its dipeptide composition: a novel approach for predicting in vivo stability of a protein from its primary sequence. *Protein Eng*. 4,155-161.

Gurvan, M., Czjzek, M. (2013). Polysaccharide-degrading enzymes from marine bacteria, *in* Marine Enzymes for Biocatalysis, ed. A. Trincone (Cambridge: Woodhead Publishing). doi: 10.1533/9781908818355.3.429.

Ha S.C., Lee S., Lee J., Kim H.T., Ko H.J., Kim K.H., Choi I.G. (2011). Crystal structure of a key enzyme in the agarolytic pathway, α-neoagarobiose hydrolase from *Saccharophagus degradans* 2-40. *Biochem. Biophys. Res. Commun*. 412:238–244.

Hehemann J.H., Correc G., Barbeyron T., Helbert W., Czjzek M., and Michel G. (2010). Transfer of carbohydrate-active enzymes from marine bacteria to Japanese gut microbiota. *Nature*. 464, 908–912 10.1038/nature08937.

Hehemann, J.H., Smyth, L., Yadav, A., Vocadlo, D.J., & Boraston, A.B. (2012a). Analysis of keystone enzymes in agar hydrolysis provides insight into the degradation of a polysaccharide from red seaweeds. *The Journal of biological chemistry*. *287*(17), 13985–13995. doi:10.1074/jbc.M112.345645.

Hehemann, J.H., Correc, G., Thomas, F., Bernard, T., Barbeyron, T., Jam, M., Helbert, W., Michel, G., and Czjzek, M. (2012b). Biochemical and structural characterization of the complex agarolytic enzyme system from the marine bacterium *Zobellia galactanivorans*. *J. Biol. Chem*. 287, 30571–30584.

Hehemann, J.H., Kelly, A.G., Pudlo, N.A., Martens, E.C., & Boraston, A.B. (2012c). Bacteria of the human gut microbiome catabolize red seaweed glycans with carbohydrate-active enzyme updates from extrinsic microbes. *Proc Natl Acad Sci USA*. 109(48), 19786–19791. doi:10.1073/pnas.1211002109

Henshaw J., Horne-Bitschy A., van Bueren A.L., Money V.A., Bolam D.N., Czjzek M., Ekborg N.A., Weiner R.M., Hutcheson S.W., Davies G.J., Boraston A.B., Gilbert H.J. (2006). Family 6 carbohydrate binding modules in beta-agarases display exquisite selectivity for the nonreducing termini of agarose chains. *J. Biol. Chem*. 281:17099–17107.

Hobbie, J.E. (1988). A comparison of the ecology of planktonic bacteria in fresh and saltwater. *Limnol.Oceanogr*, 33(4, part2), 750-764.

Hong S.J., Lee J.H., Kim E.J., Yang H.J., Park J.S., Hong S.K. (2017). Antiobesity and anti-diabetic effect of neoagarooligosaccharides on high-fat diet-induced obesity in mice. *Mar Drugs* 15(4):90.

Idicula-Thomas, S., Balaji, P.V. (2005). Understanding the relationship between the primary structure of proteins and its propensity to be soluble on overexpression in *Escherichia coli*. *Protein science : a publication of the Protein Society*, *14*(3), 582–592. doi:/10.1110/ps.041009005.

Ikai, A.J. (1980).Thermostability and aliphatic index of globular proteins. *J. Biochem*. 88, 1895-1898.

Imran, M., Pant, P., Shanbhag, Y.P., Sawant, S.V., Ghadi, S.C. (**2017).** Genome Sequence of *Microbulbifer mangrovi* DD-13T Reveals Its Versatility to Degrade Multiple Polysaccharides. *Marine Biotechnol,*(19):116-124.

Jabeen, A., Mohamedali, A., Ranganathan, S. (2018). Protocol for protein structure modelling. *In* M. Cannataro, B. Gaeta, & M. Asif Khan (Eds.), *Encyclopedia of bioinformatics and computational biology* (Vol. 3, pp. 252-272). Amsterdam; Oxford; Cambridge: Elsevier. doi:10.1016/B978-0-12-809633-8.20477-9.

Jam, M., Flament, D., Allouch, J., Potin, P., Thion, L., Kloareg, B., Czjezk M., Helbert W., Michel G., Barbeyron, T. (2005). The endo-beta-agarases AgaA and AgaB from the marine bacterium *Zobellia galactanivorans*: two paralogue enzymes with different molecular organizations and catalytic behaviours. *The Biochemical journal*, 385(Pt 3), 703–713. doi:10.1042/BJ20041044.

Joint, I., Mühling, M., & Querellou, J. (2010). Culturing marine bacteria-an essential prerequisite for biodiscovery. *Microbial biotechnology*, *3*(5), 564–575. doi:10.1111/j.1751-7915.2010.00188.x.

Jonnadula, R.., Ghadi, S.C. (2011). Purification and characterization of β-agarase from seaweed decomposing bacterium *Microbulbifer* sp. Strain CMC-5. *Biotechnol Bioproc E* 16, 513–519. doi.org/10.1007/s12257-010-0399-y.

Jutur P.P., Nesamma A.A., Shaikh K.M. (2016). Algae-Derived Marine Oligosaccharides and Their Biological Applications. *Front. Mar. Sci*. 3:83. doi: 10.3389/fmars.2016.00083.

Kanai R., Haga K., Akiba T., Yamane K., Harata K. (2004). Biochemical and crystallographic analyses of maltohexaose-producing amylase from alkalophilic *Bacillus* sp 707. *Biochemistry* (Mosc), 43, 14047–14056.

Kang D.R., Yoon G.Y., Cho J., Lee S.J., Lee S.J., Park H.J., Kang T.H., Han H.D., Park W.S., Yoon Y.K., Park Y.M., Jung I.D. (2 0 1 7 .) Neoagarooligosaccharides prevent septic shock by modulating A20-and cyclooxygenase-2-mediated interleukin-10 secretion in a septic-shock mouse model. *Biochem Biophys Res Commun*. 486(4): 998–1004.

Kazimierczak P., Palka K., Przekora A. (2019) Development and optimization of the novel fabrication method of highly macroporous chitosan/ agarose/nanohydroxyapatite bone scaffold for potential regenerative medicine applications. *Biomolecules*. 9(9):434.

Kim H.T., Lee S., Lee D., Kim H. S., Bang W. G., Kim K. H., Choi I. G.(2010). Overexpression and molecular characterization of Aga50D from *Saccharophagus*

degradans 2-40. An exo-type β-agarase producing neoagarobiose. *Appl. Microbiol. Biotechnol*. 86, 227–234.

Kim J.H., Yun E.J., Seo N., Yu S., Kim D.H., Cho K.M., An H.J., Kim J.H., Choi I.G., Kim K.H. (2017). Enzymatic liquefaction of agarose above the sol-gel transition temperature using a thermostable endo-type β-agarase, Aga16B. *Appl. Microbiol. Biotechnol*. 101:1111–1120. doi: 10.1007/s00253-016-7831-y.

Klappenbach, J. A., Dunbar, J. M., Schmidt, T. M. (2000). rRNA operon copy number reflects ecological strategies of bacteria. *Applied and environmental microbiology*, *66*(4), 1328–1333. doi:10.1128/aem.66.4.1328-1333.2000.

Klebe G. (2013) Inhibitors of hydrolyzing metalloenzymes. In: Klebe G. (eds) Drug Design. Springer, Berlin, Heidelberg. doi:/10.1007/978-3-642-17907-5_25.

Knudsen N.R., Ale M.T., Meyer A.S. (2015). Seaweed hydrocolloid production: an update on enzyme assisted extraction and modification technologies. *Mar Drugs*. 13:3340–3359. doi:10.3390/md13063340.

Kobayashi R., Takisada M., Suzuki T., Kirimura K., Usami S. (1997). Neoagarobiose as a novel moisturizer with whitening effect. *Biosci Biotechnol Biochem* 61(1):162–163.

Konstantinidis K., Tiedje J.M. (2005) Genomic insights that advance the species definition for prokaryotes. *Proc Natl Acad Sci USA*. 102, 2567-2592.

Koivula A., Ruohonen L., Wohlfahrt G., Reinikainen T., Teeri T.T., Piens K., Claeyssens M., Weber M., Vasella A., Becker D., Sinnott M.L., Zou J.Y., Kleywegt G.J., Szardenings M., Ståhlberg J. and Jones T.A. (2002). The active site of cellobiohydrolase Cel6A from *Trichoderma reesei*: the roles of aspartic acids D221 and D175. *J. Am. Chem. Soc*. 124, 10 015–10 024.

Koshland D.E. (1953). Stereochemistry and the mechanism of enzymatic reactions. *Biol. Rev. Camb. Philos. Soc*, 28, pp. 416-436.

Kraan S. (2012) Algal polysaccharides, novel applications and outlook. *In*: Chang CF (ed) Carbohydrates-comprehensive studies on glycobiology and glycotechnology. InTech, Rijeka, pp 489–532.

Kredich, N.M. (1996). Biosynthesis of cysteine**.** in *Escherichia coli* and *Salmonella typhimurium*. Cellular and Molecular Biology (Ed by Neidhard FC) pp. 514-527, *American Society for Microbiology*, Washington D.C.

Krieger, E., Nabuurs, S.B., Vriend, G. (2003). Homology modeling. *Methods Biochem. Anal.* 44, 509–523. doi: 10.1002/0471721204.ch25.

Lahaye, M. (1986). Agar from *Gracilaria* spp. *Dissertation*. Faculty of Graduate Studies and Research. Department of Microbiology and Immunology McGill University, Canada. ISBN 0-315-34443-1.

Lahaye, M. (2001), Development on gelling algal galactans, their structure, and physic chemistry. *J. Appl. Phycol*. 13, 173-184.

Lahaye, M., Robic, A. (2007) Structure and functional properties of ulvan, a polysaccharide from green seaweeds . *Biomacromol*. 8 , 1765 – 1774 .

Lahaye, M., Rochas C. (1991). Chemical structure and physicochemical properties of agar. Int. Workshop on Gelidium, *Hydrobiologia*. 221: 137–148.

Laskowski, R.A., Luscombe, N.M., Swindells, M.B., & Thornton, J.M. (1996). Protein clefts in molecular recognition and function. *Protein science: a publication of the Protein Society*, *5*(12), 2438–2452. doi:10.1002/pro.5560051206.

Lauro, F.M., McDougald, D., Thomas, T., Williams, T.J., Egan, S., Rice, S., Cavicchioli, R. (2009). The genomic basis of trophic strategy in marine bacteria. *Proc Natl Acad Sci USA*, 106(37), 15527–15533. doi:10.1073/pnas.0903507106.

Laursen, B.S., Sørensen, H.P., Mortensen, K.K., Sperling-Petersen, H.U. (2005). Initiation of protein synthesis in bacteria. *Microbiology and molecular biology reviews: MMBR*, *69*(1), 101–123. doi:10.1128/MMBR.69.1.101-123.2005.

Lee D.G., Jang M.K., Lee O.H., Kim N.Y., Ju S.A., Lee S.H. (2008). Overproduction of a glycoside hydrolase family 50 β-agarase from *Agarivorans* sp. JA-1 in *Bacillus subtilis* and the whitening effect of its product. *Biotechnol Lett* 30(5):911–918.

Lee, S., Lee, J.Y., Ha, S.C., Jung, J., Shin, D.H., Kim, K.H., Choi, I.G. (2009). Crystallization and preliminary X-ray analysis of neoagarobiose hydrolase from *Saccharophagus degradans* 2-40. *Acta crystallographica. Section F, Structural biology and crystallization communications*, *65*(Pt 12), 1299–1301. doi:10.1107/S174430910904603X.

Lee M.H., Jang J.H., Yoon G.Y., Lee S.J., Lee M.G., Kang T.H., Han H.D., Kim H.S., Choi W.S., Park W.S., Park Y.M., Jung I.D. (2017). Neoagarohexaose-mediated activation of dendritic cells via Toll-like receptor 4 leads to stimulation of natural killer cells and enhancement of antitumor immunity. *BMB Rep* 50(5):263–268

Lemoine M., Nyvall Collén P., Helbert W. (2009). Physical state of kappa-carrageenan modulates the mode of action of kappa-carrageenase from *Pseudoalteromonas carrageenovora*. *Biochem J* 419:545–53. doi: 10.1042/BJ20080619.

Lieshout J.F.T. 2007. Characterization and Engineering of Thermostable Glycoside Hydrolase. *Dissertation*. Wagenigen University. 152 p. ISBN 90-8504-586-x.

Li G., Sun M., Wu J., Ye M., Ge X., Wei W., Li H., Hu F. (2015). Identification and biochemical characterization of a novel endotype β-agarase AgaW from *Cohnella* sp. strain LGH. *Appl Microbiol Biotechnol* 99(23):10019–10029.

Lindemann, S.R. (2019). Microbial Ecology: Functional "Modules" Drive Assembly of Polysaccharide-Degrading Marine Microbial Communities. *Current Biology,* 29(9), R330–R332. doi:10.1016/j.cub.2019.03.056.

Lin B, Lu G, Zheng Y, Xie W, Li S, Hu Z. (2012). Gene cloning, expression and characterization of a neoagarotetraose-producing β-agarase from the marine bacterium *Agarivorans* sp. *HZ105*. *World J Microbiol Biotechnol*.28(4):1691–1697. doi: 10.1007/s11274-011-0977-y.

Lippert K., Galinski E.A. (1992). Enzyme stabilization be ectoine-type compatible solutes: protection against heating, freezing and drying. *Appl Microbiol Biotechnol*. 37:61–5.

Liu N., Mao X., Yang M., Mu B.,Wei D. (2014). Gene cloning, expression, and characterisation of a new β-agarase, AgWH50C, producing neoagarobiose from *Agarivorans gilvus* WH0801. *World J Microbiol Biotechnol* 30(6):1691–1698. doi:/10.1007/s11274-013-1591-y.

Liu J, Xue Z, ZhangW, Yan M, Xia Y (2018) Preparation and properties of wet-spun agar fibers. *Carbohydr Polym* 181:760–767.

Lombard V., Golaconda Ramulu H., Drula E., Coutinho P.M., Henrissat B. (2014). The Carbohydrate-active enzymes database (CAZy) in 2013. *Nucleic Acids Res.* 42:D490–D495.

Ma C., Lu X., Shi C., Li J., Gu Y., Ma Y., Chu Y., Han F., Gong Q., Yu W. (2007). Molecular cloning and characterization of a novel β-agarase, AgaB, from marine *Pseudoalteromonas* sp. CY24. *J. Biol. Chem*.;282:3747–3754. doi: 10.1074/jbc.M607888200.

Macleod R.A. (1965). The question of the existence of specific marine bacteria. *Bacteriological reviews*, 29(1), 9–24.

Maderankova, D., Jugas, R., Sedlar, K., Vitek, M., & Skutkova, H. (2019). Rapid bacterial species delineation based on parameters derived from genome numerical representations. *Computational and structural biotechnology journal*, *17*, 118–126. doi: 10.1016/j.csbj.2018.12.006.

Matsuyama, S., Tajima, T., Tokuda, H. (1995). A novel periplasmic carrier protein involved in the sorting and transport of *Escherichia coli* lipoproteins destined for the outer membrane. *The EMBO journal*, *14*(14), 3365–3372.

Matsuzawa, T., Saito, Y., Yaoi, K. (2014). Key amino acid residues for the endo-processive activity of GH74 xyloglucanase. *FEBS Lett.* 588, 1731–1738.

Mazarrasa, I., Olsen, Y.S., Mayol, E., Marbà, N., & Duarte, C.M. (2014). Global unbalance in seaweed production, research effort, and biotechnology markets. *Biotechnology Advances*, 32(5), 1028–1036. doi:10.1016/j.biotechadv.2014.05.002.

Meier-Kolthoff, J.P., Hahnke, R.L., Petersen, J., Scheuner, C., Michael, V., Fiebig, A., Rohde, C., Rohde, M., Fartmann, B., Goodwin, L.A., Chertkov, O., Reddy, T., Pati, A., Ivanova, N.N., Markowitz, V., Kyrpides, N.C., Woyke, T., Göker, M., Klenk, H-P. (2014). Complete genome sequence of DSM 30083^{T}, the type strain (U5/41^{T}) of *Escherichia coli*, and a proposal for delineating subspecies in microbial taxonomy. *Standards in Genomic Sciences* 10:2.

Michel, G.; Czjzek, M. (2013). Polysaccharide-degrading enzymes from marine bacteria. In Marine Enzymes for Biocatalysis-Sources, Biocatalytic Characteristics and Bioprocesses of Marine Enzymes; Trincone, A., Ed.; Woodhead Publishing: Cambridge, UK: pp. 429–464.

Michel G., Nyval-Collen P., Barbeyron T., Czjzek M., Helbert W. (2006). Bioconversion of red seaweed galactans: a focus on bacterial agarases and carrageenases. *Appl. Microbiol. Biotechnol.* ;71:23–33. doi: 10.1007/s00253-006-0377-7.

Miller, G. L. (1959). Use of dinitrosalicylic acid reagent for determination of reducing sugar. *Analytical chemistry* 31, 426–428.

Moh, T.H., Lau, N., Furusawa, G., Amirul A.A.A. (2017). Complete genome sequence of *Microbulbifer* sp. CCB-MM1, a halophile isolated from Matang Mangrove Forest, Malaysia. *Stand in Genomic Sci* 12, 36. doi: 10.1186/s40793-017-0248-0.

Morrice, L.M., McLean, M.W., Long, W.F., Williamson, F.B. (1983). Porphyran primary structure: An investigation using beta-agarase-I from *Pseudomonas atlantica* and $^{C-13}$-NMR spectroscopy. *European Journal of Biochemistry*. 133.673–684.

Naretto, A., Fanuel, M., Ropartz, D., Rogniaux, H., Larocque, R., Czjzek, M., Tellier, C., Michel, G. (2019). The agar-specific hydrolase ZgAgaC from the marine bacterium *Zobellia galactanivorans* defines a new GH16 protein subfamily. *J. Biol. Chem.* 294, 6923–6939.

Niepmann, M. (2007). Discontinuous native protein gel electrophoresis: pros and cons. *Expert Review of Proteomics.* 4:3, 355-361, doi: 10.1586/14789450.4.3.355.

Nishijima, M., Takadera, T., Imamura, N., Kasai, H., An, K.D., Adachi, K., Nagao, T., Sano, H., and Yamasato, K. (2009). *Microbulbifer variabilis* sp. nov. and *Microbulbifer epialgicus* sp. nov., isolated from Pacific marine algae, possess a rod-coccus cell cycle in association with the growth phase. *Int. J. Syst. Evol. Microbiol*. 59:1696-1707.

Oh, C., De Zoysa, M., Kwon, Y.K., Heo, S.J., Affan, A., Jung, W.K., Park, H.S., Lee., Son, S.K., Yoon, K.T., Kang, D.H. (2011). Complete genome sequence of the agarase-producing marine bacterium strain S89, representing a novel species of the genus *Alteromonas*. *J.Bacteriol*. 193, 5538.

Ohta Y., Nogi Y., Miyazaki M., Li Z., Hatada Y., Ito S., Horikoshi K. (2004a). Enzymatic properties and nucleotide and amino acid sequences of a thermostable beta-agarase from the novel marine isolate, JAMB-A94. *Biosci Biotechnol Biochem.* 68(5): 1073-1081. doi: 10.1271/bbb.68.1073.

Ohta Y., Hatada Y., Nogi Y., Miyazaki M., Li Z., Akita M., Hidaka Y., Goda S., Ito S., Horikoshi, K. (2004b) Enzymatic properties and nucleotide and amino acid sequences of a thermostable beta-agarase from a novel species of deep-sea *Microbulbifer. Appl Microbiol Biotechnol*. 64(4): 505-514. doi: 10.1007/s00253-004-1573-y.

Park, S.H., Lee, C., Hong, S. (2020). Implications of agar and agarase in industrial applications of sustainable marine biomass. *Appl Microbiol Biotechnol* 104, 2815–2832. doi:10.1007/s00253-020-10412-6.

Parks, D.H., Imelfort, M., Skennerton, C.T., Hugenholtz, P., Tyson, G.W. (2015). CheckM: assessing the quality of microbial genomes recovered from isolates, single cells, and metagenomes. *Genome research*, *25*(7), 1043–1055. doi:10.1101/gr.186072.114.

Patel, S.(2012). Therapeutic importance of sulfated polysaccharides from seaweeds: updating the recent findings. *3 Biotech* 2, 171–185.doi:/10.1007/s13205-012-0061-9.

Peracchi A. (2001). Enzyme catalysis: removing chemically 'essential' residues by site-directed mutagenesis. *Trends Biochem. Sci*.;26:497–503. doi: 10.1016/S0968-0004(01)01911-9.

Pereira J.d.C, Giese E.C., de Souza M.M.M., dos Santos G.A.C., Perrone O.M., Boscolo M., da Silva R., Gomes E., Martins D.A.B. (2017). Effect of metal ions, chemical agents and organic compounds on lignocellulolytic enzymes activities, enzyme inhibitors, and activators, Murat Senturk, IntechOpen, DOI: 10.5772/65934.

Pérez, V., Hengst, M., Kurte, L., Dorador, C., Jeffrey, W. H., Wattiez, R., Moline V., Matallana-Surget, S. (2017). Bacterial survival under extreme UV radiation: a comparative proteomics study of *Rhodobacter* sp., isolated from high altitude wetlands in Chile. *Frontiers in microbiology*, *8*, 1173. doi:10.3389/fmicb.2017.01173.

Pettersen E.F., Goddard T.D., Huang C.C., Couch G.S., Greenblatt D.M., Meng E.C., Ferrin T.E. (2004). UCSF Chimera--a visualization system for exploratory research and analysis. *J Comput Chem.* Oct;25(13):1605-12.

Pluvinage, B., Grondin, J.M., Amundsen, C., Klassen L., Moote, P.E., Xiao, Y., Thomas D., Pudlo, N.A., Anele, A., Martens, E.C., Inglis, G.D., Uweira, R.U., Boraston, A.B., Abbot, D.W. (2018). Molecular basis of an agarose metabolic pathway acquired by a human intestinal symbiont. *Nat Commun* 9, 1043 doi:10.1038/s41467-018-03366-x.

Pluvinage B., Hehemann J.H., Boraston A.B. (2013.) Substrate recognition and hydrolysis by a family 50 exo-beta-agarase, Aga50D, from the marine bacterium *Saccharophagus degradans*. *J Biol Chem* 288(39): 28078–28088. doi:10.1074/jbc.M113.491068.

Poletto M., Pistor V., Zattera A.J. (2013). Structural Characteristics and Thermal Properties of Native Cellulose, Cellulose - Fundamental Aspects, Theo van de Ven and Louis Godbout, IntechOpen. doi:10.5772/50452.

Pomin, V.H.., Mourao, P.A. (2008). Structure, biology, evolution, and medical importance of sulfated fucans and galactans. *Glycobiol.* 18 , 1016 – 1027.

Pulz, O., Gross, W. (2004). Valuable products from biotechnology of microalgae. *Appl Microbiol Biotechnol*. 65, 635–648. Doi:10.1007/s00253-004-1647-x.

Qian, W. Zhang, J. (2008). Gene dosage and gene duplicability. *Genetics*, 179, 2319–2324.

Rajan, S.S., Yang ,X., Collart, F., Yip, V.L., Withers, S.G., Varrot, A., Thompson, J., Davies, G.J., and Anderson, W.F. (2004). Novel catalytic mechanism of glycoside hydrolysis based on the structure of an NAD^{+}/Mn^{2+}-dependent phospho-alpha-glucosidase from *Bacillus subtilis*. *Structure.* 12, 1619-29.

Rebello, J., Ohno, M., Ukeda, H., Sawamura, M. (1997). Agar quality of commercial agarophytes from different geographical origins. 1. Physical and rheological properties. *J. Appl. Phycol.* 8: 517– 521.

Rebuffet, E., Groisillier, A., Thompson, A., Jeudy, A., Barbeyron, T., Czjzek, M., and Michel, G. (2011). Discovery and structural characterization of a novel glycosidase family of marine origin. *Environ. Microbiol.* 13, 1253-1270.

Renn D. (1997). Biotechnology and the red seaweed polysaccharide industry: status, needs, and prospects. *Trends Biotechnol*., 15.pp. 9-14. doi:10.1016/S0167-7799(96)10069-X.

Richter, M., Rosselló-Móra, R., Glöckner, F.O., and Peplies. J. (2015). JSpeciesWS: a web server for prokaryotic species circumscription based on pairwise genome comparison. *Bioinformatics*. 16. pii: btv681.

RoosmalenM.L. van, N. Geukens., J.D.H., Jongbloed, H., Tjalsma, J.Y.F., Dubois , S., Bron, J.M, van Dijl, J., Anné. (2004). Type I signal peptidases of Gram-positive bacteria. *Biochim. Biophys. Acta Mol. Cell Res.*, 1694 , pp. 279-297, 10.1016/J.BBAMCR.2004.05.006

Rosselló-Móra R.(2006). DNA-DNA reassociation methods applied to microbial taxonomy and their critical evaluation. *in* Molecular Identification, Systematics, and Population Structure of Prokaryotes, ed Stackebrandt E. Springer-Verlag, Berlin. pp 23-50.

Ruiz, D., Turowski, V,. Murakami, M. (2016). Effects of the linker region on the structure and function of modular GH5 cellulases. *Sci Rep* 6, 28504. doi.org:10.1038/srep28504.

Rye, C.S., Withers, S.G. (2000). Glycosidase mechanisms. *Curr. Opin. Chem. Biol.* 4, 573–580.

Sammond, D.W., Payne, C. M., Brunecky, R., Himmel, M. E., Crowley, M.F., Beckham G. T. (2012). Cellulase linkers are optimized based on domain type and function: insights from sequence analysis, biophysical measurements, and molecular simulation. *PloS ONE* 7, e48615, doi: 10.1371/journal.pone.0048615.

Schein, C. (1989). Production of soluble recombinant proteins in bacteria. *Nat Biotechnol* 7, 1141–1149. Doi:10.1038/nbt1189-1141.

Selleck, W., Tan, S. (2008). Recombinant protein complex expression in *E. coli*. *Current protocols in protein science*, *Chapter 5*, Unit–5.21. doi:10.1002/0471140864.ps0521s52.

Sinnott M.L. (2007). Carbohydrate chemistry and biochemistry: structure and mechanism. The Royal Society of Chemistry. ISBN:978-0-85404-256-2. 731 pages.

Smith, A. C. Hussey, M.A. (2005). Gram stain protocols. American Society for Microbiology.

Song, T., Xu H., Wei, C., Jiang, T., Qin, S., Zhang, W., Cao, Y., Hu C., Zhang, F., Qiao, D., Cao, Y. (2016). Horizontal transfer of a novel soil agarase gene from marine bacteria to soil bacteria via human microbiota. *Scientific reports*, *6*, 34103. doi:10.1038/srep34103.

Sousa, A.M., Borges, J., Silva, A.F., Goncalves, M.P. (2013). Influence of the extraction process on the rheological and structural properties of agars. *Carbohydr Polym* 96:163–171.

Souza, C.P., Almeida, B.C., Colwell, R.R., Rivera, I.N.G. (2011). The importance of chitin in the marine environment. *Mar. Biotechnol*. 13:823–30. doi: 10.1007/s10126-011-9388-1.

Sun C., Chen Y.J., Zhang X.Q., Pan J., Cheng H., Wu, M. (2014). Draft genome sequence of *Microbulbifer elongatus* strain HZ11, a brown seaweed degrading bacterium with potential ability to produce bioethanol from alginate. *Mar Genomics* 18:83–85.

Stackebrandt E., Goebel B. (1994). Taxonomic note: A place for DNA-DNA reassociation and 16S rRNA sequence analysis in the present species definition in bacteriology. *Int J Syst Evol Microbiol* 44, 846-849. doi:10.1099/00207713-44-4-846.

Stein L. (2001). Genome annotation: from sequence to biology. *Nat. Rev. Genet*. 2, 493–503. doi:10.1038/35080529.

Sterner, R., Liebl., W. (2001). Thermophilic adaptation of proteins *Crit. Rev. Biochem. Molec. Biol*. 36 39–106.

Suzuki H., Sawai Y., Suzuki T., Kawai K. (2002). Purification and characterization of an extracellular α-neoagarooligosaccharide hydrolase from *Bacillus* sp. mk03. J. *Biosci. Bioeng*. 93, 456–463. 10.1016/S1389-1723(02)80092-5.

Sugano Y., Kodama H., Terada I., Yamazak Y.I., Noma M. (1994). Purification and characterization of a novel enzyme, alpha-neoagarooligosaccharide hydrolase (alpha-NAOS hydrolase), from a marine bacterium, *Vibrio* sp. strain JT0107, *J. Bacteriol*. 176 6812–6818.

Su Q., Jin T., Yu Y., Yang M., Mou H., Li L. (2017). Extracellular expression of a novel beta-agarase from *Microbulbifer sp.* Q7, isolated from the gut of sea cucumber. *AMB Express* 7(1): p. 220 doi.org/10.1186/s13568-017-0525-8.

Takagi E., Hatada Y., Akita M., Ohta Y., Yokoi G., Miyazaki T., Nishikawa A., Tonozuka T. (2015). Crystal structure of the catalytic domain of a GH16 *β*-agarase from a deep-sea bacterium, *Microbulbifer thermotolerans* JAMB-A94. *Bioscicence, Biotechnology, and Biochemistry*. 2015;79:629–632. doi: 10.1080/09168451.2014.988680.

Tatusov R.L., Koonin, E.V., Lipman, D.J. (1997). A genomic perspective on protein families. *Science*, 278, 631–637. doi: 10.1126/science.278.5338.631.

Tatusov, R.L., Galperin, M.Y., Natale, D.A., Koonin, E.V. (2000). The COG database: a tool for genome-scale analysis of protein functions and evolution. *Nucleic acids research*, *28*(1), 33–36. doi:10.1093/nar/28.1.33.

Tawara M., Sakatoku A., Tiodjio RE., Tanaka D., Nakamura S. (2015). Cloning and characterization of a novel agarase from a newly isolated bacterium *Simiduia* sp. strain TM-2 able to degrade various seaweeds. *Appl Biochem Biotechnol.* 177(3): 610-23.

Temuujin U, Chi WJ, Lee SY, Chang YK, Hong SK (2011) Overexpression and biochemical characterization of DagA from *Streptomyces coelicolor* A3(2): an endo-type beta-agarase producing neoagarotetraose and neoagarohexaose. *Appl Microbiol Biotechnol* 92(4): p. 749-59.

Tindall B.J., Rosselló-Móra R., Busse H.J., Ludwig W., Kämpfer P. (2010). Notes on the characterization of prokaryote strains for taxonomic purposes. *Int J Syst Evol Microbiol* 60:249–266. doi:10.1099/ijs.0.016949-0.

Taylor, C.B., Payne, C.M., Himmel, M.E., Crowley, M.F., McCabe, C., & Beckham, G.T. (2013). Binding site dynamics and aromatic-carbohydrate interactions in processive and non-processive family 7 glycoside hydrolases. *The journal of physical chemistry.* B, 117 17, 4924-33.

Tostevin R., Turchyn A.V., Farquhar J., Johnston D.T., Eldridge D.L., Bishop J.K.B., McIlvin, M. (2014). Multiple sulfur isotope constraints on the modern

sulfur cycle. (Open Access). *Earth and Planetary Science Letters*, 396, pp. 14-21. doi: 10.1016/j.epsl.2014.03.057.

Trincone A. (2018). Update on marine carbohydrate hydrolyzing enzymes: biotechnological applications. *Molecules (Basel, Switzerland)*, *23*(4), 901. doi:10.3390/molecules23040901

Tsai K.C., Jian J.W., Yang E.W., Hsu P.C., Peng H.P., Chen C.T., Chen J.B., Chang J.Y., Hsu W.L., Yang A.S. (2012). Prediction of carbohydrate binding sites on protein surfaces with 3-dimensional probability density distributions of interacting atoms. *PLoS ONE* 7(7): e40846. doi:10.1371/journal.pone.0040846.

Usov, A. I. (2011). Polysaccharides of the red algae. *Adv. Carbohydr. Chem. Biochem.* 65, 115-217.

Vallenet D., Calteau A., Cruveiller S., Gachet M., Lajus A., Josso A., Mercier J., Renaux A., Rollin J., Rouy Z., Roche D., Scarpelli C., Médigue C. (2017). MicroScope in 2017: an expanding and evolving integrated resource for community expertise of microbial genomes. *Nucleic acids research*, *45*(D1), D517–D528. doi:10.1093/nar/gkw1101.

Van der Meulen, H.J., Harder, W. (1976). The regulation of agarase production by resting cells of *Cytophaga jeevensis*. *Antonie van Leeuwenhoek*. 42,277-286.

Van Hal, J.W., Huijgen, W.J.J., López-Contreras, A.M. (2014). Opportunities and challenges for seaweed in the biobased economy. *Trends Biotechnol.* 32, 231–233.

Vattuone M.A., De Flores E.A., Sampietro AR. (1975). Isolation of neoagarobiose and neoagarotetraose from agarose digested by *Pseudomonas elongata. Carbohydrate Research* 39:164-167.

Veerakumar, S., Manian, R.P. (2018). Recombinant β-agarases: insights into molecular, biochemical, and physiochemical characteristics. *3 Biotech*, *8*(10), 445. doi:10.1007/s13205-018-1470-1.

Viborg, A.H., Terrapon, N., Lombard, V., Michel, G., Czjzek, M., Henrissat, B., Brumer, H. (2019). A subfamily roadmap of the evolutionarily diverse glycoside hydrolase family 16 (GH16). *The Journal of biological chemistry*, *294*(44), 15973–15986. doi:10.1074/jbc.RA119.010619.

Vocadlo, D.J., Davies, G.J. (2008). Mechanistic insights into glycosidase chemistry. *Curr. Opin. Chem. Biol*. 12, 539–555. DOI 10.1016/j.cbpa.2008.05.010.

Vonossowski, I., Ståhlberg, J., Koivula, A., Piens, K., Becker, D., Boer, H., Harle, R., Harris, M., Divne, C., Mahdi, S., Zhao, Y., Driguez, H., Claeyssens, M., Sinn ott, M. L., Teeri, T. T. (2003). Engineering the exo-loop of *Trichoderma reesei* cellobiohydrolase, Cel7A: a comparison with *Phanerochaete chrysosporium* Cel7D. *J. Mol. Biol*. 333, 817–829.

Wagner, A. (2005). Energy constraints on the evolution of gene expression. *Mol. Boil. Evol*. 22, 1365–1374.

Wakabayashi, M., Sakatoku, A., Noda, F. Noda M., Tanaka D., Nakamura S. (2012). Isolation and characterization of *Microbulbifer* species 6532: a degrading seaweed thalli to single cell detritus particles. *Biodegradation* 23, 93–105. doi:/10.1007/s10532-011-9489-6.

Walker J.M. (2009). The Protein Protocols Handbook. Third Edition. New York (NY): Springer-Verlag New York, LLC

Walsh R. (2018). Comparing enzyme activity modifier equations through the development of global data fitting templates in Excel. *PeerJ*, *6*, e6082. doi:10.7717/peerj.6082.

Wang W., Liu P., Hao C., Wu L., Wan W., Mao X. (2017). Neoagarooligosaccharide monomers inhibit inflammation in LPS-stimulated macrophages through suppression of MAPK and NF-κB pathways. *Sci Rep* 7:44252.

Waterhouse A., Bertoni M., Bienert S., Studer G., Tauriello G., Gumienny R., Heer F.T., de Beer T.A.P., Rempfer C., Bordoli L., Lepore R., Schwede T. (2018). SWISS-MODEL: homology modelling of protein structures and complexes. *Nucleic Acids Res*. Jul 2;46(W1): W296-W303. doi: 10.1093/nar/gky427.

Wei, N., Quarterman, J., Jin, Y.S. (2013). Marine macroalgae: an untapped resource for producing fuels and chemicals. *Trends Biotechnol*. 31, 70–77.

Wolfe A.J. (2015). Glycolysis for microbiome generation. *Microbiology spectrum*, *3*(3), doi:10.1128/microbiolspec.MBP-0014-2014.

Wilson C.A., Kreychman J., Gerstein M. (2000). Assessing annotation transfer for genomics: quantifying the relations between protein sequence, structure, and function through traditional and probabilistic scores. *J Mol Biol* 297: 233–249.

Wilson K. (2010). Principles and techniques of biochemistry and molecular biology. Cambridge University Press. pp. 581–624. doi:10.1017/cbo9780511841477.016.

Xie W., Lin B., Zhou Z., Lu G., Lun J., Xia C., Li S., Hu Z. (2013). Characterization of a novel β-agarase from an agar-degrading bacterium *Catenovulum* sp. *X3. Appl Microbiol Biotechnol.*;97 (11):4907–4915. doi: 10.1007/s00253-012-4385-5.

Xu X.Q., Su B.M, Xie J.S., Li R.K, Yang J., Lin J., Ye X.Y. (2018): Preparation of bioactive neagaroligosaccharides through hydrolysis of *Gracilaria lemaneiformis* agar: a comparative study. *Food Chemistry*, 240, pp. 330-337.

Yan S., Yu M., Wang Y., Shen C., Zhang X.H. (2011). *Catenovulum agarivorans* gen. nov., sp. nov., a peritrichously flagellated, chain-forming, agar-hydrolysing gammaproteobacterium from seawater. *Int J Syst Evol Microbiol*.61:2866–73. doi: 10.1099/ijs.0.027565-0.

Yang, M., Yu, Y., Jin, T., Mou, H., Li, L. (2018). Genomic analysis of *Microbulbifer* sp. Q7 exhibiting degradation activity toward seaweed polysaccharides. *Marine Genomics*, 39, 7–10. doi:10.1016/j.margen.2017.07.003.

Yip V.L., Varrot A., Davies G.J., Rajan S.S., Yang X., Thompson J., Anderson W.F., Withers S.G. (2004) An unusual mechanism of glycoside hydrolysis involving redox and elimination steps by a family 4 beta-glycosidase from *Thermotoga maritima. J Am Chem Soc.* 126, 8354-5.

Yoon J.H., Kim H., Kang K.H., Oh T.K., Park Y.H. (2003) Transfer of *Pseudomonas elongata* Humm 1946 to the genus *Microbulbifer as Microbulbifer elongatus comb. nov. Int J Syst Evol Microbiol.* 53: 1357-1361. doi 10.1099/ijs.0.02464-0

Yoon J.H., Kim I.G., Shin D.Y., Kang K.H., Park Y.H. (2003) *Microbulbifer salipaludis* sp. nov., a moderate halophile isolated from a Korean salt marsh. *Int J Syst Evol Microbiol* 53:53–57. doi: 10.1099/ijs.0.02342-0.

Yoon, S.H., Ha, S.M., Lim, J.M., Kwon, S.J., Chun, J. (2017). A large-scale evaluation of algorithms to calculate average nucleotide identity. *Antonie van Leeuwenhoek.* 110:1281–1286.

Yooseph, S., Nealson, K., Rusch, D., McCrow J.P., Dupont C.L., Kim M., Johnson J., Montgomery R., Ferriera S., Beeson K., Williasmson S.J., Tovchigrechko A., Allen A.E., Zeigler L.A., Sutton G., Eisenstadt E., Rogers Y.H., Friedman R., Frazier M., Venter C.J. (2010). Genomic and functional adaptation in surface ocean planktonic prokaryotes. *Nature* 468, 60–66. doi.org/10.1038/nature09530.

Young K.D. (2007). *Bacterial morphology: why have different shapes? Curr Opin Microbiol*,. 10(6): p. 596-600.

Yun E.J., Lee S., Kim J.H., Kim B.B., Kim H.T., Lee S.H., Pelton J.G., Kang N.J., Choi I.G., Kim K.H. (2013) Enzymatic production of 3,6-anhydro-Lgalactose from agarose and its purification and in vitro skin whitening and anti-inflammatory activities. *Appl Microbiol Biotechnol* 97(7):2961–2970.

Yun E.J., Yu S, Kim K.H. (2017). Current knowledge on agarolytic enzymes and the industrial potential of agar derived sugars. *App. Microbio. and Biotech*. 101(14): 5581-5589.

Zhang D.S., Huo Y.Y., Xu X.W., Wu Y.H., Wang C.S., Xu E.F., Wu M. (2012). *Microbulbifer marinus* sp. nov. and *Microbulbifer yueqingensis* sp. nov., isolated from marine sediment. *Int J Syst Evol Microbiol*;62:505–510.

Zhang N., Mao X., Li R.W., Hou E., Wang Y., Xue C., Tang Q. (2017). Neoagarotetraose protects mice against intense exercise-induced fatigue damage by modulating gut microbial composition and function. *Mol Nutr Food Res* 61(8):1600585.

Zhao, Q., Li, S., Lv, P. Sun S., Ma C., Xu P., Su H., Yang C. (2019). High ectoine production by an engineered *Halomonas hydrothermalis* Y2 in a reduced salinity medium. *Microb Cell Fact.* 18, 184. doiI10.1186/s12934-019-1230-x.

Zinder S.H., Dworkin M. (2013). Morphological and physiological diversity. In: Rosenberg E., DeLong E.F., Lory S., Stackebrandt E., Thompson F. (eds) The Prokaryotes. Springer, Berlin, Heidelberg.

Appendices

Appendix 1.

Table 1.1 . Amplification of gene insert for cloning

Gene insert	Note
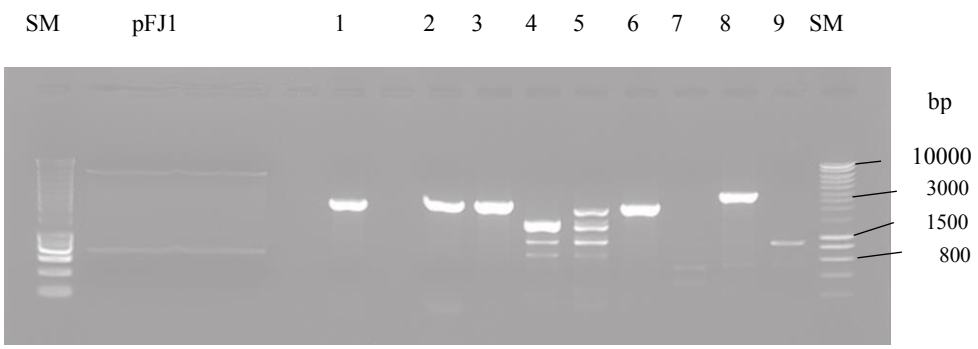	Sample : agarase genes insert digestion;1% w/v agarose, 100 V, 20 min, @5 µL

1=agaA50(BamHI-HF&EcoRI-HF); 2=agaB50(XhoI&NsiI-HF); 3=agaC50; 4=agaD86-1b(XhoI&NsiI-HF); 5=agaD86-2by(XhoI&NsiI-HF); 6=agaE86-1y(XhoI&NsiI-HF); 7=agaE86-2wy(XhoI&NsiI-HF); 8=agaE86-3bwy(EcoRI-HF); 9=agaF16-1y(BamHI-HF&EcoRI-HF); pFJ1=pFO4 modified(5,7 kb+690 bp) (BamHI-HF&EcoRI-HF); SM=smart ladder 1700-10

Appendix 1. continued

Table 1.2. Plasmid Validation Using HincII Map

Cut Plasmid	Note
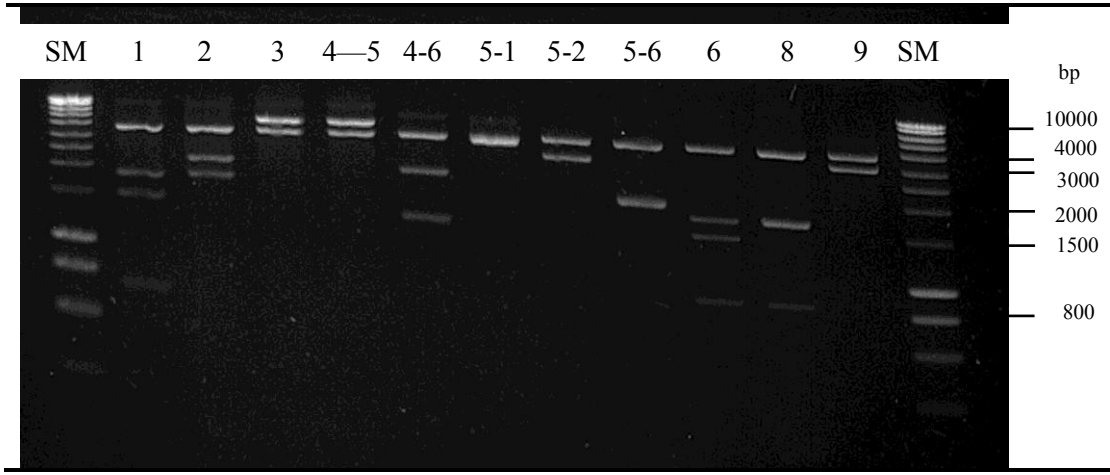	Sample : agarase plasmids (pME) digestion HincII; 1,2% w/v agarose, 100 V, 40 min, @ 7 µL 1=agaA50; 2=agaB50; 3=agaC50; 4-5&4-6=AgaA86T (agaD86-1b); 5-1; 5-2; 5-6=agaD86-2by; 6=agaE86-1y; 8=agaE86-3bwy; 9=agaF16-1y; SM=smart ladder 1700-10

Appendix 2.

Table 1. Characteristics of *Microbulbifer elongatus* PORT2 among other *Microbulbifer* species

Characteristics	***M. elongatus* PORT2**	***M. elongatus* DSM 6810^T**	***M. elongatus* CMC5**	***M. hydrolyticus* DSM11525^T**	***M.salipaludis* SM-1^T**
Cell shape	Rods, coccoid	Rods or cocci,	short rods	Rods	Rods
Gram Staining	negative	negative	negative	negative	negative
Motility	Non-motile, non-spore forming	Motile, non-spore forming, encapsulated	Non-motile, non-spore forming	Non-motile, non-spore forming	Non-motile, non-spore forming
catalase activity	+	+	+	NA	+
oxidase activity	+	NA	+	NA	+
use of nitrate as a sole nitrogen source	NA	+	NA	NA	NA
Na+ requirement	2-10 % (w/v)	2-3% (w/v)	2-8% (w/v)	0.1 to 1 M	2–3% (w/v)
agar hydrolysis	+	+	+	NA	weakly
amylase activity	+	´+		+	+
Gelatine hydrolysis	-	+	+	+	-
utilization of :					
lactose,	-	+	+	NA	+
sucrose,	-	+	-	NA	+
glucose,	+	+	+	+	+
sodium citrate	NA	+	NA	NA	NA
H2S production	-	+	-	NA	NA
Indole production	-	-	NA	NA	NA
Fermentation of glucose	-	-	NA	+	+

Table 1. Continued

Characteristics	***M. elongatus* PORT2**	***M. elongatus* DSM 6810^T**	***M. elongatus* CMC5**	***M. hydrolyticus* DSM11525^T**	***M.salipaludis* SM-1^T**
Antibiotic Resistance -Ampicillin (100 µg/mL) -Gentamycin (20 µg/mL) Kanamycin Streptomycin	 + - - +	NA	NA	NA	NA
Colony color on Marine Agar (MA)	Opaque-yellowish brown	Yellowish-brown	cream	Greyish-yellow	Yellowish-brown
pH range	6-8	NA	NA	6.5-8.5	5–8
Temparature range (^{0}C)	28-37	25-30	30-37	10 to 41	10 to 45
GC content	57.6	58	65.6	58	59

NA= Not Available

Appendix 3. Clone Constructs

>pME1 Ligation of N341_nt-SP PCR* into pFO4*

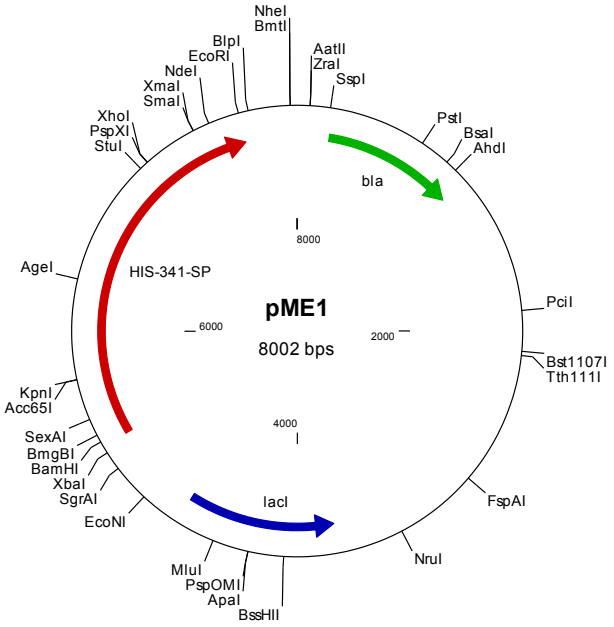

Details: HIS-341-SP, 5317 to 7665, CDS, Draw as Gene

Translation product 782 aas

Mol Wt 87942.1, Isoelectric Pt (pI) 4.67

Translation:
MGSSHHHHHHGSEQKGGETAANVTATSDSNLLAQDLLLEGFDQGGIPASV
QVNNGTANLVDDGAGGKALQVKLKLADNNNAGLVIQPAEAWDWSEFSDFN
LAFDVANHGVESVQIDVTMADKNGDFYTRGLVVPADGTARTYYAKLHGHD
QEDPKAAAQNEFNFASGLRSNPPTWQSDDIMLHSFWGKKLLDLSGITQIS
FGSDGSLSDRQYTIDNLRLRANPPMDENFLTGLLDKYGQNAKVDYEGKIH
SDEELKKVVEEELASLSGKPNVDRSKFSGWKSGPQLEATGYFRTEKVNGK
WAIVDPEGYLYFSTGIDIIRLSNSSTITGYDYDQELIPKRSADEVIAEDD
QPLNRVDEKAWATRELISETRAKMFNWLPGYDDELGNHYGYRRETQSGPL
KHGETFSFYSANLERRYGETYPESYLDTWQKVTVDRMLDWGFTSLGNWAA
EPFYQQERIPFVAFADIIGEFGTLSSGFDFWHPVPDPYDPRFYQRSVVAA
KSVSEQIENSPWCMGVFFDNEQSFGRLESDELHYGIVINTLTRDAADTPA
KGVFTKVLREKYGTIEALNKAWNKEVKSWEAFEKGMDSSLTTDAQREDYA
TLLFEYGNQYFGTIRKAMKSVMPNHLYLGSRLPSWGMPPEIVKAAGKNVD
IISYNLYEEGLVPSKWEFLAEIDKPSLIGEFSFGSDDQGHFHPGIVISAD
QKDRGRMFKNYMHSFIDNPWFVGVHMFQYMDSPITGRAYDGENYANGFVS
VADVPYVELVKAAKEVHEDLYERRFGDVKPAE

>pME2 Ligation of 342_nt PCR* into pFO4*

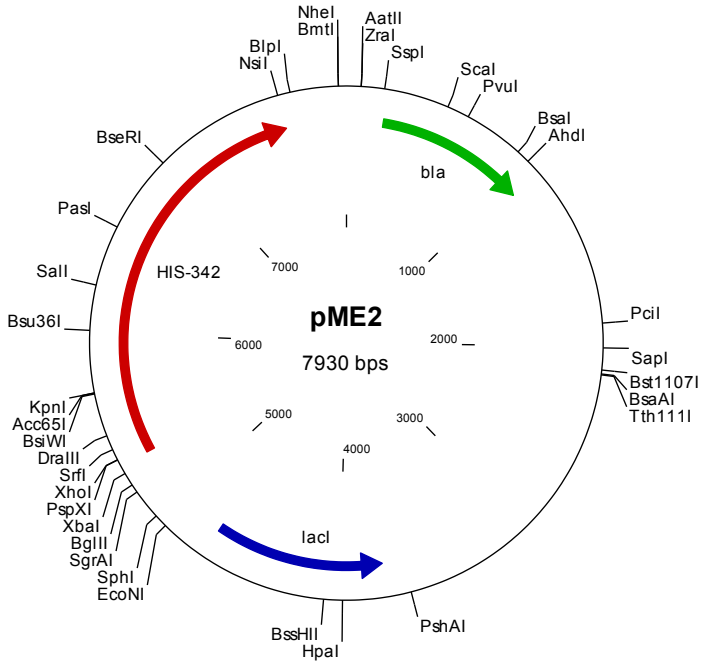

Details: HIS-342, 5317 to 7587, CDS, Draw as Gene

Translation product 756 aas

Mol Wt 84020.1, Isoelectric Pt (pI) 4.79

Translation:

MGSSHHHHHHGSLELLSACGQSGEEGAVAAGPGNDREYQQPLLTGGRGIP
AGVEGHGVSLSRVPVDTGIAPLHAVFSKNTYEPRLDLAPESGWDWSGVGE
NIGLSLKVTNPGEHSAQLFVTVYDHETYGTRSFNVPAGGIGTYYFDLNGP
ALALDTGMRDAPALYDNAATAMTWMWGSKSLDLSNIRRIELNMKSILSDR
PLVFEDIALAPNGEFKPQKLQKIFDQYGQYAPQDYPEKIHSDDELRASAQ
REAEAFSESSIFPDRSRFGGWAEGPRYKSTGYFRTQKIDGQWALIDPEGY
LFFATGVDNMRMDNTVTMTGVDFADPDTGLGETIVSELRRDLFQWLPEKG
DPLAAHYFYRPVVHMGPVEKGQGYSFYRANLQRKYGPDYLQRWREVTVDR
QLNWGFTTLGNWADPSLYDNGKVAYVANGWIRGEHKRVSSGNDYWGPLHD
PFDPEFVNSVKRTVAQVAAEVQGDPWCMGVYIENELSWGNTKTDAGHFGL
IIHTLTRDAAESPAKAAFVEILKRKYPSVESLSRAWFSSMPSRSIPSWEA
FAAGFSLSQAAGGEPQIEGQLREDFSLLLESLSARFFSVVQRELADVMPD
HLFLGARFADWGMTPEVVRGAAAYVDVVSYNLYTEGLAADNWEFLAEIDK
PSIIGEFHMGATDSGSFHAGLVSAESQQERGEMFRDYMHTIIDNPWFVGA
QWFQYIDSPASGRAWDGENYNVGFVTVADEPYGPLVAAAQALNRELYPRR
YGQKND

>pME3 Ligation of 451_nt-SP PCR* into pFO4*

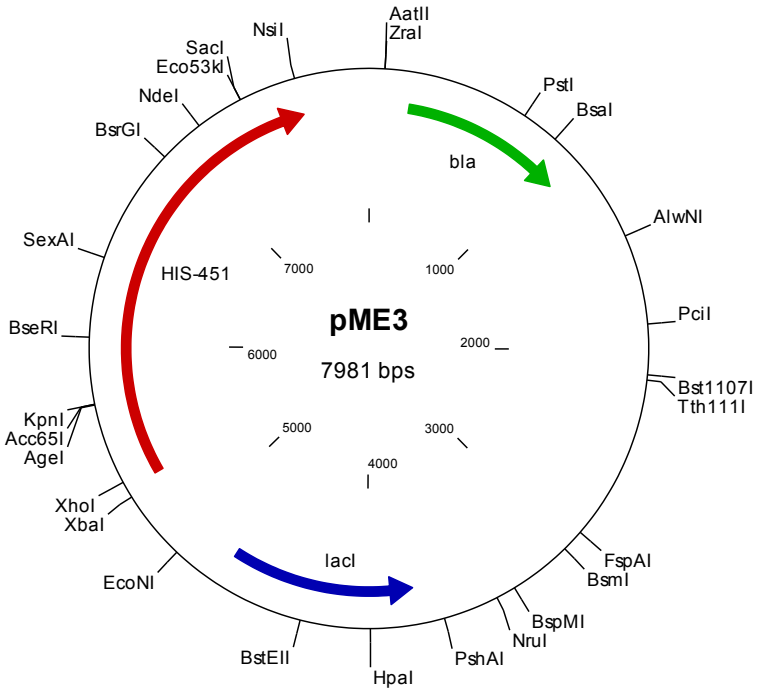

Details: HIS-451, 5317 to 7638, CDS, Draw as Gene

Translation product 773 aas

Mol Wt 86981.5, Isoelectric Pt (pI) 4.89

Translation:
MGSSHHHHHHGSLENDVRSTITEATTGNTEVAAENSNTLWTFDQGEMPSA
IQVENADARVIDGESGKALEVQLRTKSHYSANITFAAEQPWDWSGLGNFA
FALDITNPKQSSVHLYVRAADKHGKVQSRSFAVPENSTGTYYMELKGPDL
MVDTGIRSNPPSWDSEFQDMIYRGGVKQIDVSAVKSIALSVIGVLEDKAL
VIDNVRLIQPKSLDESYLKDLVDEFGQNNKLDFASKVDSLEELRAISEEE
QSQLRKTPMDGRSRFGGWAEGPKLEATGYFRTEKVDGKWALVDPEGHLFF
STGIANVRLANTSTITGYDFDKARVPQRTPGDLTPEDSLGLNRVPDAAIP
TRHISSPLRADMFTWLPEYDEPLGQNFGYRREVHTGVIEHGETFSFYRAN
LQRKYDIADEERLMAKWRETTIDRMLSWGFTSFGNWIDPAYYQMNRIPYF
ANGWIIGNFKTVSSGNDYWSPLPDPFDPLFKERAYITAEQIAKEVANNPW
CVGVFVDNEKSWGQEGSTASQYGIVINTLGRAAGESPTKAQFVQLMQDKY
GEIGRLNTAWNIQLADWDAFANGVALTEFSDAMIEDFSTMLEHYTGQYFK
IVREAIKHFMPNHMYLGARFADWGMTPEVRRAAAKYADVVSYNYYKEGVS
NKFWSFLEEIDRPSIIGEFHNGSLDSGLLSPGLIHASSQADRGKKFAEYM
NSVIDNPYFVGAHWFQYIDSPLTGRAYDGENYNVGFVSVTDTPYQPLVVA
VKEVNENLYQRRFGEAKLAVAPE

>pME4 Ligation of 452_nt-1b PCR* into pFO4*

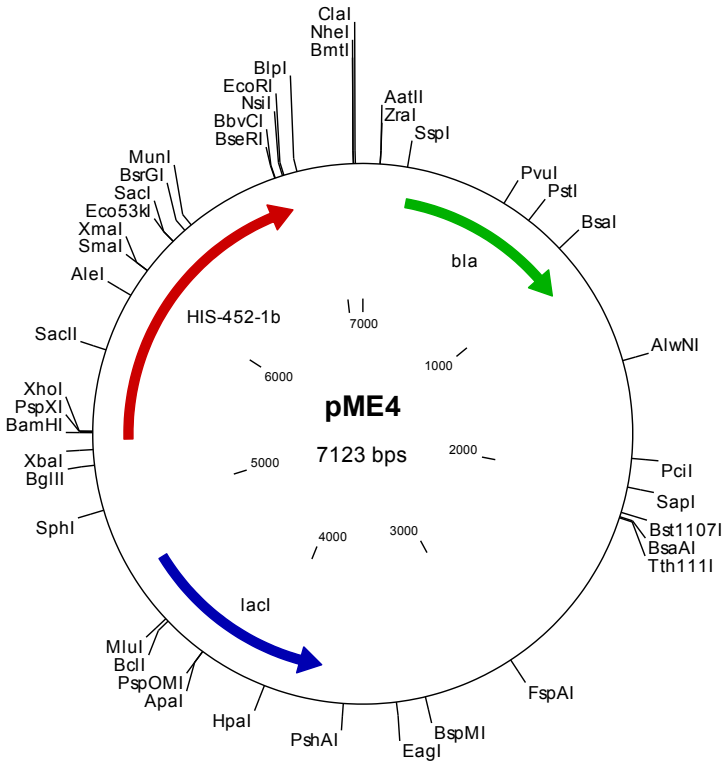

Details: HIS-452-1b, 5317 to 6780, CDS, Draw as Gene

Translation product 487 aas

Mol Wt 54809.2, Isoelectric Pt (pI) 4.43

Translation:
MGSSHHHHHHGSLEQPKPVFLEVMNEPLYDLVDYPKDKDAGTTPEDVFKFHNA
VANEVRAYRDQWGLASHDNLLIGGYTVAFPDFEKDNFNRWEERDKLFIDIAGA
NMDFLSVHFYDFPAFQGTRQLRRGSNVEATFDMLEQYSLMATGERKPFVVSEIG
ATVHSMMNDPWSPERDGYKLRALNGLTMNMLERPDQILKSIPFVTIKAEWGRTE
VPYTNRLMRQKFEAAGETGDAWVYTEFVKFYQLWSDVKGTRVDSWASDLDIQ
VNAYVDDKTAYLVLNNLEQEDTDLNLAALGADGNSLQSVTIKELYYDADGKPV
LDISDSTELPQMYTLKSEATTILQLTYTNPIAIDGDGTETKYYADKYKQPITADAK
LQFAINDVVVGNAGEAVLRLGIGREHGKSLTPSVTVNSNAVTVPEDYQGYDQYY
GGKGRAQFFGVLEIPVDLEYLNEDNTVEIVFEDEGGFVSTATLQVFNTSSALVRG
ARE

>pME5 Ligation of 452_nt-2by PCR* into pFO4*

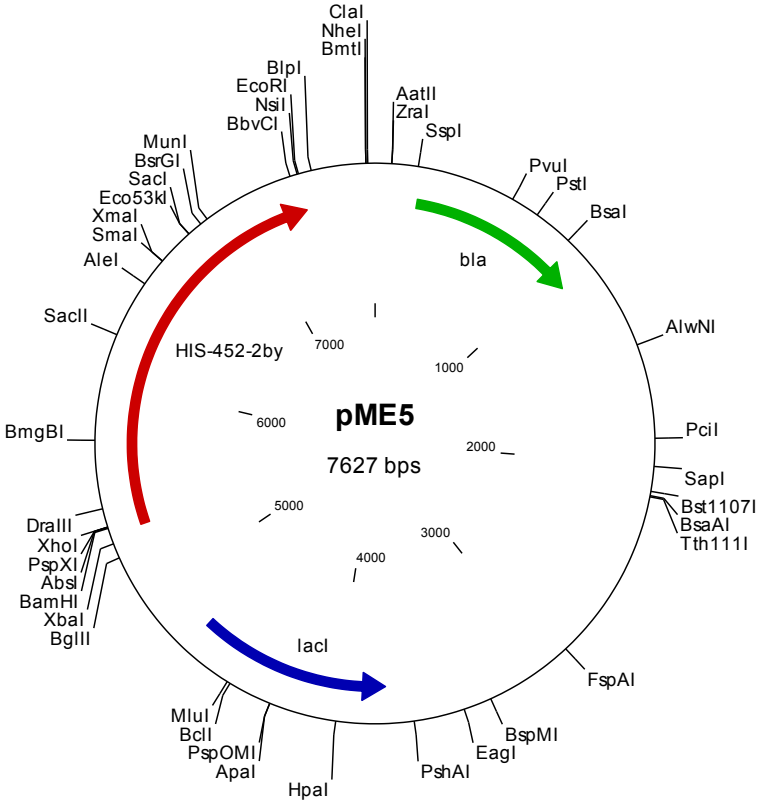

Details: HIS-452-2by, 5317 to 7284, CDS, Draw as Gene

Translation product 655 aas

Mol Wt 73462.9, Isoelectric Pt (pI) 4.38

Translation:
MGSSHHHHHHGSLEESEFDRRKFITVHASNTENDWFGSNSQSAGAPNDDP
DLMTSFLEGYDVYFGRDTGGMKWQLSQLPEDGTRPGFIDEGAASTNGGNA
RWNYTEGTTANAALARKHEHRATDMIVGGQQHPYWPNGDDVGMGWSFSQT
DTEEEPLGTAVGHYMANYLYEYFNRGSNDTYGQPKPVFLEVMNEPLYDLV
DYPKDKDAGTTPEDVFKFHNAVANEVRAYRDQWGLASHDNLLIGGYTVAF
PDFEKDNFNRWEERDKLFIDIAGANMDFLSVHFYDFPAFQGTRQLRRGSN
VEATFDMLEQYSLMATGERKPFVVSEIGATVHSMMNDPWSPERDGYKLRA
LNGLTMNMLERPDQILKSIPFVTIKAEWGRTEVPYTNRLMRQKFEAAGET
GDAWVYTEFVKFYQLWSDVKGTRVDSWASDLDIQVNAYVDDKTAYLVLNN
LEQEDTDLNLAALGADGNSLQSVTIKELYYDADGKPVLDISDSTELPQMY
TLKSEATTILQLTYTNPIAIDGDGTETKYYADKYKQPITADAKLQFAIND
VVVGNAGEAVLRLGIGREHGKSLTPSVTVNSNAVTVPEDYQGYDQYYGGK
GRAQFFGVLEIPVDLEYLNEDNTVEIVFEDEGGFVSTATLQVFNTSSALV
RGARE

>pME6 Ligation of 453_nt-1y PCR* into pFO4*

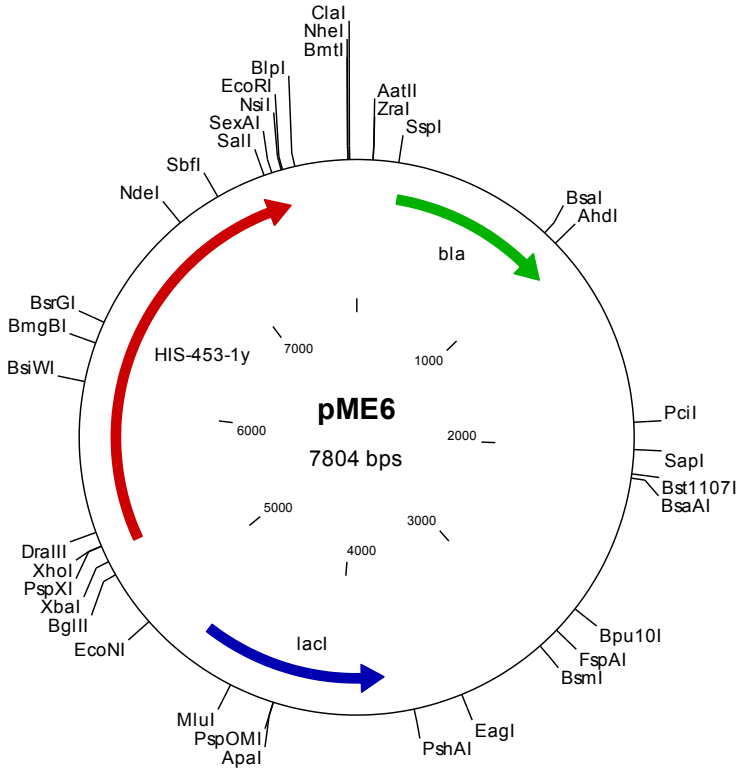

Details: HIS-453-1y, 5317 to 7461, CDS, Draw as Gene

Translation product 714 aas

Mol Wt 80902.6, Isoelectric Pt (pI) 4.86

Translation:
MGSSHHHHHHGSLESASQVGNSNSATVTVNANIKHSVNGVSDFGRNRHIT
AHTTIYEKDWDGHADKLNYLVNTLDVTLGRDNGTASWKFRDTKEDPNKPS
WPDMDYMVDRGQELRELYEGNPFYKRFDAESTELIAGTNPHPTYPTLSWY
ENGKTWHNWQPMTIETSAAWMGQYMKHYYANSSNGYLGDPMPKYWEVINE
PDMEMKTGKFMVTNQEALWEYHNLVAQEIRSKLGNEAPMIGGMTWGQHDF
YRRDGISRYGDNAYDQWITAEDPAEEAAAEEFFRNAMATTVDDTRAQDWY
QWDVMWKGFMDAAGHNMDFYAVHVYDWPGVSDDSTSRLRRNGHLPAMLDM
MEWYDVYKNGQSNRKPIVLSEYGSVQGGWDTLAHHPRFESEVLKSFNAML
MQILDRPDYVIKSMPFTPAKPLWGYYPGGCGYEEPRTCSAAYHYSLLIEP
VLNQGNWQWSDYIKFFELWADVDGTRVDSVSSDADVQVQSYVDGNELFVI
VNNLETVDTTVNLDVAGLGGAQLQNVEMRNMRFDSGSDTHVDRQHMKQMP
SNLTLAANATVVLRYTLGNNIAVNQSMNEKKYFGNSVSGGSEPHRISVAG
GAKTLQVNNVTVPAGYAEAQLRLTVALYPGEDDSPDSMLQIDSLTINGQT
VETPLDWRGRKQNSTERYFNTLEIPVPADVLQANNTISVDFRHNGELTVANLVVK
DFSTVPVRN

>pME7 Ligation of 453_nt-2wy PCR* into pFO4*

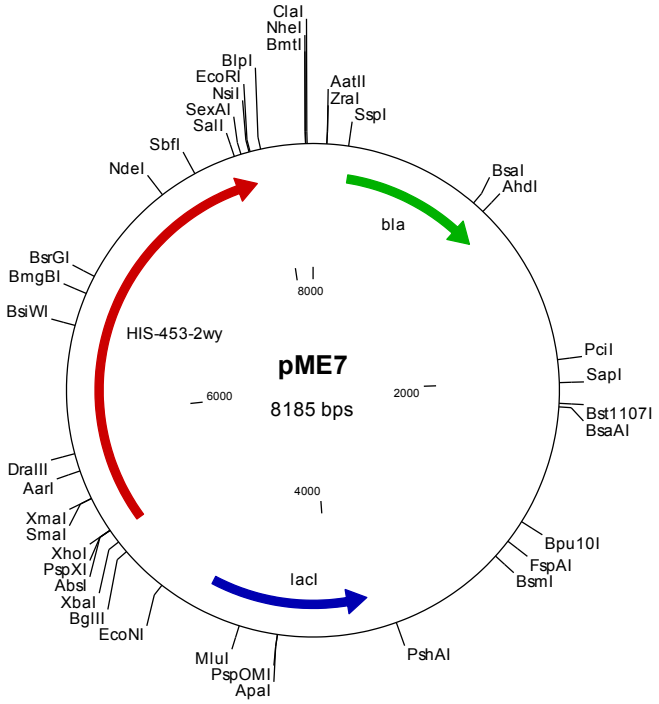

Details: HIS-453-2wy, 5317 to 7842, CDS, Draw as Gene

Translation product 841 aas

Mol Wt 93447.2, Isoelectric Pt (pI) 4.34

Translation:

MGSSHHHHHHGSLEDGDGDGTPDVSDQCPSTDPAETANSVGCAPSQLDTD
EDGITDNLDQCPTTAAGEFVNAVGCASPGGDDDDFDGVMNSADQCANTPF
GQNVDPSGCSGFADSDNDGIANSVDNCPATPAGEFANESGCSASQVGNSN
SATVTVNANIKHSVNGVSDFGRNRHITAHTTIYEKDWDGHADKLNYLVNT
LDVTLGRDNGTASWKFRDTKEDPNKPSWPDMDYMVDRGQELRELYEGNPF
YKRFDAESTELIAGTNPHPTYPTLSWYENGKTWHNWQPMTIETSAAWMGQ
YMKHYYANSSNGYLGDPMPKYWEVINEPDMEMKTGKFMVTNQEALWEYHN
LVAQEIRSKLGNEAPMIGGMTWGQHDFYRRDGISRYGDNAYDQWITAEDP
AEEAAAEEFFRNAMATTVDDTRAQDWYQWDVMWKGFMDAAGHNMDFYAVH
VYDWPGVSDDSTSRLRRNGHLPAMLDMMEWYDVYKNGQSNRKPIVLSEYG
SVQGGWDTLAHHPRFESEVLKSFNAMLMQILDRPDYVIKSMPFTPAKPLW
GYYPGGCGYEEPRTCSAAYHYSLLIEPVLNQGNWQWSDYIKFFELWADVD
GTRVDSVSSDADVQVQSYVDGNELFVIVNNLETVDTTVNLDVAGLGGAQL
QNVEMRNMRFDSGSDTHVDRQHMKQMPSNLTLAANATVVLRYTLGNNIAV
NQSMNEKKYFGNSVSGGSEPHRISVAGGAKTLQVNNVTVPAGYAEAQLRL
TVALYPGEDDSPDSMLQIDSLTINGQTVETPLDWRGRKQNSTERYFNTLE
IPVPADVLQANNTISVDFRHNGELTVANLVVKDFSTVPVRN

>pME8 Ligation of 453_nt-3bwy PCR* into pFO4*

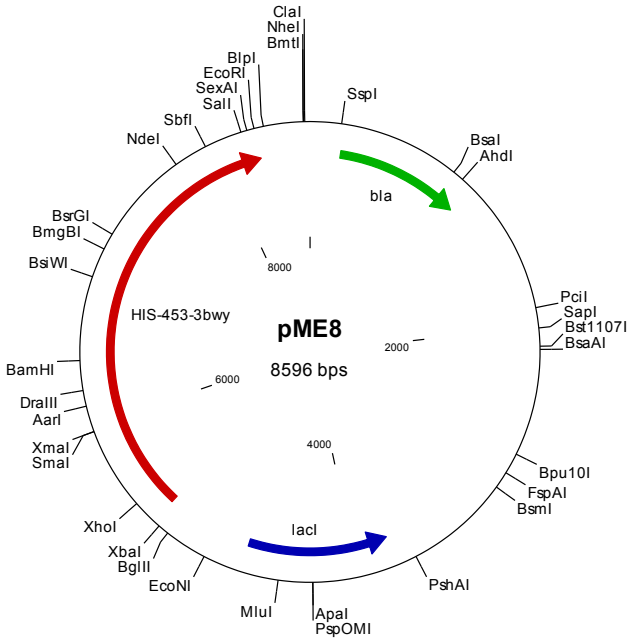

Details: HIS-453-3bwy, 5317 to 8259, CDS, Draw as Gene

Translation product 980 aas

Mol Wt 108365.1, Isoelectric Pt (pI) 4.26

Translation:
MGSSHHHHHHGSSGTFTLQAEAAHAVGGEIDTYAINGGTAVNYFNSGDYL
EYNLTLDQSGLYRPKYFVGTANTSGTAVGLMATDHEGELVVKNTTDVQSQ
GDWDTFYLLNASSEVNLFAGDLTIRIYGAGSQDFQFNIDYATFERVGDAD
LALDGDGDGTPDVSDQCPSTDPAETANSVGCAPSQLDTDEDGITDNLDQC
PTTAAGEFVNAVGCASPGGDDDDFDGVMNSADQCANTPFGQNVDPSGCSG
FADSDNDGIANSVDNCPATPAGEFANESGCSASQVGNSNSATVTVNANIK
HSVNGVSDFGRNRHITAHTTIYEKDWDGHADKLNYLVNTLDVTLGRDNGT
ASWKFRDTKEDPNKPSWPDMDYMVDRGQELRELYEGNPFYKRFDAESTEL
IAGTNPHPTYPTLSWYENGKTWHNWQPMTIETSAAWMGQYMKHYYANSSN
GYLGDPMPKYWEVINEPDMEMKTGKFMVTNQEALWEYHNLVAQEIRSKLG
NEAPMIGGMTWGQHDFYRRDGISRYGDNAYDQWITAEDPAEEAAAEEFFR
NAMATTVDDTRAQDWYQWDVMWKGFMDAAGHNMDFYAVHVYDWPGVSDDS
TSRLRRNGHLPAMLDMMEWYDVYKNGQSNRKPIVLSEYGSVQGGWDTLAH
HPRFESEVLKSFNAMLMQILDRPDYVIKSMPFTPAKPLWGYYPGGCGYEE
PRTCSAAYHYSLLIEPVLNQGNWQWSDYIKFFELWADVDGTRVDSVSSDA
DVQVQSYVDGNELFVIVNNLETVDTTVNLDVAGLGGAQLQNVEMRNMRFD
SGSDTHVDRQHMKQMPSNLTLAANATVVLRYTLGNNIAVNQSMNEKKYFG
NSVSGGSEPHRISVAGGAKTLQVNNVTVPAGYAEAQLRLTVALYPGEDDS
PDSMLQIDSLTINGQTVETPLDWRGRKQNSTERYFNTLEIPVPADVLQAN
NTISVDFRHNGELTVANLVVKDFSTVPVRN

>pME9 Ligation of 454_nt-1y PCR* into pFO4*

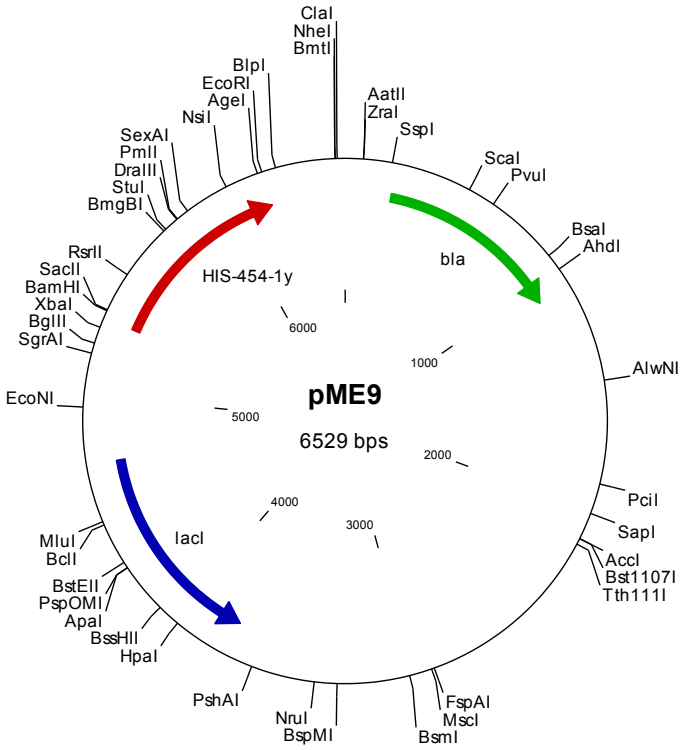

Details: HIS-454-1y, 5317 to 6192, CDS, Draw as Gene

Translation product 291 aas

Mol Wt 32752.5, Isoelectric Pt (pI) 5.16

Translation:
MGSSHHHHHHGSADWDGIPVPADPGAGKVWELHPLSDDFNYEAPAAGKSA
AFYERWKEGFINPWTGPGLTEWHPEYSLVSNGRLQIKSGRKPGTNQVYLG
SITSKTTLTYPLYMEARAKLSNMVLASDFWLLSADSTEEIDVIEAYGSDR
PGQEWFAERLHLSHHVFIREPFQDYQPTDPGTWYADGNGTRWADSYHRVG
VYWRDPWHLEYYVDGQLVRTASGPDIIDPNGFTNGTGLSKPMHAIINMED
QSWRSDNGITPTDAELADPNRNTYNVDWVRFYKPVATGGGS

Acknowledgements

Alhamdulillahi Rabbil Aalamiin

I would like to praise Allah Subhanahu wa Taala, the Wise and the Most Great who guides and teaches me the knowledge I did not know before.

I would like to acknowledge and gratitude to Prof. Marion Bettina Ansorge Schumacher who has given me trust, opportunity, encouragement, and support to become a scientist in Molecular Biotechnology.

I am particularly grateful to Dr. Christoph Loderer who has been very kind and patient donating his time, experiences, feedback, and encouragement. You are an extraordinary warm-hearted and humble scientist I have ever met and I owe you much than I can express in words.

I am especially indebted to Dr. Mirjam Czjzek, Robert Laroque, Dr. Thomas Francois, Tristan Barbeyron, and colleagues in the Station Biology Roscoff for sharing their expertise in an encouraging environment that developed my insight about marine polysaccharides-active enzymes.

I am also grateful to Prof. Michael Rother and Prof. Thorsten Mascher for the generous support of lab facilities.

I am lucky and honored to work at the Molecular Biotechnology Group. Thank you to Eugen Schell, Dr. Axel Wobus, Dr. Zhiyong Sun, Alexander Bolt, Frances Morgenstern, Thomas Krause, Jana Stephan, Silke Hoffman for becoming pleasant colleagues during my study. Special thanks to Ningning Zhang who is willing to become more than a colleague but also a friend. Last but not least to all colleagues in the Institute for Microbiology thank you for making me feel at home.

I would like to express sincere gratitude to the Indonesia Endowment Fund for Education for funding my study, to the International Office of TU Dresden, and the Association for Friends and Alumni TU Dresden for financial assistance during my writing time.

I owe my loving and caring husband, Hera Hendrasana, our pleasant children, Hafshah Nur Fadhilah, Muhammad Hafizh Rantisi, Imad Aqil Rabbani, and my parent for their unconditional support, praying, patience, and encouragement.